Results: We show identical molecular signature in the original leukemic blasts and the subsequent histiocytic neoplasms in two pediatric patients with TALL. Using FISH, one case had the same biallelic deletion of the CDKN2A (TP16) locus on 9p21, while using next generation sequencing, the other had the same G13D mutation in the NRAS gene.
Conclusions: This confirms a common clonal origin and highlights the need to perform appropriate molecular studies in such patients to better understand the mechanism and etiology behind histiocytic neoplasm seemingly born out of other hematopoietic malignancies.

1893 Assessment of PD-L1 Expression in Pediatric High-Grade Gliomas

Mariona Suñol, Iban Aldecoa, Ofelia Cruz, Angel Montero, Eva Rodríguez, Teresa Ribalta. Sant Joan de Déu Barcelona Children's Hospital, Barcelona, Spain.
Background: Programmed death-ligand 1 (PD-L1) is an immune-inhibitory receptor expressed in some tumors, including high-grade gliomas (HGG). Expression of PD-L1 has been associated with poorer outcomes and may predict response to anti-PD-1 agents. Immune checkpoint-inhibitor therapies can facilitate tumor regression and clinical studies of PD-1 blockade are now being initiated in pediatric patients with high-grade gliomas (HGG), however, little is known regarding PD-L1 expression in these childhood tumors. In the present study, we aimed to investigate the expression of PD-L1 in a series of pediatric HGGs of our institution.
Design: We measured the incidence of PD-L1 expression in 54 pediatric HGGs (ages 0-17 y. o.). Whole slide sections were evaluated by IHC using the rabbit anti-PD-L1/CD274 (clone SP142) monoclonal antibody. Nineteen of the tumors were autopsy cases. Tumor locations included pons (23), cerebral hemispheres (12), supratentorial deep structures (7), spinal cord (4), and other (8). The percentage of PD-L1-expressing cells was assessed semi-quantitatively.
Results: Fifty-seven percent (34/59) of tumors (28/40 biopsies; 6/19 autopsies) expressed PD-L1 in at least 1% of tumor cells. Staining was heterogeneous, with the vast majority of the cells demonstrating both membrane and cytoplasmic staining. Small clusters of strongly positive tumor cells were observed in 7 cases; a faint diffuse cytoplasmic staining was seen in 7 cases and scattered positive cells were identified in 20 cases. Many of the scattered PD-L1 expressing cells had either the morphology of either normal neurons, or inflammatory cells. A combination of patterns was observed in 7 cases. Two cases showed a weak nuclear stain.
Conclusions: Similar to adult HGG that have been recently profiled for PD-L1 expression, expression in our series of pediatric HGG patients using anti-PD-L1/CD274 (clone SP142) is frequent, although is largely confined to a minority subpopulation of tumor cells.

1894 Histopathologic Correlation with the Newly Defined "Term" Placenta

Ashley N Vogel, Jordyn B Tumas, Dan de Cotiis, Amanda Roman, Joanna Chan. Thomas Jefferson University, Philadelphia, PA; Einstein Medical Center, Philadelphia, PA.
Background: Previously, uncomplicated "term" pregnancies were considered a homogeneous group defined as 37-41 weeks gestational age. However, neonatal outcomes, especially respiratory morbidity, varied significantly within this time frame. In 2013, the American Congress of Obstetrics and Gynecology (ACOG) reclassified term pregnancy into early (37 0/7-38 6/7 weeks), full (39 0/7-40 6/7 weeks), late (41 0/7-41 6/7 weeks), and postterm (>42 0/7 weeks) pregnancies to reflect these clinical differences. This study examines the correlation between this new stratification and placental pathology.
Design: From 2012-2016, 674 consecutive singleton placentas were evaluated for gestational age, placental weight, cord insertion, malperfusion, fetal/maternal vascular stasis, meconium, fetal/maternal inflammatory response and decidual vasculopathy. Statistical analysis used single and multiple variable ANOVA as well as single and multiple variable logistical regression based on gestational age. When stratified into early, full, and late term, data was evaluated using Chi-Square and Fischer exact test analysis on a contingency table basis.
Results: Retrospective evaluation shows that placental weight ($p<0.0003$) and increased perivillous fibrin ($p<0.001$) directly correlate to gestational age. In addition, acute chorioamnionitis and funisitis correlate to increasing gestational age when compartmentalized as previously described ($p<0.023$ and $p<0.001$, respectively). The remainder of the tested variables show no significant difference between early, full and late term placentas.
Conclusions: Stratifying placentas by the new ACOG terminology significantly correlates to placental weight, increased perivillous fibrin, chorioamnionitis and funisitis. The correlation between placental weight and gestational age is consistent with improved clinical outcome at increased gestational age. However, increased perivillous fibrin, chorioamniionitis and funisitis are each independently associated with poorer neonatal outcomes. Exact gestational age should be noted when evaluating placentas as it correlates with pathologic findings. Clinicians should be made aware of these risk factors as they advise their gravid patients. Future studies include correlating neonatal outcomes and maternal comorbidities with placental pathology in early, full and late term pregnancies.

1895 Norovirus Infection in Pediatric Small Intestine Allografts: A Clinicopathological Study of a Cohort of 23 Patients

Wei Xu, Stuart Kaufman, Joeffrey Chahine, Brandi Higgins, Nada Yazigi, Cal Matsumoto, Khalid Khan, Bhaskar VS Kallakury. Medstar Georgetown Univeristy Hospital, Washington, DC.
Background: Human Norovirus in the family Caliciviridae is a major cause of epidemic gastroenteritis. Norovirus infections are typically acute and self-limited. However, Norovirus infection, the most frequent cause of acute pediatric gastroenteritis in the era of Rotavirus vaccine, produces a prolonged and chronic diarrhea in immunocompromised host, particularly in pediatric small intestine transplant recipients. This study aimed to characterize histological and immunohistochemical features of small bowl allograft biopsies before and after Novovirus infection.
Design: We retrospectively reviewed H&E slides and performed IHC staining for proliferation index (Ki67), apoptosis (Caspase 3), T lymphocytes (CD3) on pre and post Novovirus enteritis (11 to 204 days from symptom onset to PCR diagnosis) in 23 small bowel transplant recipients at MGUH between 2007 and 2014. We studied immunohistochemical features by counting the number of intraepithelial T lymphocytes, proliferation index and apoptotic bodies in both villi and crypts per 100 enterocytes.
Results: Comparison was made between pre Novovirus infection group (controls) and PCR confirmed Novovirus infection group. Compared with controls, biopsies with Novovirus infection group showed significantly increased in intraepithelial T lymphocytes (15.1 ± 6.0 versus 7.7 ± 2.9 cells/100 enterocytes, $P < .05$), higher proliferation index in villi (7.3 ± 4.0 versus 2.9 ± 1.8 cells/100 enterocytes, $P < .05$) and crypts (78.7 ± 12.1 versus 50.3 ± 11.7 cells /100 enterocytes, $P < .05$), higher apoptosis activity in superficial lamina propria (1.0 ± 0.5 versus 0.4 ± 0.3 cells/100 enterocytes, $P < .05$). There was no significant difference in crypts apoptosis activity between Novovirus infection group and control group.
Conclusions: In summary, all Novovirus infection biopsies showed increased intraepithelial T lymphocytes and villi blunting, increased proliferation index in both villi and crypts and increased lamina propria apoptosis, deemed characteristic of Novovirus infection. These features may be helpful in designing a test group to differentiate Novovirus enteritis from mild acute rejection, warranting further study.

Pulmonary Pathology (including Mediastinal)

1896 *MET* Exon 14 Splicing Mutations and Intragenic Deletions in Non-Small Cell Lung Cancer: A Study of Co-Occurring Genomic Mutations and Copy Number Alterations

Deepu Alex, Joseph Montecalvo, William Travis, Maria E Arcila, Marc Ladanyi. Memorial Sloan Kettering Cancer Center, New York, NY.
Background: Splicing mutations of *MET* exon 14 at the splice acceptor and donor sites have been previously reported to cause exon skipping, resulting in loss of the CBL E3-ubiquitin ligase-binding site which is responsible of MET protein turnover. The presence of these oncogenic mutations makes the tumor responsive to MET-targeted therapies.
Design: Comprehensive cancer genomic profiling was performed using a hybridization capture-based next-generation sequencing (NGS) assay for targeted deep sequencing of all exons and selected introns (inclusive of *MET*) of 410 key cancer genes in formalin-fixed, paraffin-embedded tumors. Bar-coded libraries from patient-matched tumor and normal samples are captured, sequenced, and subjected to a custom analysis pipeline to identify somatic mutations, copy number alterations and select structural rearrangements. Next generation sequencing results from 1682 NSCLCs were reviewed to identify cases with *MET* exon 14 alterations.
Results: *MET* exon 14 alterations were detected in 58 patients [male=27, female=31] with a median age of 72 years (44-89). Tumor morphologies were variable and included pleomorphic sarcoma, lung adenocarcinoma (lepidic, acinar and mixed patterns), squamous cell carcinoma and adenosquamous carcinoma. 42 cases had sequence variants at the splice donor site (6 not previously reported), 11 cases had sequence variants at the splice acceptor site and 5 cases had deletions within exon 14 that included the CBL E3-ubiquitin ligase-binding site, Y1003 (3 not previously reported). Based on the analysis of 410 genes of the sequencing panel, *MET* exon 14 mutated NSCLCs frequently showed the following co-mutations: *TP53* alterations (32%), *MDM2* and *CDK4* amplifications (25 and 21% respectively), and *TERT* alterations (21%). Concurrent *MET* amplification (as determined by the hybrid capture NGS assay) involving the mutated allele was detected in 5 cases (9%). One case with *CBL* p.R420L was identified. No other known lung cancer driver alterations were identified in these cases, indicating strong mutual exclusivity with alterations in *EGFR*, *KRAS*, *ALK*, *RET* and *ROS*.
Conclusions: *MET* exon 14 alterations represent a distinct molecular subtype of NSCLC. Our study describes the spectrum of alterations identified in this region, including alterations not previously reported. The detection of these alterations is important as it allows the identification of patients who can be treated with already existing targeted therapies.

1897 The Development of Brain Metastasis in Lung Adenocarcinoma Is Associated with a High Rate of Tumor Necrosis in the Primary Tumor and the Selection of Cribriform and Solid Growth Patterns

Khaleel I Al-Obaidy, Fulvio Lonardo. Wayne State Univeristy/ Detroit Medical Center/ Karmanos Cancer Institute, Detroit, MI.
Background: In lung adenocarcinoma (LADC), growth patterns- as recently re-defined- and necrosis have a well-established prognostic value, yet it is not known whether they may be specifically linked to the development of brain metastasis.

Design: We compared the predominant growth patterns of 69 resected brain metastases from LADC (BM), accrued over 10 years, to that of a control series (C-LADC), composed of 87 consecutively resected LADC, accrued over 3 years, including 66 stage I and 21 stages II-IV.
Among patients with resected brain metastases, we identifed a subgroup who had undergone resections of their primary LADC (*BM-1ary-LADC*), (n=12, including 6 stage I and 6 stages II-IV). We compared the % of tumor necrosis occuring in these cases with that of the *C-LADC*.
We studied whether an association exists between growth patterns and tumor necrosis in *C-LADC*.
We compared growth patterns changes occurring between *BM-1ary-LADC* and their matching brain metastases.
Results: 1- BM show a higher rate of solid and cribriform patterns of *C-LADC* ($p<0.05$).
2- *BM-1ary-LADC* show a higher average percentage of necrosis of stage matched *C-LADC*. Taking ≥10% tumor necrosis as a cut-off, the differences are statistically significant ($p<0.05$) across all stages.
3-In *C-LADC* the cribriform pattern is associated with high (≥10%) tumor necrosis ($p<0.05$).
4- A direct comparison of growth patterns between *BM-1ary-LADC* and their matching brain metastases reveals the following changes. In seven *BM-1ary-LADC* with solid predominant pattern, this remains the same (n=5), changes to acinar (n=1) or cribriform (n=1) in the metastasis. In four *BM-1ary-LADC* with an acinar predominant pattern, this changes to cribriform (n=3) or mucinous (1). One *BM-1ary-LADC* maintains its mucinous pattern in the brain metatasis.
Conclusions: 1- An apparent selection of solid and cribriform growth patterns is associated with the development of brain metastases in LADC. The cribriform pattern is associated with high tumor necrosis. These collective data are consistent with other studies, pointing out that the cribriform pattern, although not formally recognized by the current classification, may represent a high grade variant of LADC.
2-Our preliminary observations on a small series of *BM-1ary-LADC* raise the possibility that necrosis may foster the development of brain metastasis.

1898 Comparative Immunohistochemical Analysis of Programmed Death-Ligand 1 (PD-L1) Utilizing 22C3 and 28.8 Clones for Targeted Drug Therapy in Primary and Metastatic Tumor Resections

Fatimah I Alruwaii, Weihua Song, Howard Wu, Muhammad Idrees. Indiana University School of Medicine, Indianapolis, IN.

Background: Programmed death-ligand 1 (PD-L1) expression by tumor cells protects the tumor from destruction by cytotoxic T cells. Recent early-phase trials in different carcinomas targeting the PD-L1 have shown clinical efficacy that correlated PD-L1 tumor expression and responses. Recently two PDL-1 clones 22C3 and 28.8 for targeted drug therapy (Pembrolizumab and Nivolumab respectively) for non-small cell lung carcinoma (NSCLC) were marketed. There is perplexity in reporting and analyzing these antibodies due to different cut offs for expression. We comparatively analyzed the immunoexpression of these antibodies in cases of NSCLC.
Design: 45 Primary NSCLC resection specimens were selected with appropriate amount of tissue (>100 tumor cells). All these cases had clinical metastasis. Immunohistochemical stains for 22C3 were performed on all 45 cases while 28.8 were performed on 21 matched cases using the Dako ready to use kit. Only membranous staining in tumor cells was considered for scoring. Staining Intensity (0, 1+, 2+, 3+) and Tumor proportion score (TPS) were evaluated and differences were recorded for the expression patterns of two antibodies. The TPS was evaluated as Negative 0, 1-25% 1+, 26-49% 2+, >50% 3+.
Results: For 22C3, 28 of 45 (66%) cases were positive. The tumor proportion score ranged 1% to 90% (1+ 20; 2+ 2; 3+ 6) while intensity ranged from 1+ to 3+ (1+ 14, 2+ 10, 3+ 4). For 28.8 clone 12 of 21 (57%) were positive. The tumor proportion score ranged 1% to 90% (1+ 9, 2+ 2, 3+ 1) while intensity ranged from 1+ to 3+ (1+2, 2+ 7, 3+ 3). Among two antibodies 19 matched (90%) tumors showed similar TPS and intensity. Alveolar and tissue macrophages were intensely positive more with 22C3 and to lesser extent with 28.8 which made analysis challenging.
Conclusions: Both antibodies showed similar expression patterns in NSCLC and can provide valuable information regarding the use of different therapeutic agents. Careful evaluation of tumor cells is of utmost importance as majority of the alveolar macrophages and immune cells will react with both antibodies.

1899 Validation of a Rapid Point-of-Care Test to Detect *Epidermal Growth Factor Receptor* Gene Mutations in Patients with Lung Cancer by Using Cell-Free DNA Supernatants

Shiho Asaka, Akihiko Yoshizawa. Shinshu University Hospital, Matsumoto, Nagano, Japan; Kyoto University Hospital, Kyoto, Japan.

Background: *Epidermal growth factor receptor* (*EGFR*) gene mutations are associated with a response to tyrosine kinase inhibitors in non-small-cell lung cancer. We have reported on a rapid *EGFR* mutation assay using a real-time droplet-polymerase chain reaction machine (Seiko Epson) (*EGFR* d-PCR) with a reaction time less than 10 minutes. The purpose of this study was to validate the performance of the *EGFR* d-PCR assay using cell-free DNA supernatants compared to pellets of fresh liquid cytology specimens (FLCSs) (e.g., bronchial lavage fluid [BLF] and pleural effusion [PE]).
Design: We analyzed three main *EGFR* mutations (L858R in exon 21, E746_A750del in exon 19, and T790M in exon 20) in 31 FLCSs (25 BLFs and 6 PEs) from consecutive patients clinically diagnosed as having lung cancer, and we performed bronchoscopic examination or aspiration cytology of pleural effusion for 2 months at Shinshu University Hospital. Specimens were centrifuged and divided into pellet and supernatant fractions. Among 31 specimens, malignant cells were identified in 17 specimens by cytological examination, whereas no malignant cells were identified in 14 specimens.
Results: The positive rates of *EGFR* mutations in cell-free DNA supernatants were highly concordant with those of the pellets (L858R: 4 [12.9%] vs. 4 [12.9%]; E746_A750del: 3 [9.68%] vs. 4 [12.9%]; and T790M: 2 [6.5%] vs. 2 [6.5%]). In 2 of 9 mutation-positive specimens of cell-free DNA supernatants, malignant cells were not identified during cytological examination of the pellets.

	pellet	cell-free DNA supernatant
Positive	7 (22.6%)	6 (19.4%)
Exon 21 L858R	4 (12.9%)	4 (12.9%)
Exon 19 E746_A750del	4(12.9%)	3 (9.68%)
Exon 20 T790M	2 (6.5%)	2 (6.5%)
Negative	24 (77.4%)	25 (80.6%)
Total	31	31

Conclusions: The *EGFR* d-PCR assay with cell-free DNA supernatants of FLCSs may be a rapid and sensitive point-of-care test for patients with lung cancer, even in those with cytologically negative specimens. This method would be useful because the pellets that enable morphological and multiple molecular analyses are reserved. Currently, we are continuing to validate this method with additional specimens of cell-free DNA supernatants of FLCSs, and we are developing a new *EGFR* d-PCR assay using blood serum.

1900 A Semi-Quantitative Approach to Biopsy Diagnosis of Large Cell Neuroendocrine Carcinoma of the Lung

Marina K Baine, Robert J Homer. Yale University, Yale New Haven Hospital, New Haven, CT.

Background: Large cell neuroendocrine carcinoma (LCNEC) of the lung is a seemingly rare entity for which current WHO diagnostic criteria require resection material. As a result, a therapeutic approach is not well defined. Modified criteria for diagnosis of LCNEC on biopsy have been proposed by Watanabe et al., which resulted in a high frequency of a correct diagnosis. These criteria incorporate the use of Ki-67 proliferative index in place of mitotic count, in addition to other histomorphologic and immunophenotypic features. The reliability of this approach, however, has not been validated in an independent cohort.
Design: A tissue microarray (TMA) composed of 27 cases diagnosed as large cell neuroendocrine carcinoma was created from the files of Yale New Haven Hospital. An additional array of 283 non-small cell carcinomas (NSCLC) and other neuroendocrine tumors was analyzed for comparison. The TMAs were used as a biopsy surrogate, and were stained for Ki-67, standard neuroendocrine markers, Napsin A, and p40. The tumors were also analyzed by standardized morphologic criteria.
Results: A scoring system was devised, which assigned a score of 1 for each of the three classical architectural patterns of LCNEC (peripheral palisading, organoid nesting, and rosettes). An additional 1 point was assigned for the presence of prominent nucleoli (at 20x magnification), 1 point for necrosis (excluding single-cell necrosis), 1 point for high Ki-67 (>40%), and 3 points for one or more neuroendocrine marker positivity (chromogranin, synaptophysin, or CD56/NCAM), with a maximum possible total score of 9. The total scores for NSCLC ranged from 0 to 6 with a median and average scores of 1 and 1.1 (± 1), respectively. The range for LCNEC cases was 3 to 8 with a median of 6 and a mean of 6.2 (± 1.4). Utilizing a cut-off score of ≥5 resulted in the correct diagnosis of LCNEC in 20 of 24 cases (83%), with a 99% specificity and 83% sensitivity.

SCORE	Non-Small Cell Lung Carcinoma	Large Cell Neuroendocrine Lung Carcinoma
0-2	168 (94%)	0 (0%)
3-4	9 (5%)	4 (17%)
≥5	2 (1%)	20 (83%)
TOTAL	179	24

Conclusions: On the basis of these results we propose a semi-quantitative approach to the diagnosis of LCNEC on biopsy based on a combination of specific morphologic and immunohistochemical features.

1901 Non-Mesothelial Neoplasms in Individuals with Malignant Mesothelioma

Kelly Butnor, Elizabeth N Pavlisko, Thomas A Sporn, Victor L Roggli. University of Vermont Medical Center, Burlington, VT; Duke University Medical Center, Durham, NC.

Background: Malignant mesothelioma (MM) has been recognized as a component of the BAP1 tumor predisposition syndrome. Other than familial studies of *BAP1* mutation carriers, the prevalence and spectrum of non-mesothelial neoplasms in individuals with MM has not been comprehensively assessed.
Design: Individuals with both MM and other neoplasms were identified from a database of approximately 4000 MM cases. Using data from Surveillance, Epidemiology, and End Results (SEER) and other published sources, the expected prevalence of each type of non-mesothelial neoplasm was calculated and compared to the actual prevalence in the study population.
Results: Other neoplasms were identified in 241 individuals with MM (6% of study population). The majority of MM were pleural (84%) and remainder were peritoneal. Prostate adenocarcinoma was the most common non-mesothelial neoplasm (n=51), but along with chronic lymphocytic leukemia (n=13), colorectal carcinoma (n=16), cutaneous melanoma (n=6), soft tissue sarcomas (n=8), thyroid carcinoma (n=4), and testicular neoplasms (n=3), did not exceed expected prevalence. Renal cell carcinoma (n=19), non-Hodgkin lymphoma (n=20), Hodgkin lymphoma (n=19), lung carcinoma (n=18), urothelial carcinoma (n=18), breast carcinoma (n=17), multiple myeloma/

plasmacytoma (n=5), meningioma (n=5), ocular melanoma (n=3), and Wilm tumor (n=2) all were more prevalent than expected. In 32 cases (0.8%), MM developed subsequent to radiation therapy of another malignancy.

Conclusions: Non-mesothelial neoplasms are uncommon in individuals with MM, but certain tumor types are increased in prevalence. Not surprisingly, there is an increased prevalence of lung carcinoma, which like MM, is associated with asbestos exposure. Malignancies typically treated with irradiation, such as Hodgkin lymphoma, are also overrepresented. Interestingly, in our unselected study population with respect to *BAP1* status, there was an increased prevalence of tumors described in *BAP1* germline mutation carriers, which in addition to lung carcinoma, include renal cell carcinoma, multiple myeloma, meningioma, and ocular melanoma, suggesting that individuals with both MM and other neoplasms may benefit from *BAP1* mutational testing.

1902 Microcrystalline Cellulose Identification in a Series of 9 Lung Transplant Recipients

John Carney, Alice L Gray, David N Howell, Elizabeth N Pavlisko. Duke University Medical Center, Durham, NC.

Background: Microcrystalline cellulose (MCC) is an insoluble material commonly used as a binder and filler in oral medications. Identification of pulmonary intravascular deposition of MCC in transbronchial biopsies from lung transplant (LT) recipients following parenteral injection of oral medications has only been reported once. The identification of MCC can be facilitated via polarization microscopy, and if intravascular crystalline material is observed, it can be confirmed via GMS and Congo red histochemical stains.

Design: A search of our surgical pathology electronic database was performed from 1/1/2000 to 8/15/2016 using the text "TRANSPLANT TRANSBRONCHIAL." The diagnosis field for all cases retrieved was then searched for the text "CELLULOSE." These cases were queried for patient demographics and outcomes.

Results: Between 1/1/2000 and 8/15/2016, 1436 lung transplants were performed in 1358 individual patients at our institution; 9 were identified to have MCC in their lung tissue (Table 1). Patients most at risk for parenteral use of oral medications are those transplanted for cystic fibrosis in their teens and twenties. The 45-year-old patient, at time of transplant, had had a history of chronic pain with prescription of narcotics. Of the 9 patients, 5 (56%) are known to be deceased.

Table 1. Microcrystalline Cellulose Identification in 9 Lung Transplant Recipients

Age (years)at transplant	Sex	Reason for Lung Transplant	Months from transplant to identification of MCC	Outcome
20	Male	CF	3	Deceased
25	Male	CF	8	Deceased
27	Male	CF	2	Deceased
23	Female	CF	34	Alive
24	Female	CF	5	Lost to follow-up
17	Female	CF	51	Alive
20	Female	CF	96	Deceased
22	Male	CF	8	Alive
45	Female	Alpha-1 antitrypsin deficiency	142	Deceased

Abbreviations: CF (Cystic Fibrosis)

Conclusions: Identification of MCC within the pulmonary vasculature may be an indicator of increased complications, mortality, or shortened survival in LT recipients. Detecting intravascular MCC and distinguishing it from aspirated medication fragments is a diagnostic challenge. Awareness of the differential diagnosis for pulmonary foreign material and open communication with transplant pulmonologists are of paramount importance for the pathologist.

1903 Pulmonary Ciliated Muconodular Papillary Tumor (CMPT) with Classic and Non-Classic Morphology: Expanded Morphologic and Molecular Spectrum of Bilayered Lesions with Bronchiolar-Type Differentiation

Jason C Chang, Joseph Montecalvo, Shaohua Lu, Dean Wallace, Wichit Sae-Ow, Laetitia Borsu, Hyunjae R Kim, Marc Ladanyi, William Travis, Natasha Rekhtman. MSKCC, NY, NY; UCLA, LA, CA.

Background: Ciliated muconodular papillary tumor (CMPT) is a relatively new entity in the lung that is characterized by nodular proliferation of bronchiolar-type epithelium containing basal cells and luminal ciliated and mucinous cells. Classic description of CMPT includes prominent papillary architecture, and predominance of ciliated and mucinous cells entirely surrounded by basal cells. Two recent studies identified the presence of *BRAF V600E* and uncommon *EGFR* exon 19 deletion (L747_S752) in CMPTs. We have encountered several non-classic CMPTs, defined by the absence or only focal presence of papillary architecture, and paucity of ciliated and mucinous cells. Here we report on the clinicopathologic features and molecular profile for classic and non-classic CMPTs.

Design: Twelve tumors from 9 patients were identified. Clinical, morphologic and immunophenotypic features were reviewed. Genomic analysis included next-generation sequencing by a 98-gene AmpliSeq panel (n=8), 410-gene hybrid capture panel (n=2), Amplification Refractory Mutation System (n=1), and *EGFR* pyrosequencing (n=1).

Results: All tumors were composed of nodular proliferation of bland bronchiolar-type epithelium, containing continuous p40-positive basal cells. Three tumors had classic CMPT morphology, whereas 9 tumors were non-classic. Of the classic group, 2 showed *BRAF V600E* mutations and 1 was negative for all mutations tested. Of the non-classic group, 3 (33%) showed *BRAF V600E* mutations and 2 (22%) showed *EGFR* deletions involving L747_S752. In addition, 2 (22%) tumors showed *EGFR* exon 20 insertions, 1 (11%) showed *KRAS G12C* mutation, and 1 (11%) was negative for all mutations tested. Patients with classic and non-classic lesions had a similar distribution of age (p=0.46), smoking status (p=0.85), and tumor size (p=0.46).

Conclusions: Lesions with classic and non-classic CMPT morphology share overlapping clinicopathologic and molecular features, dominated by *BRAF V6000E* mutation and uncommon *EGFR* deletion. This supports our morphologic impression that these lesions represent a spectrum of the same entity, possibly reflecting differentiation toward central bronchial epithelium (classic CMPT) versus more peripheral bronchial/bronchiolar epithelium (non-classic CMPT). *EGFR* exon 20 and *KRAS* mutations in CMPTs are a novel finding. These data expand on the morphologic and molecular spectrum of CMPTs, overall supporting their neoplastic nature despite the bland hamartomatous-like morphology.

1904 Aerogenous Intrapulmonary Metastasis of Lung Adenocarcinomas: Pathologic and Radiologic Features and Correlation

Nina Chang, Joao R Inacio, Carolina A Souza, Chi K Lai, Harman S Sekhon, Marcio M Gomes. The Ottawa Hospital, Ottawa, ON, Canada.

Background: In addition to accepted mechanisms of metastases in primary lung cancer (hematogenous, lymphatic & transcoelomic), cumulative evidence suggests that lung adenocarcinoma spreads through the airways: cell discohesiveness, cytokine-induced migration and anchorage-independent survival have all been described in lung cancer cells. We define aerogenous intrapulmonary metastasis (AIM) as the intrapulmonary, discontinuous spread of neoplastic cells through airspaces and airways. Here, we describe pathologic and radiologic features of AIM.

Design: Of all patients with multiple resected lung adenocarcinomas from 2003-2016, 45 cases (with 1° and 2° tumors) were identified with at least one feature previously described in AIM. Histology slides were blindly reviewed and 2° tumors classified as AIM, vascular intrapulmonary metastasis (VIM) or synchronous primary tumors (SPT), according to an adapted comprehensive histologic assessment that included previously proposed criteria for AIM. Corresponding CT images were blindly reviewed to similarly classify patients.

Results: Histologic assessment showed 13 AIM, 4 VIM, 20 SPT and 8 indeterminate (IND: AIM versus VIM) cases. Two main patterns of AIM were seen: mucinous with papillary/lepidic patterns and non-mucinous papillary-predominant. Common histologic features of all AIM 2° tumors included: same histologic patterns as the 1° tumor, predominant airspace disease (lepidic, papillary & micropapillary), centrilobular distribution, "floater" tumor cells and absence of stromal/vascular invasion. Two of 13 (15%) AIM cases were positive for ALK by immunohistochemistry. Radiologic assessment showed 9 AIM, 5 VIM, 20 SPT and 11 IND cases. Radiologic features of AIM included centrilobular distribution, airspace disease (ground-glass opacities & consolidation), and slower progression than infection but faster progression than new 1° tumors on follow-up. Radiology was concordant for 8/13 (62%) AIM, 20/20 (100%) SPT and 7/8 (88%) IND. Clinical follow-up showed that 5 patients with histologic AIM developed contralateral lung metastases without distant metastases.

Conclusions: Our study provides strong evidence of AIM, with excellent radio-pathologic concordance in distinguishing metastases from SPT. Tumors with AIM show distinct biological behavior compared to SPT and tumors with VIM, which impacts staging, management and prognosis. Recognition of AIM features on imaging or in tissue samples should thus influence choice of therapy and provide prognostic information.

1905 Transbronchial Lung Cryobiopsy in Idiopathic Pulmonary Fibrosis: Useful or Not?

Adeline Chelliah, Hadeel Jawad, Nicola Ronan, Darren Dahly, Barry Plant, Michael Henry, Alberto Cavazza, Louise Burke. Cork University Hospital, Cork, Ireland; University College Cork, Cork, Ireland; S. Maria Nuova Hospital I.R.C.C.S., Reggio Emilia, Italy.

Background: Idiopathic pulmonary fibrosis (IPF) is defined by the presence of usual interstitial pneumonia (UIP) histology in the appropriate clinico-radiological context. Currently, surgical lung biopsy (SLB) is the recommended method to obtain tissue samples for histological diagnosis. Transbronchial lung cryobiopsy (TLC) is a proposed novel alternative to obtaining alveolated lung parenchyma samples.

The objecive of this study is to evaluate the usefulness, including interobserver reproducibility, of TLC in the diagnosis of IPF.

Design: A defined group of 13 patients with confirmed multidisciplinary consensus diagnosis of IPF were enrolled in this study. Each patient had undergone middle and lower lobe lung TLCs both pre- and post-treatment with Pirfenidone, yielding a total of 56 H/E-stained cryobiopsies for retrospective review. Patient demographics, biopsy size and any associated complications were noted. Diagnostic confidence (DC) was scored as low, high or non-diagnostic by two pathologists with a special interest in thoracic pathology, based on the presence of patchy interstitial fibrosis, fibroblastic foci and honeycombing.

Results: There were 9 male (69.2%) and 4 female (30.8%) patients with a mean age of 67.5 years (range 46-82 years). The mean biopsy size pre-treatment was 9.39mm^2 (range 2.0-32.0mm^2) and post-treatment 15.42mm^2 (range 1.62-43.0mm$^{2)}$.

Biopsies obtained from the lower lobe of lung had a higher degree of diagnostic confidence than middle lobe lung biopsies. UIP diagnosis was confirmed in all cases with good concordance between the pathologists using the histological criteria of patchy interstitial fibrosis, fibroblastic foci and honeycombing.

The complication rate was comparablke to that of standard transbronchial lung biopsy and consisted of either pneumothorax or moderate bleeding.

Conclusions: TLC is a relatively safe, novel technique with encouraging results for the diagnosis of IPF. However, larger studies are needed and currently SLB remains the gold standard for obtaining tissus samples.

1906 Radiological and Histopathogical Features of Benign and Malignant Lung Nodules

Jason L Cheng, Eric Hart, Malcolm Decamp, Rishi Raj, Kirtee Raparia. Northwestern University, Chicago, IL.

Background: The objective of our study was to correlate the histopathological and radiological features, and to evaluate whether the radiological features on computered tomography with contrast and positron emission tomography (PET) scan can be used to differentiate malignancies from granulomas.

Design: This study included 285 lung nodules in 285 consecutive patients. One hundred and thirty-seven (48%) were malignant nodules (all Stage 1a lung cancer) and 148 (52%) were granulomas. We studied clinical, radiological (lung nodule size, density, margins, presence and pattern of calcifications, PET metabolic activity and SUVmax) and histopathological characteristics of these nodules. Statistical analysis was calculated using appropriate parametric and non-parametric test with Stata software (StataCorp).

Results: Patients with malignant nodules are likely to be older (74 vs 60 years; p=0.0001). The average size of nodules in malignant and granuloma groups were 17.7 and 16.5 mm respectively. There was no difference in SUVmax in both the groups (5.9 for malignant and 5.5 for granulomas). Granulomas were much more likely to have a higher Hounsfield unit density; 1.21 (SD 11.04) for granuloma vs -65.08(SD 21.13) for malignant nodules; p = 0.02. Hilar lymph nodes were much more likely to be enlarged in patients with granulomas (20%) vs. malignant nodules (4%); p=0.001. Granulomas were more likely to have soft tissue density (83% vs. 46%) and malignant lesions were much more likely to be of mixed density (43% vs 16%) and ground glass opacity (11% vs 1%); p=0.001. Granulomas were much more likely to have necrosis (caveating or non caveating) than malignant nodules (21% vs. 6% p =0.001). Granulomas were more likely to be calcified (9% vs 3%; p= 0.030 and more likely to have smooth margins (32% vs 9%; p=0.001) and malignant nodules more likely to have poorly defined margins (22% vs 6%; p= 0.001). There was no statistical difference between the two type of nodules in relation to presence or absence of pleural effusion, calcification pattern, and metabolic activity.

Conclusions: Granulomas cannot be distinguished from malignant nodules based on the size and SUVmax . Significant radiologic differences exist between granulomas and malignant nodules in terms of absolute radio density (Hounsfield unit), subjective radio density, presence of necrosis and calcifications. These differences are clinically useful and can be used by clinicians to assign a pre-test probability of malignancy and potentially avoid excision in a subset of these patients.

1907 Steroid Hormone Receptor Protein Expression by Gender and Smoking in Non-Small Cell Lung Cancer: SWOG S0424

Ting-Yuan David Cheng, Amy K Darke, Mary W Redman, Gary R Zirpoli, Warren Davis, Rochelle Payne Ondracek, Wiam Bshara, Robert Kratzke, Julian R Molina, Jill M Kolesar, Yuhchyau Chen, Robert M MacRae, James Moon, Philip Mack, David R Gandara, Karen Kelly, Regina M Santella, Kathy S Albain, Christine B Ambrosone. Roswell Park Cancer Institute, Buffalo, NY; SWOG Statistical Center/Fred Hutchinson Cancer Research Center, Seattle, WA; University of Minnesota, Minneapolis, MN; Mayo Clinic, Rochester, MN; University of Wisconsin-Madison, Madison, WI; University of Rochester Medical Center, Rochester, NY; The Ottawa Hospital Cancer Centre, Ottawa, ON, Canada; UC Davis Cancer Center, Sacramento, CA; Columbia University, New York, NY; Loyola University Chicago, Chicago, IL.

Background: Research has suggested that sex hormones could be related to lung cancer risk in women. However, the influence of gender, reproductive factors, and hormone use at the tumor level in smokers and nonsmokers is not entirely clear.

Design: Newly diagnosed, histologically confirmed stages I-IIIA, or selected IIIB NSCLCs (525 females and 432 males) were recruited from the NCI Lung Cancer Intergroup and SWOG Lung Committee investigators, 2005-11. All never smokers (149 F, 39 M) matched to ever smokers (138 F, 37 M) with the same sex, age, and, stage were selected for analyses. Tissue microarray (79% cases) or whole tissue sections were stained with anti-estrogen receptor (ER)-α, ER-β, progesterone receptor (PR), and human epidermal growth factor receptor 1 (EGFR) and 2 (HER2). Expressions shown as H-score (Σ intensity [0, 1, 2, 3] × % cells) and positivity defined *a priori* were compared by reproductive/hormonal factors, and between ever and never smokers by gender.

Results: ER-α nucleus expression was higher in post- than premenopausal women (63% vs. 42% positive, p=0.038). ER-β nucleus (95% vs. 86% positive, P=0.018) and total (nucleus+cytoplasmic: 96% vs. 87%, P=0.011) expression was higher in postmenopausal women who ever used hormone therapy (HT) than the never users. Ever- (vs. never-) smoking was associated with a higher ER-α (nucleus: 68% vs. 54% positive, P=0.021; cytoplasmic: 87% vs. 72% positive, P=0.003) and ER-β cytoplasmic (H-score 109 vs. 76, P=0.012), but a lower PR total (H-score 76 vs. 97, P=0.005) expression among women. The associations remained significant adjusted for gender, age, and race. No differences in EGFR and HER-2 expression were observed by hormonal factors and smoking.

Conclusions: Menopausal status and HT use may have etiological roles in female NSCLC, potentially by influencing ER-α, ER-β, and PR expression. Smoking could act as a promoter of ER-related carcinogenesis in women.

ClinicalTrials.gov Identifier: NCT00450281. Support: NIH/NCI CA180888, CA180819, CA189974, CA180799, CA180820, CA180821

1908 Concordance Between Biopsy and Resection Specimens in Assessing Lung Adenocarcinoma Histologic Growth Patterns

Hannah M Christensen, Emilian Racila. University of Minnesota, Minneapolis, MN.

Background: Predominant growth pattern subtyping of lung adenocarcinoma (lepidic, acinar, papillary, micropapillary and solid) has prognostic value. For example, micropapillary and solid tumors are associated with worse outcome. However, many patients are not candidates for tumor resection, therefore the predominant pattern must be established on the limited biopsy material. The aim of this study is to determine the concordance between biopsy and resection material in evaluating histologic growth patterns of lung adenocarcinoma.

Design: We identified and reviewed 49 specimens of lung adenocarcinoma with biopsy followed by resection at the University of Minnesota Medical Center between 2006-2016. The specimens included 35 lobectomies, 2 segmentectomies and 12 wedge resections, that were collected from 47 patients (38 females and 9 males) ranging from 41-85 years old (66 years old average). One patient had three primary lung adenocarcinomas that were biopsied then resected. Only one patient received pre-operative chemotherapy. Histologic subtype in biopsy and resection specimens was assessed semi-quantitatively and recorded in 5% increments.

Results: We found concordance between the predominant pattern in the biopsy and resection specimens in 28 of 49 cases (57%), with the following concordance for each pattern as percentage calculated per total number of biopsies: solid (100%), papillary (83%), acinar (71%) and lepidic pattern (20%). The under-represented minor components that were present in the resection specimen and absent in corresponding biopsy were (as percentage of all cases): solid (29%), papillary (29%), lepidic (14%), micropapillary (12%) and acinar (6%). Micropapillary pattern was not predominant in any biopsy or resection specimens, although a micropapillary minor component was present in one biopsy specimen and six resection specimens.

Conclusions: Our results indicate that the value of biopsy specimen in determining the predominant pattern of growth in lung adenocarcinomas is limited, with concordance found only in a slight majority of cases. We also found that solid, papillary and micropapillary patterns are under-represented in biopsy specimens when present as minor components in resected tumors, a fact that may have direct impact on estimating clinical outcome since solid and micropapillary patterns are associated with worse prognosis in lung adenocarcinoma. Current efforts are in progress to expand the study population and to establish a collaborative study that will include pathologists from other institutions.

1909 The Proposal of User-Friendly Formula to Separate CTD-IPs and IIPs

Mutsumi Dairiki, Mikiko Hashisako, Shuntaro Sato, Kensuke Kataoka, Yasuhiro Kondoh, Hiroyuki Taniguchi, Hiromi Ichikawa, Junya Fukuoka. Nagasaki University Hospital, Nagasaki, Japan; Tosei General Hospital, Seto, Aichi, Japan.

Background: Idiopathic interstitial pneumonias (IIPs) and Connective tissue disease (CTD)-associated interstitial pneumonias (IPs) are the two most common types of IPs. IIPs and CTD-IPs share common histological features, yet the clinical managements are different. We prepared 2 different case cohorts, derivation and validation, semi-quantitatively evaluated several histological markers, and elicit a practical calculation formula based on statistical analysis, and applied the formula to the validation cohort to confirm the usability for daily cases.

Design: We selected 154 and 65 consecutive cases of CTD-IPs and IIPs, for derivation and validation cohorts, respectively. For derivation, 14 histological markers were evaluated by 2 observers and graded into score of 0 to 3. Stepwise Logistic regression analysis was used to select histological candidates to differentiated CTD-IPs and IIPs. The calculation formula to obtain the probability coefficient for IIPs was further determined. Another pathologist scored for 65 validation cases for selected histological candidates. The scores were applied for the formula and cases with probability coefficients were obtained. Clinical data and the probability was further compared.

Results: Among evaluated 14 scored histological findings along with ATS/ERS histological pattern, 8 markers were identified by regression test: smooth muscle hyperplasia(S), fibroblastic focus(F), cellular IP(C), fatty change(F), dense perivascular collagen(D), plasmacytic infiltration(P), lymphoid follicle with germinal center(L), airspace fibrin(A).

The formula to calculate the probability was:

$P(Y=IIP|\ Markers) = \exp(Z)/1+\exp(Z)$.

$Z=-1.65+0.81xS + 1.09xF - 2.47xA - 0.86xP + 0.86xD - 0.64xL + 0.85xC + 0.57xF$.

Case with P more than 0.5 was judged as P-idiopathic, and the rest as P-CTD. ROC curve for the derivation cohort using this formula was constructed and its AUC was 0.85. The probability divided 65 cases of validation cohort for 37 P-idiopathic and 28 P-CTD. The 65 cases were clinically 32 IIPs, 10 CTD-IPs, and 23 IIPs with autoantibodies. The agreements for IIPs and CTD-IPs were 30/32 (94%) and 8/10 (80%). 23 IIPs with autoantibodies composed of 18 P-CTD and 5 P-idiopathic cases.

Conclusions: We identified 8 histological markers and suggested the user-friendly formula to calculate the probability to separate CTD-IPs and IIPs. The high reproducibility of the formula was confirmed by the validation cohort.

1910 A Subset of Malignant Mesotheliomas in Young Adults Are Associated with Recurrent *EWSR1-ATF1* Fusions

Patrice Desmeules, Philippe Joubert, Hikmat Al-Ahmadie, Christopher DM Fletcher, Deborah Delair, Natasha Rekhtman, Marc Ladanyi, William Travis, Cristina R Antonescu. Memorial Sloan Kettering Cancer Center, New York, NY; Quebec Heart and Lung Institute, Quebec City, QC, Canada; Brigham and Women's Hospital, Boston, MA.

Background: Malignant mesothelioma (MM) is a rare, aggressive tumor often associated with asbestos exposure and characterized by complex genetic abnormalities, including deletions of chromosome 22. *EWSR1* gene fusion with *YY1* has been already reported in peritoneal MM of two patients over age of 60. However, the incidence of *EWSR1* rearrangement and the spectrum of its fusion partners remain unknown.

Design: We recently encountered two MM cases with *EWSR1-ATF1* fusions, and sought to investigate the prevalence and clinicopathologic features associated with this abnormality. As both cases occurred as intra-abdominal tumors of young adults and displayed epithelioid morphology, we searched our files for pleural and peritoneal MM occurring in adults younger than 40 years old, an age group estimated to represent only 2% of all MM. All cases were tested by FISH using custom BAC probes for *EWSR1, FUS* and *ATF1* genes. When available, immunohistochemistry for BAP1 was performed.

Results: The first index case occurred in the peritoneum of a 21 year old man, raising the differential diagnosis of desmoplastic round cell tumor and triggering *EWSR1* FISH. Based on FISH screening, both *EWSR1* and *ATF1* genes showed break-apart signals. The second index case was a tumor from a 33 year old woman. Targeted next-generation sequencing assay of 410 cancer genes revealed *EWSR1-ATF1* fusion as the sole abnormality. We then screened additional patients (total of 19) with MM from peritoneum (n = 9) and pleura (n = 10) in young patients (median 33 years; range 19-39). Males were predominant in peritoneal (89%) and females in pleural (70%) tumors. An additional case from pleura displaying *EWSR1-ATF1* fusions was identified, for a total of 3 cases (16%), all lacking asbestos exposure history. All positive cases displayed classic mesothelioma morphology, immunohistochemical expression of cytokeratins and WT1, and negativity for S-100. BAP-1 expression was retained in the two fusion-positive cases with available material for testing, and in 70% of the fusion-negative cases.

Conclusions: Our results expand the spectrum of tumor types harboring *EWSR1-ATF1* gene fusions to include a subgroup of conventional epithelioid MM. Features of this unique MM subset suggest young age at presentation, lack of asbestos exposure and retained BAP1 expression.

1911 Metastatic Lung Carcinoid Tumors: Evidence of Proliferation Rate Progression at Metastatic Sites

Patrice Desmeules, Joshua K Sabari, Maria Laureana Santos-Zabala, Anna M Litvak, Maria C Pietanza, John T Poirier, Charles M Rudin, David S Klimstra, William Travis, Natasha Rekhtman. Memorial Sloan Kettering Cancer Center, New York, NY.

Background: The criteria for the classification of lung carcinoid tumors were developed based on surgically-resected primary tumors. There is a paucity of data on the spectrum and evolution of proliferation rates of carcinoid tumors at metastatic sites, particularly in matched primary and metastatic samples.

Design: Seventy-five patients with stage IV lung carcinoids were identified. Patients had a total of 157 tissue samples (mean 2 samples per patient, range 1-5), of which 130 samples were available for re-review, including samples from metastatic/recurrent (n=97) and primary (n=33) sites. Manual mitotic count was performed on all non-cytology samples (n=112), and MIB1 proliferation marker was assessed on 106 samples. For samples with fewer than 10 high-power fields (HPF; 2 mm^2) of tumor volume (n=20), a derived mitotic score per 10 HPF was calculated based on the count in the available fields.

Results: Most common sites of metastasis included liver (38%), bone (11%) and brain (6%). Hot-spot MIB1 rate was on average higher in metastatic (17.5%) than primary (10.5%) sites; *P*=0.018. Similarly, mitotic rate tended to be on average higher in metastatic (7/10 HPF) than primary (4/10 HPF) sites; *P*=ns. Among metastatic samples, 15/81 (18%) exhibited mitotic rate of >10/10 HPF, and 22/79 (28%) exhibited MIB1 rate of >20%, with overall 36% of metastatic samples exceeding either of the above parameters. In matched primary/metastatic samples, 13/28 (46%) showed an increase in MIB1 rate (mean increase by 16%), and 19/33 (58%) showed an increase in mitotic count (mean increase by 9.7/10 HPF) at metastatic sites. Brain metastases showed significantly higher MIB1 (*P*=0.0007) and mitotic (*P*=0.004) rates than other metastatic sites.

Conclusions: Metastatic lung carcinoids frequently display proliferation rates that exceed the current criteria used to separate carcinoid tumors from small cell and large cell neuroendocrine carcinomas, which is most pronounced in brain metastases.We document the progression of proliferation rate in matched primary and metastatic samples in approximately half of the cases. These findings parallel the emerging data on elevated proliferation rates in some well-differentiated gastroenteropancreatic neuroendocrine tumors. Clinical behavior of this subgroup of tumors will need further investigation.

1912 Discordant PD-L1 Expression in Non-Small Cell Lung Carcinoma Tissue Microarray Cores Compared to Corresponding Whole Tissue Sections

Brandon Driver, Ross A Miller, Michael Deavers, Eric Bernicker, Philip T Cagle. Houston Methodist Hospital, Houston, TX.

Background: Accurate assessment of programmed death ligand-1 (PD-L1) expression is important as PD-L1 expression tends to correlate with response to immunotherapy. A recent study of PD-L1 expression assessed by immunohistochemistry with clone SP142 in non-small lung carcinoma (NSCLC) showed major discordances between surgically resected specimens and matched biopsies. The biopsy specimens always underestimated PD-L1 expression, and the discordance was usually due to lack of PD-L1 expression in tumor-infiltrating immune cells in matched biopsies. In this study we test the hypothesis that PD-L1 expression in a NSCLC cohort is discordant when comparing whole tissue sections to matched tissue microarray (TMA) cores.

Design: A total of 86 adenocarcinomas and 23 squamous cell carcinomas were included in the study. Tissue microarrays were constructed with triplicate cores from tumor blocks. Whole tissue sections were obtained of separate tumor blocks from identical cases used in TMA construction. PD-L1 immunohistochemistry was performed with the SP142 clone and scored according to percent of PD-L1-positive tumor cells (TC0 for <1%, TC1 for 1-4%, TC2 for 5-49%, and TC3 for ≥50%) and percent tumor area with PD-L1-positive tumor-infiltrating immune cells (IC0 for <1%, IC1 for 1-4%, IC2 for 5-9%, IC3 for ≥10%).

Results: PD-L1 expression was compared in TMA cores and corresponding whole tissue sections by TC score (TC0 vs TC1/2/3), IC score (IC0 vs IC1/2/3), and TC/IC subgroups (1% and 5% cutoffs). Analyses yielded a consistent pattern of agreement and discordance. Agreement ranged from 54% to 59%. In all analyses, the majority of discordant cases (18% to 34%) exhibited PD-L1 expression in whole tissue sections but not corresponding TMA cores, while a minority of discordant cases (7% to 17%) exhibited PD-L1 expression in TMA cores but not corresponding whole tissue sections. Kappa coefficients comparing PD-L1 expression in TMA cores to corresponding whole tissue sections ranged from -0.023 (95% CI -0.25 to 0.21) to 0.098 (95% CI -0.086 to 0.28) signifying poor agreement.

Conclusions: Although PD-L1 expression was underestimated in TMA cores more often, occasionally (7% to 17%) PD-L1 expression was underestimated in whole tissue sections. This result implies PD-L1 status is dependent on the tumor block chosen for testing, as the TMA cores and whole tissue sections were derived from different tumor blocks of identical cases. Further, this result suggests PD-L1 status could potentially be underestimated by any NSCLC specimen most likely owing to heterogeneity of the tumor.

1913 Correlation Between Programmed Death-1 (PD-1) Expression in Tumor Infiltrating Lymphocytes and Programmed Death Ligand-1 (PD-L1) Expression in Non-Small Cell Lung Carcinoma

Brandon Driver, Ross A Miller, Michael Deavers, David Tacha, Eric Bernicker, Philip T Cagle. Houston Methodist Hospital, Houston, TX; Biocare Medical LLC, Concord, CA.

Background: Programmed death-1 (PD-1) is a surface receptor expressed by activated T cells and mediates an inhibitory signal when engaged with its ligand, programmed death ligand-1 (PD-L1), on tumor cells. PD-1 expression in tumor-infiltrating lymphocytes (TIL) strongly correlated with tumor cell PD-L1 expression in melanoma brain metastases. Little is known about the relationship of TIL PD-1 expression and PD-L1 expression in non-small cell lung carcinoma (NSCLC). This study aims to test the hypothesis that PD-1 expression in TIL correlates with PD-L1 expression in tumor cells and/or TIL.

Design: A total of 124 adenocarcinomas and 37 squamous cell carcinomas were included in the study. Whole tissue sections were used. PD-1 immunohistochemistry (clone NAT105) was scored according to percent positive TIL (IHC0 for <1%, IHC1 for 1-4%, IHC2 for 5-9%, IHC3 for ≥10%). PD-L1 immunohistochemistry (clone SP142) was scored according to percent of PD-L1-positive tumor cells (TC0 for <1%, TC1 for 1-4%, TC2 for 5-49%, and TC3 for ≥50%) and percent tumor area with PD-L1-positive tumor-infiltrating immune cells (IC0 for <1%, IC1 for 1-4%, IC2 for 5-9%, IC3 for ≥10%).

Results: PD-1 expression in TIL was observed in 147 of 161 (91%) NSCLC cases and usually (42%) with the highest score. All 14 cases lacking PD-1 expression (IHC0) also lacked PD-L1 expression in tumor cells, although one case (7%) exhibited PD-L1 expression in tumor-infiltrating immune cells. The 68 cases with the highest PD-1 expression in TIL (IHC3) included 33 (49%) with PD-L1 scores of TC1/2/3, 32 (47%) with PD-L1 scores of IC1/2/3, and 44 (65%) with PD-L1 scores of either TC1/2/3 or IC1/2/3. Strong correlations were observed between PD-1 expression in TIL and PD-L1 expression in tumor cells (IHC0, IHC1, IHC2, IHC3 vs TC0, TC1, TC2/3; χ^2; $p = .014$), PD-L1 expression in tumor-infiltrating immune cells (IHC0, IHC1, IHC2, IHC3 vs IC0, IC1/2/3; χ^2; $p = .0025$), and PD-L1 expression in either tumor cells or tumor-infiltrating immune cells (IHC0, IHC1, IHC2, IHC3 vs TC0 and IC0, TC1/2/3 or IC1/2/3; χ^2; $p < .0001$).

Conclusions: PD-1 expression in TIL strongly correlated with PD-L1 expression in both tumor cells and tumor-infiltrating immune cells in NSCLC. If confirmed, our result may help explain the mechanisms of PD-1 and PD-L1 expression in NSCLC. Further, negative PD-1 expression may be useful to help predict negative PD-L1 status, especially since PD-L1 status may be underestimated on small biopsies.

1914 Molecular Injury and Repair Assessment in Ex Vivo Perfused Swine Lung Transplants

Peter Dromparis, Siegfried Wagner, Nader Aboelnazar, Sayed Himmat, Jessica GY Luc, Darren Freed, Jayan Nagendran, Michael Mengel, Benjamin Adam. University of Alberta, Edmonton, AB, Canada.

Background: Brain death, organ procurement and preservation cause acute lung injury (ALI). As a result, only about 20% of donated lungs are suitable for transplantation and a quarter of these develop primary dysfunction. With the recent development of ex vivo perfusion, previously inadequate donor lungs can now potentially be used for transplantation. However, mechanisms of ex vivo repair remain poorly understood. The aim of this large animal study is to define and validate a set of molecular markers for the quantification of ALI and monitoring of ex vivo repair.

Design: 41 samples were collected at different time points from swine lung donor organs in vivo (IV, n=4), after cold static preservation (CSP, n=13), and following ex vivo lung perfusion (EVLP, n=24). Functional parameters were recorded during EVLP. Samples were assessed by histology for features of ALI. RNA was isolated from

FFPE samples and 53 genes previously shown to be up-regulated in different models of ALI were quantified with the NanoString nCounter system. Data were analyzed with nSolver and R.

Results: Heat map analysis highlighted two subsets of genes separating EVLP from IV and CSP: 28 "repair" genes with relative up-regulation in EVLP and 9 "injury" genes with relative down-regulation in EVLP (Fig. 1). Expression of "repair genes" was inversely correlated with neutrophil infiltration by histology (r=-0.330, p=0.047) but showed a positive correlation with P/F-ratio (r=0.687, p=0.005) and compliance (r=0.738, p=0.002). Principal component analysis confirmed the association between "repair" gene expression and EVLP duration, with maximum values after 12 hours (Fig. 2).

Conclusions: We defined a gene set for quantification of ALI that can be used for molecular monitoring of tissue repair during EVLP and thus as a tool for tailoring ex vivo protocols in individual patients.

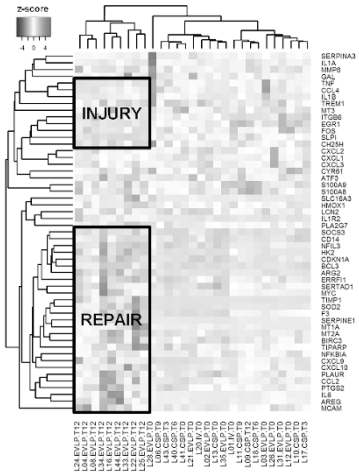

Fig. 1 Relative expression of 53 acute lung injury-related genes in peripheral swine lung samples (n=29). CSP, cold static preservation; EVLP, ex vivo lung perfusion; IV, in vivo.

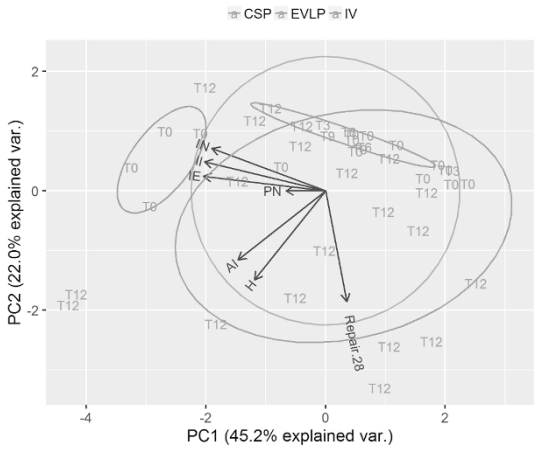

Fig. 2 Principal component analysis showing relationship between 28 "repair" genes and various histology, time, and preservation variables. AI, airspace inflammation; CSP, cold static preserv.; EVLP, ex vivo lung perfusion; H, hemorrhage; IE, interstitial edema; II, interstitial inflammation; IN, interstitial neutrophils; IV, in vivo; PC, principal component; PN, perivascular neutrophils.

1915 Primary Pulmonary Artery Sarcoma: A Single-Center Retrospective Case Series of 41 Patients

Zeljko Dvanajscak, Jennifer Katzenberg, Kim M Kerr, Eunhee S Yi, Grace Y Lin. UCSD, San Diego, CA; Mayo, Rochester, MN.

Background: Pulmonary artery sarcoma (PAS) is a rare, poorly differentiated mesenchymal tumor thought to arise from the pluripotent intimal cells of pulmonary arteries. Studies of PAS to date are limited and mostly include case reports and limited case series. We report the largest single center retrospective case series of PAS to date.

Design: Retrospective pathologic and clinical review of 41 cases, including an autopsy, of PAS were done. Routine histology and immunohistochemistry methods were employed for pathologic analysis. Kaplan-Meier estimates were computed to compare survival between treatment regimens.

Results: PAS is bilateral at presentation in 98% of cases. Histomorphology shows variable cellular density with spindled/stellate tumor cells within a myxoid stroma. 78% of cases were undifferentiated spindle cell tumors or pleomorphic undifferentiated sarcomas with a few cases with chondrosarcoma, osteosarcoma, angiosarcoma, liposarcoma, rhabdomyosarcoma, and inflammatory myofibrobastic tumor morphology. 44% showed ≥50% necrosis, while only 15% showed no necrosis. Mitotic activity was as follows: 62% had 0-9 mf/10 hpf, 19% had 10-19 mf/10 hpf, and 19% had ≥20 mf/10 hpf. Tumor grading was as follows: 69% were grade 3, 20% were grade 2, and 11% were grade 1. Of the cases that were immunostained, 100% were positive for vimentin, 71% were positive for smooth muscle actin, 43% were positive for desmin, 20% were positive for pankeratin, 8% were positive for S-100. None of the cases that were stained showed positivity for CD117, myogenin, CD34, CD31, or factor VIII related antigen. Pulmonary endarterectomy (PEA) resulted in statistically significant hemodynamic improvements. Post-PEA nuclear perfusion scans improved in 83% of cases. Peri-operative mortality was 9.7%. Median survival was 12 months following surgery, but increased to 19 months post-adjuvant therapy. One patient with tumor isolated to the left lung has been alive and tumor free for 15 years.

Conclusions: We report the largest, single center study of PAS to date. PAS typically presents as a bilateral, undifferentiated, high-grade malignancy. PAS is typically positive for vimentin and SMA, variably positive for pankeratins and desmin, and negative for endothelial markers, CD117 and myogenin. Histology and tumor grade were not associated with survival. PEA treatment is typically palliative, leading to improvement of hemodynamics and perfusion scans, but is rarely curative due to advanced stage of disease at diagnosis. Adjuvant therapy improves overall survival.

1916 CD44 Expression in Mucinous Adenocarcinomas of the Lung and the Potential for Targeted Therapy

Liz Edmund, Shaolei Lu, Li Juan Wang. Brown University, Providence, RI.

Background: Mucinous lung adenocarcinoma (MLA) is a unique variant of lung adenocarcinoma that is commonly associated with KRAS mutations. CD44 is required for activation of KRAS mediated signaling and tumor proliferation. As cancer stem cell markers, CD44 and CD166 have recently emerged as important factors in the regulation of tumor microenviroment, promoting cell proliferation, adhesion and invasion. Expression of CD44 and its isoforms has been found to be of prognostic significance in multiple tumors including squamous cell carcinoma (SCC) of the lung and colorectal adenocarcinoma, and may have clinical applications as a therapeutic target. The role of CD44 in promoting KRAS-dependent lung adenocarcinoma has been reported in animal models. However CD44/CD166 expression has not been investigated in mucinous adenocarcinoma of the lung.

Design: Tissue microarrays were created for 80 randomly selected cases of MLA at our institution from 1995 to 2015, 33 diagnosed at pT1, 31 at pT2, 8 at pT3 and 4 at pT4. Lymph node metastases were present in 16 cases. IHC was performed using CD44, CD44v6, stromal CD44, and CD166. Moderate staining in at least 10% of cells was considered to be positive. CD44 expression, specifically isoform v6, was correlated with pathologic stage at diagnosis, lymph node metastasis, and KRAS mutation status.

Results: CD44 was positive in 37 of 80 MLAs (46%), 57 of 80 cases were positive for CD44v6 (71%)and CD44 stromal was postive in 66 cases (82.5%). Sixty four cases were CD166 positive (80%). KRAS positive cases all harbored mutations in codon 12. Analysis of the results using Fisher's two tailed test showed no association between CD44v6 expression and lymph node metastasis (p=0.76), nor CD44v6 with advanced pathologic stage at diagnosis (p=0.67). Tumors with mutated and wild type KRAS both showed comparable expression of CD44 proteins. There was also no correlation between CD44 and CD166 expression (p=0.7), nor association with CD166 and clinical behaviour of the tumors or KRAS mutation status.

Conclusions: Unlike previous studies in SCC of the lung and colorectal tumors, where CD44v6 expression portended an unfavourable clinical outcome, no association was established in mucinous lung adenocarcinomas in our study. The findings support previous studies which demonstrated that KRAS mutations in mucinous lung adenocarcinoms are not associated with poor prognosis. However, since over 71% of the mucinous lung tumors in this study were positive for CD44v6 , this may represent a great potential therapeutic target for treatment of these tumors.

1917 The Role of SATB2 and TCTE3 as Diagnostic Markers for CDX-2 Positive/TTF-1 Negative Primary Mucinous Adenocarcinomas of the Lung

Liz Edmund, Shaolei Lu, Madhu Ouseph, Kara A Lombardo, Dongfang Yang, Maria L Garcia-Moliner, Bassam Aswad, Li Juan Wang. Brown University, Providence, RI.

Background: Primary mucinous lung adenocarcinomas (PMALs), particularly those with enteric differentiation, often have immunophenotypic features in common with metastatic mucinous colorectal adenocarcinomas (MMACs), including CK20 and CDX2 expression. In the absence of TTF-1 immunoreactivity, accurate diagnosis can be challenging. Here we explore the utility of Special AT-rich sequence binding protein 2 (SATB2) and cadherin 17, which are newly recognised colorectal tumor markers, and t-complex-associated-testis-expressed 3 (TCTE3), in aiding to solve the diagnostic dilemma.

Design: Eighty primary mucinous lung adenocarcinomas, 36 metastatic mucinous colorectal carcinomas and 42 primary mucinous colonic adenocarcinomas (PMACs) were randomly selected at our institution from 1995 to 2015. Analysis of the expression of CK7, CK20, CDX2, TTF-1, cadherin 17, TCTE3 and SATB2 using tissue microarray was performed for each group. Moderate staining in 10% of cells was considered as positive. The PMACs were used as the control group.

Results:

Markers	Primary mucinous lung adenocarcinoma, n=80 (%)*	Metastatic colon tumors, n=36, (%)	Primary mucinous colonic carcinomas, n=42 (%)	p value
CK7	80 (100)	0 (0)	0 (0)	<0.0001
CK20	19 (23.5)	23 (63.9)	32 (76.1)	<0.0001
CDX-2	10 (12.5)	36 (100)	38 (90.5)	<0.0001
Cadherin	22 (27.5)	36 (100)	36 (85.7)	<0.0001
TCTE3	68 (84)	0 (0)	0 (0)	<0.0001
SATB2	0 (0)	25 (69.4)	34 (81.7)	<0.0001

TTF-1 was positive in 40 of 80 PMALs (50%). Analysis of CK7 and CDX2 showed that 90% of PMALs were CK7+/CDX2-, with PPV and NPV of 100% and 81% respectively (p<0.0001). The PPV of CK7-/CDX2+ for MMACs was 100% with a NPV of 99% (p<0.0001). However, 12.5% of PMALs were positive for both markers, 50% of which were TTF-1 negative. Analysis of SATB2 and TCTE3 identified 85% of TCTE3+/SATB2- PMALs with PPV of 100% and NPV of 75% (p<0.0001), and 70% of TCTE3-/SATB2+ MMACs with PPV of 100% and NPV of 99% (p<0.001).
Conclusions: In this study all primary mucinous lung adenocarcinomas were negative for SATB2 and both primary and metastatic mucinous colorectal adenocarcinomas were all negative for TCTE3. Although less sensitive for tumors of colorectal origin than CDX2, SATB2 has a higher specificity. In combination with TCTE3, it may be helpful in differentiating CDX2+/TTF-1- primary mucinous lung tumors from metastatic colonic adenocarcinoma to lung.

1918 "A Study of Random versus Directed Lymph Node Biopsies in Lung Cancer Staging"

Siba El Hussein, Roy Williams, John Alexis. Mount SInai Medical Center, Miami Beach, FL.
Background: Lymph node dissection for lung carcinoma is a subject lacking consensus,and no specific recommendations for the number of lymph nodes required for staging have been proposed by the Society of Thoracic Surgeons.There is a recent trend amongst thoracic surgeons to remove more than 10 lymph nodes during lung carcinoma surgery, the rationale being to detect occult nodal metastasis.The goal of this study was to determine whether examining more than 10 lymph nodes improves the chances of finding metastases,leading to upstaging and potential changes in treatment.
Design: 244 surgical resections of carcinoma performed at Mount Sinai Medical Center between March 2013 and March 2016 were included.The cases were divided into two groups.The first group consisted of cases with more than 10 lymph nodes dissected by the surgeon,or found during gross or microscopic examination of the specimen (122 cases). The second group consisted of cases with fewer than 10 lymph nodes dissected by the surgeon, or found during gross or microscopic examination of the specimen (122 cases).
Results: In the first group,21 cases harbored nodal metastatic disease (17.2%),17 (80.9 %)of the positive cases had positive sentinel nodes (stations #10, 11, 12) included among positive lymph nodes, or as the only positive lymph node.In the second group,23 harbored metastatic disease (18.9%),14 (60.9%) of the positive cases had positive sentinel nodes included among positive lymph nodes, or as the only positive lymph node.In 17 out of the 44 positive cases (38.6%),positive sentinel nodes were detected by the pathologist post-operatively,during grossing of the specimen.
Conclusions: Increasing the number of lymph nodes dissected from less than 10 to 10 or more did not increase the yield of nodal metastases.31 out of 44 positive cases (70.5%) had positive sentinel node(s).In cases with positive "non-sentinel" nodes,the sentinel nodes had been either partially sampled or not sampled at all,precluding determination of the patient's sentinel lymph node status.Targeting sentinel lymph nodes first and thorough examination of the specimens post-operatively,may increase the chances of detection of metastatic disease.During surgery,if the sentinel nodes are positive,mediastinal lymph node dissection is warranted.If the sentinel nodes are negative,mediastinal lymph node dissection may not be necessary,preventing sampling of numerous lymph nodes,and protecting patients from well-known complications of mediastinal lymph node dissection.

1919 The Role of Serum Amyloid A Staining of Granulomatous Tissues for the Diagnosis of Sarcoidosis

Tony El Jabbour, Albert Huho, Llewellyn Foulke, Timothy Jennings, Efstratios Koutroumpakis, Siddhartha Dalvi, Haroon Chaudhry, Amit Chopra, Aakash Modi, Neha Rane, David J Prezant, Christine E Sheehan, Recai Yucel, Mehul Patel, Marc Judson. Albany Med Col, Albany, NY; Univercity of NM, Albuquerque, NM; Albert Einstein Col of Med, New York, NY; Fire Department of NYC, New York, NY; SUNY, Albany, NY.
Background: Previous studies demonstrated that SAA staining of sarcoidosis granulomas was qualitatively and quantitatively different from that of all other granulomatous diseases. These data suggest that positive SAA staining of granulomatous tissue may be specific enough to be used as a diagnostic test for sarcoidosis. This study was designed to determine the specificity of SAA staining for the diagnosis of sarcoidosis relative to other granulomatous disorders.
Design: Pathological specimens that demonstrated granulomatous inflammation were retrospectively identified at one institution over a 10-year period. Specimens were included in this analysis only if the associated patient had a specific diagnosis related to the granulomatous inflammation confirmed through medical record review. We also obtained 4 histological specimens from New York City firefighters with biopsy-confirmed World Trade Center "sarcoidosis-like" pulmonary disease. SAA staining was performed using previously developed methods that were modified to increase the specificity of the stain for the diagnosis of sarcoidosis at the potential expense of lowering the sensitivity. This was gauged by repeatedly staining 10 known sarcoidosis specimens and 10 known granulomatous specimens with a specific diagnosis other than sarcoidosis. After the SAA stain technique was modified, two pathologists, blinded to each other and the diagnoses, determined if the stained material was SAA positive or negative. Discordant results were adjudicated by the two pathologists.
Results: 106 histology specimens were analyzed from 100 patients, with 36 biopsies (34%) from sarcoidosis tissues and 70 (66%) from other granulomatous disorders. The Cohen Kappa correlations between the two pathologists for SAA staining positivity were excellent (0.85, 0.73- 0.98). The overall specificity of SAA staining for the diagnosis of sarcoidosis was 84% (59/70). The sensitivity was 44% (16/36). The pathologists independently agreed on the SAA staining results of 93/106 (88%), and the specificity of these specimens was 92% (55/60).
Conclusions: We have demonstrated that although SAA staining of various granulomatous tissues is fairly specific for the diagnosis of sarcoidosis, the specificity is inadequate for SAA staining to be used as a diagnostic test for sarcoidosis in isolation. These data suggest that SAA production may not be a universal mechanism in the development of sarcoidosis.

1920 Profiling of Tumor Mutational Burden and PD1/PDL1 Immunohistochemistry (IHC) in Non-Small Cell Lung Cancer

Julia A Elvin, Michael E Goldberg, Laurie M Gay, James Suh, Jo-Anne Vergilio, Shakti H Ramkissoon, Siraj M Ali, Alexa Schrock, David Fabrizio, Garrett Frampton, Vincent Miller, Philip Stephens, Jeffrey Ross. Foundation Medicine, Inc., Cambridge, MA; Albany Medical College, Albany, NY.
Background: IHC for PD1 and/or PD-L1 expression is used to identify patients potentially suitable for treatment with immune checkpoint inhibitors (ICPi). High tumor mutational burden (TMB) is an additional biomarker that strongly associates with response to immunotherapy. We analyzed 616 clinical NSCLC tumors using comprehensive genomic profiling and PD1 and PDL1 IHC to identify patients who may benefit from ICPi treatment.
Design: DNA (≥50ng) was extracted from 15,096 NSCLC (adenocarcinoma, NOS, or SCC) and CGP was performed (mean coverage depth >550X) for up to 315 cancer-related genes plus select introns from 28 genes commonly rearranged in cancer. TMB was calculated over 1.1 Mb by counting somatic, non-driver GA and scored high (TMB-H, ³20 mut/Mb) or low (TMB-L, <20 mut/Mb). For 616 tumors, PD1 and/or PDL1 expression were measured by IHC and scored in tumor infiltrating lymphocytes (TIL) and tumor cells (t) for distribution (0, 1-24%, >24% of cells) and intensity (0, 1+, 2+) as negative (Neg), low positive (LP) or high positive (HP).
Results: Of 616 NSCLC, 88 (14.3%) were TMB-H. TMB score did not significantly associate with PD1 status (HP or Neg), although a trend toward TMB-H in PD1 HP exists. TMB-H was more common in PD-L1 HP tumors (p<0.01), but was also observed in 13.2% of PD-L1 Neg samples and 10% (7/70) of PD-L1 Neg/PD1 Neg samples. *CD274* amplification was observed in 4/616 (0.6%) samples and demonstrated variable tPDL1 tumor staining (3 LP, 1 HP). Changes in alteration frequencies were noted in IHC-defined subgroups for *BRAF, EGFR, STK11, RICTOR,* and *ERBB2*, compared to all NSCLC, and additional genomic analyses will be presented. *MET* alterations (amp, 8.8%, or exon 14 splice site, 5%) were more common in TMB-L/PD-L1 HP samples, compared with other TMB-L samples (PD-L1 LP or Neg) (p<0.001).

	PD1 Lymphocyte Compartment			PD-L1 Tumor Compartment		
	Neg (n=97)	LP (n=137)	HP (n=59)	Neg (n=291)	LP (n=172)	HP (n=104)
TMB Low (n=528)	87	126	48	257	144	80
TMB High (n=88)	10	11	11	34	28	24

Conclusions: 616 NSCLC were stratified by TMB and PD1 and/or tPDL1 expression. TMB score did not associate with PD1 expression in TIL, but TMB-H is more common in tPD-L1 HP tumors. CGP of TMB-L/PD-L1 HP samples reveals that a significant fraction harbor *MET* alterations. As PD1, tPDL1, and TMB identified non-overlapping patient subsets, immunotherapy response data will be needed to validate the relative predictive efficacy of each biomarker.

1921 Nodular Fibrinous Organizing Pneumonia with Atypical Septal Lymphocytes: An Under-Recognized Presentation of Lymphoma

Arash Eslami, Kirk Jones. University of California - San Francisco, San Francisco, CA.
Background: Acute fibrinous organizing pneumonia is a pattern of lung injury presenting idiopathically or most commonly in association with autoimmune disease, environmental and occupational exposure, or infection (Beasley et al, 2002). We describe three cases of nodular fibrinous organizing pneumonia with atypical septal lymphocytes which were ultimately diagnosed as lymphoma.
Design: A retrospective search of internal and consult cases from January 2000 through June 2016 was performed to identify cases of fibrinous organizing pneumonia and lymphoma. Review of clinical data was performed for referral diagnosis and ancillary testing. Cases were evaluated with standard histology and supplemental immunohistochemical stains.
Results: Three cases were identified that showed a nodular pattern of alveolar filling by polypoid plugs of fibrin with sparse inflammation. The septa were thickened in the nodular regions by scattered large atypical lymphocytes and occasional eosinophils. Immunohistochemical staining along with bone marrow biopsy, T-cell receptor gamma gene rearrangement PCR, and B-cell receptor IGH gene rearrangement PCR revealed two cases of peripheral T-cell lymphoma and one case of diffuse large B-cell lymphoma. A definitive referring diagnosis had not been made in two of the cases although infection was favored in both. In the final case, a referring diagnosis of an inhalational type hypersensitivity pneumonia overlap with eosinophilic pneumonia had been proposed.
Conclusions: Lymphoma typically presents in the lung as a densely cellular nodule of monotonous or atypical lymphocytes, often with peripheral lymphangitic extension. Fibrinous organizing pneumonia is seen as a pattern of acute lung injury with alveolar consolidation by plugs of fibrin, and has not been commonly associated with lymphoma. We identified an unusual primary presentation of lymphoma as nodular fibrinous organizing pneumonia with atypical alveolar septal lymphocytes. This pattern of inflammation and lung injury is a close mimic of infectious and immunologic reactions and a potential cause for misdiagnosis. Recognition of this unusual pathologic pattern with subsequent immunohistochemical and clonality studies allows for accurate diagnosis.

1922 Correlation Between *MET* Gene Copy Number and Molecular Profiling in Non-Small Cell Lung Cancer

Lianghua Fang, Hui Chen, L Jeffrey Medeiros, Shimin Hu, Lin Pei, Raja Luthra, Rajesh R Singh, Mark J Routbort, David Hong, Xinyan Lu. The University of Texas MD Anderson Cancer Center, Houston, TX; Jiangsu Province Hospital of Traditional Chinese Medicine, Nanjing, Jiangsu, China; Feinberg School of Medicine Northwestern University, Chicago, IL.

Background: *MET* is a receptor tyrosine kinase encoded by the *MET* proto-oncogene. *MET* amplification (*MET*amp) can promote cell proliferation, survival and metastases and is a therapeutic target for non-small cell lung cancers (NSCLC). However, many clinical trials used fluorescence *in situ* hybridization (FISH) to assess *MET*amp have been unsuccessful, suggesting that other concurrent gene abnormalities may be involved that promote NSCLC despite MET inhibitors.

Design: FISH for *MET* copy number was evaluated in 416 patients. Mutational analysis using hotspot cancer gene panels by next Generation Sequencing or orthogonal sequencing were performed in 408 patients.

Results: Thirty three (7.9%) tumors showed *MET*amp, 17 (4.1%) had *MET* copy number gain (*MET*cng), and 366 (88%) were *MET* negative (*MET*neg). A total of 387 cases (94.9%) showed at least one or more mutations in 27 genes. Hotspot mutations were detected in 242 of 358 (67.6%) *MET*neg tumors, 13 of 17 (76.5%) *MET*cng tumors, and 27 of 33 (81.8%) *MET*amp tumors (P =. 02). The most common mutations were in *TP53* followed by *KRAS* and *EGFR*. *TP53* mutation was detected in 135 of 385 (35.1%) tumors, with a frequency of 36.8%, 47.1% and 37.5% in the *MET*neg, *MET*cng and *MET*amp groups, respectively. *KRAS* mutation was found in 93/405 (23%) tumors. *EGFR* mutation was observed in 86/402 (21.4%) tumors: 18.8% in *MET*neg, 35.3% in *MET*cng, and 42.4% in *MET*amp tumors. *MET*amp was associated with *EGFR* mutation (P = .001). Twenty seven of 33 (81.8%) patients with *MET*amp tumors had concomitant mutations involving 8 genes. Median overall survival was 21.8 *vs*. 65.75 *vs*. 36. 5 months in patients with *MET*amp, *MET*cng and *MET*neg tumors, respectively (P = .0005). Patients with tumors that were *MET*amp and had co-mutations in other genes had a worse outcome than those with *MET*amp only tumors (35.9 *vs*. 17.6 months, P = .047).

Conclusions: *MET*amp in NSCLC is associated with a high frequency of additional gene mutations. Patients have *MET*amp and co-mutations showed a worse outcome. These patients might not benefit from MET inhibitor alone, and might require additional therapies that target multiple genes.

1923 FISH Analysis of Crizotinib Target Genes MET/ALK/ROS-1 in Malignant Mesothelioma

Franco Fedeli, Sandra Salvi, Simona Boccardo, Serena Varesano, Paolo Dessanti, Alessandro Valentino, Paola Ferro, Pier Aldo Canessa, Jean Louis Ravetti, Maria Pia Pistillo, Silvio Roncella. Azienda Sanitaria Locale n° 5 Spezzino, La Spezia, Italy; IRCCS AOU San Martino-IST, Genova, Italy.

Background: Malignant mesothelioma (MM) is a particularly aggressive tumour with limited possibility of treatment. New therapeutic hopes may arise from the receptor tyrosine kinases-based targeted therapies that significantly progressed in many cancers. Crizotinib is a small-molecule tyrosine kinase inhibitor with high antitumor activity against amplified *MMNG HOS Transforming proto-oncogene* (*MET*), rearranged *Anaplastic lymphoma kinase proto-oncogene* (*ALK*) and rearranged *ROS proto-oncogene-1* (*ROS-1*) thus showing broad potential activity and could be used to treat MM.

In this study, we evaluated *MET, ALK* and *ROS-1* status, by fluorescence in situ hybridization (FISH), in order to select MM patients who might benefit from treatment with crizotinib.

Design: We analyzed 106 MM (male: 66%, median age: 64, age range: 5-85), including 60 epithelioid, 34 sarcomatoid, 12 biphasic. Seventy nine MM were from a tissue microarray (MS801 29 cases and MS1001 50 cases) (US Biomax Inc, Rockville, MD, USA), 16 MM were from the Unit of Pathology, IRCCS AOU San Martino-IST (Genova, Italy) and 11 MM were from the Unit of Histopathology, ASL n°5 (La Spezia, Italy). The study protocol was approved by the Liguria Regional Ethics Committee and all patients were enrolled in the study after written informed consensus was given. *MET* gene positivity was investigated by FISH, according to the University Colorado Cancer Center-scored system (amplification if *MET*/*CEP7* ratio≥2 or at least 15 copies of *MET* signals in ≥10% of the tumour cells; high polysomy if *MET* mean≥4 copies/cells in ≥40% of tumour cells) using *MET/CEP7* probe cocktail (Vysis MET Spectrum Red FISH Probe Kit reagent/Vysis CEP 7 (D7Z1) (Abbott Molecular, Des Plaines, IL USA). *ROS-1* gene rearrangement was investigated by FISH using Spectrum Green Probe, Vysis 6q22 ROS1 Break Apart FISH Probe (Abbott). *ALK* gene rearrangement was investigated by FISH using Vysis LSI ALK Dual-Color Break Apart Rearrangement Probe (Abbott).

Results: All 106 (100%) MM were negative for *ALK* or *ROS-1* gene rearrangement. In contrast, we found 8/106 (7.6%) FISH-positive cases, of which two (1.9%) epithelioid MM showed *MET* gene amplification (*MET*/*CEP7* ratio=4, *MET*/*CEP7* ratio=6) and six (5.7%) MM (4 epithelioid, 1 sarcomatoid, 1 biphasic) showed high polysomy of *MET* gene in a range of 6-10 spots of *MET* gene in about 60-80% of tumour cells.

Conclusions: The results indicate that, for treatment of MM with crizotinib, *MET* is the only one candidate target gene and, consequently, only *MET* should be evaluated by FISH.

1924 Hybrid-Capture Based Comprehensive Genomic Profiling of Lung Adenocarcinoma Identifies Patients Who May Benefit from Targeted Therapies as Well as Immunotherapies Using Tumor Mutational Burden (TMB), a New Predictive Biomarker of Response to Immune Checkpoint Inhibitors

Garrett Frampton, Anika Gupta, Caitlin Connelly, David Fabrizio, Alexa Schrock, Laurie M Gay, Shakti Ramkissoon, Julia A Elvin, Jo-Anne Vergilio, Siraj M Ali, Vincent Miller, Philip Stephens, Jeffrey Ross, James Suh. Foundation Medicine, Inc., Cambridge, MA.

Background: The development of multiple immunotherapies for non-small cell lung cancer (NSCLC) within the past two years has created a need for predictive biomarkers of response. Currently, PD-L1 IHC for pembrolizumab is the only FDA-approved companion diagnostic. Tumor mutational burden (TMB) has emerged recently as a potential biomarker in this context. Comprehensive genomic profiling (CGP) is a hybrid capture-based next-generation sequencing (NGS) test that may help oncologists optimize targeted therapy and immunotherapy regimens for advanced stage lung adenocarcinoma patients.

Design: DNA was extracted from 40 microns of FFPE sections from 10908 consecutive cases of lung adenocarcinoma (2013-16). CGP of up to 315 cancer-related genes was performed using a hybrid-capture, adaptor ligation based NGS assay. TMB was calculated over 1.1 megabase (Mb) as the number of somatic, coding point mutations and indels per Mb of genome (low: <6; intermediate: 6-19; high: ≥20 mutations/Mb). Genomic alterations (GA: point mutations, small indels, copy number changes and rearrangements) involving *EGFR*, *ALK*, *BRAF*, *ERBB2*, *MET*, *ROS1*, *RET* and *KRAS* were recorded for each case.

Results: The median age was 65 years (range 13 to >90) and 56% were female. In this series, TMB was low in 4245 (39%), intermediate in 5258 (48%) and high in 1405 (13%) patients. Overall, the proportion of patients with at least one GA involving *EGFR* (20%), *ALK* (4.4%), *BRAF* (5.9%), *ERBB2* (5.7%), *MET* (5.4%), *ROS1* (1.5%), *RET* (2.0%) or *KRAS* (35%) was within the ranges of other Western lung adenocarcinoma cohorts. Samples with high TMB were significantly less likely to harbor GA involving *EGFR* (5.3 vs. 31%), *ALK* (1.1 vs. 8.9%), *ROS1* (0.6 vs. 2.3%) and *RET* (0.9 vs. 3.4%) than those with low TMB (all four p-values < 0.0001). Interestingly, 90% of patients with high TMB harbored a GA involving *TP53*.

Conclusions: Immunotherapies for NSCLC have brought tremendous excitement as well as confusion regarding the optimal selection of biomarker tests and medications for advanced stage lung adenocarcinoma patients. Without additional time, tissue or cost, CGP offers the potential to efficiently, rapidly and accurately identify patients with high TMB who may benefit from immunotherapies as well as GA involving all seven oncogenes listed within the National Comprehensive Cancer Network (NCCN) guidelines.

1925 Comprehensive Assessment of PD-L1 Staining Heterogeneity and Expression by Histologic Pattern in Pulmonary Adenocarcinomas: Clinical Implications

Andréanne Gagné, William Enlow, Marc-Antoine Pigeon, Michèle Orain, Stéphane Turcotte, Philippe Joubert. Laval University, Quebec City, QC, Canada; Quebec Lung and Heart University Institute, Quebec City, QC, Canada; CHU de Québec, Quebec City, QC, Canada.

Background: Molecules directed against Programmed cell death-1 (PD-1) have brought new hopes for the management of patients diagnosed with advanced non-small cell lung carcinomas. In pulmonary adenocarcinomas (AC), the efficacy of the treatment is closely associated with the levels of expression of PD ligand-1 (PD-L1) on tumor cells, as assessed by immunohistochemistry (IHC). For the vast majority of patients, this evaluation is made on small biopsies that do not allow an optimal assessment of the entire tumor. The current literature suggests that staining of PD-L1 varies in different zones of the same tumor. However, the extent of this heterogeneity has never been quantified, nor the association between PD-L1 expression and the histologic patterns of AC within the same tumor.

Design: A cohort of 226 patients that underwent pulmonary resection for lung cancer in our centre was selected. Tissue microarrays were constructed with five 1 mm cores representative of all histologic patterns found in each tumour and stained for PD-L1 (E1L3N, Cell Signalling Technology, Cambridge, UK). For each core, the histologic tumoral pattern and the percentage of tumor cells positive for PD-L1 were noted. Descriptive statistics were used to show clinical data, to quantify heterogeneity of the stain and to show the link between PD-L1 and histologic pattern. Staining heterogeneity was defined as cases with discordant results (positive versus negative) in at least 2 cores.

Results: 86 patients (38.2%) were positive for PD-L1 (≥50% of stained cells in at least one core). Among all patients, 22.0% showed staining heterogeneity. Within patients negative in at least one core, 26.2% were positive in one of the other cores and could have been considered as false negatives. Mean staining of PD-L1 was more important and homogenous in solid (47.2%) and micropapillary (24.9%) patterns and lower with acinar (15.9%), papillary (1.1%) and lepidic (7.2%) architectures.

Conclusions: Our study shows that a significant proportion of patients diagnosed with AC presents a heterogeneous pattern of PD-L1 staining. More than 25% of patients negative on one core proved to be positive in another core. This raises the consideration of rebiopsy in patients with initial negative PD-L1, in particular with patients showing a solid lesion on the chest CT-scan and a lepidic, acinar or papillary pattern on the biopsy.

1926 SMARCA4 Loss in Lung Cancer Is Associated with Distinct Clinicopathologic Features

Carolyn H Glass, Amanda J Redig, Yin P Hung, Christopher French, Lynette M Sholl. Brigham and Women's Hospital, Boston, MA; Dana-Farber Cancer Institute, Boston, MA.

Background: *SMARCA4* is a tumor suppressor gene that encodes a catalytic subunit of the SWI/SNF complex. Loss of *SMARCA4* gene expression portends a poor prognosis in lung cancer. However, patients with SMARCA4-deficient lung cancers may benefit from specific cytotoxic therapies or targeted EZH2 inhibitors (Fillmore, Nature 2015). SMARCA4-deficient thoracic sarcomas of the mediastinum have recently been identified as a potentially distinct clinicopathologic entity (LeLoarer, Nature Genet. 2015). We hypothesized that SMARCA4-deficient lung tumors represent a distinct subset of lung carcinomas.

Design: We reviewed an institutional cohort of 1876 lung cancers sampled between 2009-16 (1473 lung adenocarcinoma [LUAD], 239 lung squamous cell carcinomas [LUSC], 73 small cell carcinomas [SCLC], 2 lung adenosquamous carcinomas [LUAS] and 89 other) that previously underwent next generation sequencing (NGS) of 309 cancer-associated genes, for *SMARCA4* variants. Nonsense, frameshift, and splice site variants were defined as loss of function (LOF). SMARCA4 immunohistochemistry (IHC) was performed to confirm loss of expression and to screen an additional cohort of lung cancer biopsies from 2002-10 without NGS data.

Results: *SMARCA4* mutations were detected in 164 (8.7%) lung tumors, predominantly LUAD (n=135) including 54 (2.8%) LOF variants, also predominantly LUAD (n=42). Tumor tissue was available for SMARCA4 IHC in 29 cases, of which 13 showed total loss of expression. Among these 13 cases with SMARCA4 loss by IHC and NGS, 7 had concomitant oncogenic driver alterations in *KRAS*, *HRAS* or *ERBB2* and included LUAD (n=8), LUAS (n=3), and poorly differentiated non-small cell carcinoma (n=2). SMARCA4 loss was more common in men (9/13) and smokers (12/12), and associated with high rates of metastatic disease at diagnosis (11/13). SMARCA4 loss was also highly correlated with LOF (12/12), but not missense (1/17) variants ($p<0.001$). *SMARCA4* wild type lung cancers (n=23) were stained as a control group; all showed intact expression. IHC screening of an additional 127 lung cancers identified 4 (3.1%) with SMARCA4 loss in 2 LUSC, 1 LUAD and 1 LUAS. Two of these cases showed *SMARCA4* LOF variants by NGS.

Conclusions: SMARCA4 loss occurs in ~3% of lung carcinomas and coexists with oncogene mutations in some cases. LOF genomic variants and protein loss are highly correlated. Notably, 3/13 SMARCA4-deficient cases had adenosquamous histology. SMARCA4 loss appears to be associated with aggressive tumor behavior in smokers and may serve as potential prognostic and predictive factors.

1927 Concordance of PD-L1 Expression Between Core Biopsy and Resection Specimens of Non-Small Cell Lung Cancer

Jacob Grange, Edward B Stelow. University of Virginia School of Medicine, Charlottesville, VA.

Background: Programmed death ligand 1 (PD-L1) inhibitors, such as pembrolizumab, have demonstrated efficacy in treatment of non-small cell lung carcinomas (NSCLCs). Immunohistochemical detection of PD-L1 expression in ≥50% of tumor cells predicts response to pembrolizumab. Among the many challenges with this assay is the recognized heterogeneity of tumoral PD-L1 expression. Given this heterogeneity, it has not been determined what method of tissue sampling is necessary for an accurate result. Ideally, this assay could be performed on core needle biopsies which are commonly employed in initial diagnosis of NSCLCs. However, it is not known if the sampling performed on core needle biopsies is sufficient to predict the expression of PD-L1 within the tumor as a whole.

Design: We retrospectively compared tumoral expression of PD-L1 in lung core needle biopsies to subsequent resection specimens. Of 28 tumors analyzed, 15 were adenocarcinomas and 13 were squamous cell carcinomas. We employed the anti-PD-L1 antibody clone 22C3 (Dako). Scoring of membranous staining was categorized as 0%, 1-49%, and ≥50% of tumor cells, with ≥50% staining considered positive.

Results: Positive tumoral PD-L1 expression was detected in 5/28 (17.9%) of core biopsy specimens and 4/28 (14.3%) of resection specimens. Core biopsy and resection results were concordant in 96.4% of cases (κ 0.87; 95% CI 0.61-1.00). A single discordant result occurred in a lung adenocarcinoma with positive staining (50%) on the core biopsy, and negative staining (5%) on the resection specimen. The data are summarized in Table 1.

Table: Tumoral PD-L1 expression on core biopsy vs. resection specimens

		Core Biopsy Specimens		
		Negative	Positive	Total
Resection Specimens	Negative	23	1	24
	Positive	0	4	4
	Total	23	5	28

Conclusions: Despite tumor heterogeneity, detection of tumoral PD-L1 expression in NSCLC appears to be largely concordant between lung core biopsy and resection specimens. These findings suggest that core biopsy may be adequate for determining PD-L1 expression in NSCLC.

1928 PD-L1 Expression in Non-Small Cell Lung Carcinoma (NSCLC): Feasibility of Cytology and Its Comparison with Resection and Small Biopsies

Jonas J Heymann, Carlos Pagan, John Crapanzano, Ladan Fazlollahi, Mehrvash Haghighi, William Bulman, Mark Stoopler, Joshua Sonett, Adrian Sacher, Catherine Shu, Naiyer Rizvi, Anjali Saqi. Columbia University Medical Center, New York, NY.

Background: There are several FDA-approved immunotherapy (ITx) agents for NSCLC. Pembrolizumab, which targets programmed cell death-1 (PD-L1), has an immunohistochemistry (IHC)-based companion assay with positivity defined as staining in ≥50% of tumor cells. Eligibility for some ITx/clinical trials requires IHC. IHC is typically performed on histology (HY) specimens, but cytology (CY) aspirates and/or effusions may represent the only specimen. This feasibility study sought to determine if CY provides adequate tissue and how it compares to resection (RE) and other small biopsy (SB) specimens for PD-L1 IHC testing.

Design: All NSCLC were reflexively submitted for PD-L1 IHC testing (22C3 pharmDx). IHC on CY was performed on cell blocks. To render an interpretation, ≥100 viable tumor cells are required; cells with complete or partial ≥1+ membrane staining were quantified. IHC was compared among CY, SB and RE.

Results: NSCLC specimens (200) were collected from 183 patients (76 men, 107 women; median age 72, range 44-93). They comprised lung (129), regional lymph nodes (17), pleura/pericardium (15), distant metastases (28), and other sites (11) and included resections (83), CY (37, including 20 endobronchial ultrasound aspirates and 12 effusions), and other SB (80). Diagnoses included adenocarcinoma (ADC, 132), squamous cell carcinoma (SQ, 31), and other carcinoma (20).

Specimen type (n)	Adequate (%)	PD-L1 Positive (%)	Diagnosis (ADC,SQ,OCA)
CY (37)	34 (92)	13 (38)	25,5,7
Other SB (80)	76 (95)	19 (25)	55,16,9
RE (83)	82 (99)	18 (22)	66,11,6
Total (200)	192 (96)	50 (26)	146,32,22
OCA=other carcinoma			

IHC was PD-L1 expression negative in 142 specimens (71%), positive in 50 (25%), and unsatisfactory due to insufficient cellularity in 8 (1 RE, 2 CY, 5 other SB; 4%). There was no significant difference in PD-L1 positivity between ADC (27%) and SQ (19%, p=0.38). More than 1 specimen was collected from 15 patients, including 4 SB-RE and 3 CY-HY. Expression was concordant between all samples.

Conclusions: The current study demonstrates that results among RE, CY and other SB, including a limited number from patients with more than one specimen, are comparable, and CY provides sufficient cellularity for PD-L1 IHC in a majority of cases. This is important as CY may represent the only specimen, and an additional procedure may not be necessary.

1929 Isolated Small Airways Inflammation in Lung Allograft Transbronchial Biopsies Is More Often Associated with Increased B-Cells and Concurrent Infection

Ying-Han R Hsu, Marie C Aubry, Sarah Jenkins, John P Scott, Anja C Roden. Mayo Clinic, Rochester, MN.

Background: The significance of isolated small airways inflammation (lymphocytic bronchiolitis) in lung allograft transbronchial biopsies (TBB) is unclear. Our study aims to examine the difference in lymphocytic constituents in isolated small airways rejection with or without acute cellular rejection, and its association with concurrent infection and development of bronchiolitis obliterans syndrome (BOS).

Design: The TBB database of one of the authors (2009-2016) was queried for cases with isolated small airways inflammation (ISHLT grades A0B1R; A0B2R) and control cases (ISHLT grades A1-4B1R; A1-4B2R). Consecutive sections were stained with H&E and antibodies to CD3, CD4, CD8 and CD20. Marker-positive cells were counted over 10 high power fields. Medical records were studied. Statistical analysis was performed.

Results: 52 TBB (42 patients) including 23 TBB (18 patients) with ISHLT grade A0B1R were evaluated. No A0B2R biopsy was identified. The results of lymphocyte counts and ratios are summarized in Table 1.

Median (range)	ISHLT grade A0B1R (N = 23)	ISHLT grade A1-A4B1R (N = 29)	p-value
# CD20+ cells	5 (0-37)	0 (0-23)	<0.0001
# CD3+ cells	95 (10-310)	45 (5-270)	0.04
# CD4+ cells	47 (2-209)	16 (0-180)	0.02
# CD8+ cells	40 (8-160)	27 (2-200)	0.23
CD20:CD3	0.04 (0.00-0.39)	0.00 (0.00-0.40)	0.0001
CD4:CD8	1.10 (0.15-3.35)	0.67 (0.00-2.50)	0.08

The A0B1R group, as compared to the control, had both a higher absolute number of CD20+ B-cells (median 5 vs 0, $p < 0.0001$) and a higher CD20:CD3 ratio (median 0.04 vs 0.00, $p = 0.0001$). The increase in CD20+ B-cells was independent of CD3+ T-cells. The rate of concurrent infection was also higher in the A0B1R group than the control (47.8% vs 20.7%, $p = 0.04$). There was no significant difference in the rate of development of BOS in the A0B1R vs the control group (21.7% vs 41.4%, $p = 0.42$).

Conclusions: Isolated low grade small airways inflammation is associated with a higher absolute and relative number of B-cells and concurrent infection. Therefore, this finding might not represent rejection and is more likely associated with an infectious process. The lack of a significant difference in the development of BOS between cases of isolated small airways inflammation and small airways inflammation in cases with acute rejection is not surprising, as both are known risk factors for BOS.

1930 Genomic Profiling of Sarcomatoid and Biphasic Malignant Pleural Mesotheliomas Using Targeted Next Generation Sequencing

Albert Huho, Khalil Sheibani, Patrick Leach, Kassandra Jiron, Robert Ramos, Gwyneth Olson, Mohammad Vasef. University of New Mexico, Albuquerque, NM; Western Pathology Consultation, Tustin, CA.

Background: Pleural malignant mesothelioma (PMM) remains an aggressive tumor with a median survival of less than one year. Treatment modalities including combined surgery, chemotherapy and radiation are aimed mainly at palliation. Among different histologic subtypes, the biphasic and in particular sarcomatoid subtypes have a particularly dismal prognosis with poor response to all treatment modalities. Given the dismal prognosis, we studied the genomic profile of these prognostically very poor histologic subtypes

Design: Eleven morphologically and immunohistochemically confirmed PMM including 8 biphasic and 3 sarcomatoid cases were selected for this study. Briefly, representative H&E stained from each diagnostic specimen were reviewed and areas with >20% tumor were marked. Tissues corresponding to marked areas were scraped off slides using a razor blade for DNA extraction. Following multiplex PCR covering hot spot regions of 50 genes including oncogenes and tumor suppressor genes, libraries were prepared and subjected to sequencing (Ion AmpliSeq Cancer Hotspot Panel v.2, Thermo Fisher). Sequence analysis was performed by analysis of variant caller and second software (NextGENe).

Results: Out of eleven sequenced cases of PMM, 2 cases failed due to poor quality reads and low coverage. Among remaining 9 cases a total of 4 genomic alterations were identified: One out of 9 cases with adequate depth of read demonstrated mutations in *CDKN2A* including a p.A134V. The second case showed a *CDKN2A* (p.R131C) and a *PIK3CA* (p.E545K). One additional case showed a mutation in *PIK3CA* (p.E545K). The remaining 6 cases showed no pathogenic mutations.

Conclusions: Approximately one third (33%) of patients examined in our study harbored recurrent genomic alterations with mutations in *PIK3CA* and *CDKN2A*. These potentially targetable alterations, could influence personalize therapy in patients with PMM. Based on our results it appears that mutations in *CDKN2A* identified in our study is consistent with previously published data, though with lower frequency in these histologic subtypes. However, the *PIK3CA* (p.E545K) mutation identified in 2 out of 9 cases (22%) has not been reported in malignant mesotheliomas in prior studies. These mutations could represent a recurrent mutation in sarcomatoid and biphasic PMM. Given the limited treatment options and poor prognosis particularly in patients with sarcomatoid mesotheliomas, these genetic alterations may provide a potential for targeted therapy in a subset of these patients.

1931 A Subset of Diffuse Malignant Peritoneal Mesothelioma Have Novel *ALK* Rearrangements and Distinct Clinicopathologic Features

Yin (Rex) Hung, Fei Dong, Valentina Nardi, Jaclyn C Watkins, John Godleski, Paola Dal Cin, Christopher P Crum, Lucian R Chirieac. Brigham and Women's Hospital, Boston, MA; Massachusetts General Hospital, Boston, MA.

Background: Diffuse Malignant Peritoneal Mesothelioma (DMPM) generally has a poor prognosis, with a median survival of 1-2 years, but rare cases with survival of more than 15 years have been reported, particularly in young patients. Molecular characteristics of DMPM in these patients remain largely unknown. After encountering one index case of *ALK*-rearranged DMPM, we explored the presence of *ALK* alterations in DMPM.

Design: This study included 89 consecutive DMPM patients (40 men and 49 women, median age 61 years, range 17-84 years) with available pathology material at our institution between 2005 and 2015. Nine (10%) patients were younger than 40 years of age at presentation. We reviewed clinicopathologic data and performed immunohistochemistry (IHC) for ALK in all cases. We confirmed *ALK* rearrangement by fluorescence in situ hybridization (FISH) and identified *ALK* fusion partners by targeted next generation sequencing of tumor DNA and RNA. In select cases, we performed combined scanning electron microscopy and energy dispersive X-ray spectroscopy to quantify asbestos and other mineral fibers.

Results: ALK was positive by IHC in 11 (12%) cases (weak/focal in 8, strong/diffuse in 3). In cases with focal weak ALK immunoreactivity, no *ALK* rearrangement was detected by FISH or sequencing. However, in all 3 cases with strong/diffuse ALK expression, FISH confirmed the presence of *ALK* rearrangements. Targeted DNA and RNA sequencing identified novel *ALK* fusion partners: *STRN*, *ATG16L1*, and *TPM1* in one of each case. All DMPM patients with *ALK* rearrangements were women, two of whom were under 40 years of age at presentation. Tumors were epithelioid or biphasic, with focal areas resembling well-differentiated papillary peritoneal mesothelioma, and showed retained BAP1 and strong PAX8 expression by IHC. Ultrastructural studies confirmed a mesothelial phenotype. No asbestos fibers were detected in all 3 *ALK*-rearranged cases. One patient with *ALK*-rearranged DMPM is still alive with no evidence of disease at 10 years after diagnosis.

Conclusions: This study has identified unique molecular alterations in a subset of DMPM patients with distinctive clinicopathologic features. *ALK* rearrangements were present in 3 of 89 (3.4%) DMPM patients and enriched in young women with DMPM. The presence of *ALK* rearrangements, which are therapeutically targetable in other ALK-positive malignancies, may open new therapeutic promises in this devastating malignancy.

1932 Next Generation Sequencing Frequently Contradicts Surgical Pathology Impression of Relatedness of Multiple Tumors in the Lung

David H Hwang, Steven J Mentzer, Bruce E Johnson, Lynette M Sholl. Brigham and Women's Hospital, Boston, MA; Dana-Farber Cancer Institute, Boston, MA.

Background: The distinction between multiple lung cancer primaries versus a single primary with metastatic disease using anatomic staging and pathological analyses has profound implications for treatment decisions and patient outcome. Surgical pathology diagnosis of lung cancer is complicated by morphologic heterogeneity, processing artifacts and limited sampling. Next generation sequencing (NGS) can be informative in this scenario, as individual tumors accumulate distinct genomic alterations that can distinguish between related and unrelated tumors. This study examines NGS versus surgical pathology in determining relatedness of multiple lung tumors.

Design: An institutional cohort of cancers with available NGS data for all exonic and selected intronic regions of 309 cancer-associated genes was reviewed, including 1898 non-small cell lung carcinomas. We identified all patients with sequencing results for two or more synchronous or metachronous tumors of presumed lung origin obtained from 2007-2016. Patients with repeat testing for known relapse on targeted therapies were excluded. Surgical pathology relatedness was determined based on histomorphologic and immunohistochemical assessment as stated in the final pathology reports. Molecular relatedness was defined as the presence of shared somatic alterations between tumors.

Results: We identified 28 patients with sequencing data for two or more tumors. A median of 6 mutations was detected per case (range 1-26). In 20 patients, surgical pathology suggested that tumors were different; NGS confirmed different mutational signatures in 16 (80%), with related mutational signatures detected in 4 (20%). In 8 cases, surgical pathology suggested that multiple tumors were the same; NGS confirmed related tumor signatures in 5 patients (63%), but different signatures in 3 (38%). Overall, NGS contradicted the surgical pathology impression in 7 out of 28 patients (25%). There were no shared mutations in any of the cases that were deemed genomically distinct. The number of shared mutations in related cases ranged from 1 to 8.

Conclusions: NGS contradicts the surgical pathology impression of tumor relatedness in a quarter of patients with multiple synchronous or metachronous lung tumors. These findings suggest that a comprehensive diagnostic approach incorporating histology and molecular analysis may be essential to drawing this critical distinction in current clinical practice.

1933 Programmed Death Ligand-1 and Tumor Infiltrating Immune Cells in Non-Small Cell Lung Carcinoma, a Report from India

Deepali Jain, Varsha Singh, Prabhat Malik, Sunil Kumar. All India Institute of Medical Sciences, New Delhi, Delhi, India.

Background: Blockade of the immune checkpoint programmed death receptor ligand-1 (PD-L1)/PD-1 pathway has well-established immunotherapeutic value across many tumor types. Widespread use of immune checkpoint inhibitors will need knowledge of PD-L1 expression and its interaction with immune cells from different geographic regions and in different ethnicities. The aim of this retrospective study was to investigate the prevalence of PD-L1, its prognostic role and correlation with tumor infiltrating immune cells (TICs) in non-small cell lung carcinoma (NSCLC) in Indian patients.

Design: Formalin-fixed paraffin embedded resected tumor samples from 82 patients with NSCLC were retrieved. PD-L1 expression was evaluated by immunohistochemistry (IHC) using a rabbit monoclonal anti-PD-L1 antibody (SP142). PD-L1 positivity on tumor cell membrane was defined as ≥5% of tumor cell membrane staining. The extent of TICs as well as PD-L1 IHC expression on TICs were evaluated and IHC was scored from 0 to 4. A score of 2, 3, or 4 was considered PD-L1 positive. Clinico-pathological variables including various oncogenic driver mutations were documented.

Results: There were 37 adenocarcinomas (ADC) and 45 squamous cell carcinomas (SQC). The median age was 46 years (range, 29-78), and 79% of patients were men. Stromal lymphoplasmacytic inflammation was seen in 70% tumors however focal TICs were seen only in 10 tumors. Tumor PD-L1 membranous positivity was seen in 27 cases (32.9%). TICs were score 2 positive. PD-L1 expression was associated with high histologic grade (solid pattern in ADC and poor differentiation in SQC), smoking status, lymph nodal involvement, EGFR and Kras mutations. There was no association of PD-L1 expression with extent and score positivity of TICs and overall survival (p=0.45). No association was seen with ALK and ROS-1 rearrangement, cMET and FGFR-1 amplification and Her-2/neu mutation.

Conclusions: This is the first study of PD-L1 expression in Indian sub-population which suggests a positive correlation of tumor PD-L1 with high histologic grade and tumor stage. Approximately one third of NSCLC show PD-L1 expression. Tumor PD-L1 expression may be oncogenically driven however there was no correlation with TICs. Our data indicate that clinical studies should investigate the value of checkpoint inhibitors in Indian patients who are also potential candidates for immunotherapeutic regimens.

1934 Targeted Next Generation Sequencing Identifies Distinct Mutational Profiles of Thymomas and Thymic Carcinomas

Tyler Janovitz, Lynette M Sholl, Fei Dong. Brigham and Women's Hospital, Boston, MA.

Background: Thymic epithelial neoplasms, including thymomas and thymic carcinomas, are uncommon primary mediastinal neoplasms. The molecular pathogenesis of thymic neoplasia is not well characterized.

Design: Targeted next generation sequencing of 275 cancer-associated genes was performed on 16 thymic carcinomas and 17 thymomas. Analysis was restricted to pathogenic driver alterations in oncogenes, mutations of *TP53*, and loss of function variants (nonsense, frameshift, and splice site variants) and focal deletions in tumor suppressor genes.

Results: Driver variants in oncogenes were identified in three thymic carcinomas (19%), involving *KIT* (2) and *HRAS* (1) and were not identified in thymomas. *TP53* mutations

were identified in five thymic carcinomas (26%) and were not identified in thymomas. Inactivation of *CDKN2A* was observed in nine thymic carcinomas (56%) due to two copy deletion (8) and frameshift mutation (1). *CDKN2A* alterations were not present in thymomas. Loss of function variants in tumor suppressor genes were observed in 10 thymic carcinomas (63%) and 3 thymomas (18%), including recurrent loss of function variants in *CYLD*, *TET2* and *BAP1* in thymic carcinomas.

Conclusions: Thymic carcinomas have distinctive patterns of gene mutations compared to thymomas, including infrequent mutations of *KIT* and *HRAS* and frequent *TP53* mutations and *CDKN2A* copy loss. Targeted sequencing of thymic epithelial neoplasms identifies the molecular drivers of thymic carcinomas and may aid the diagnosis of thymic epithelial neoplasms and guide therapeutic decision making in the appropriate clinical context.

1935 Intratumoral Programmed Cell Death-Ligand 1 (PD-L1) and Intratumoral CD8⁺ T Cell Expression in Lung Cancer

Yasuto Jin, Osamu Matsubara, Kazuki Yamanaka, Eugene Mark. Hiratsuka Kyosai Hospital, Hiratsuka, Japan; Massachusetts General Hospital and Harvard Medical School, Boston, MA.

Background: Cancer immunotherapy plays an important role in the treatment of many cancers, including lung cancer. Blockade of the PD-1/PD-L1 pathway could reverse the tumor microenvironment and enhance the endogeneous antitumor immune responses. Immune checkpoint inhibitors against advanced, refractory non-small cell lung cancer have shown significant progress. Nivolumab, anti-PD-1 antibody, has been approved for the treatment of advanced non-small cell lung cancer after first-line treatment and it has been reported that the PD-L1 positive (≥1%) expression status was associated with a favorable response. However, detection of PD-L1 protein by immunohistochemistry is a complementary rather than a companion diagnostic test. It has been reported that PD-L1 over-expression with tumor infiltrating lymphocytes (TILs) plays a key role in tumor immune escape and formation of the tumor microenvironment, closely related to tumor progression. However, in lung cancer, the precise condition and diagnostic value of these immunological factors remains uncertain and specific biomarkers to predict those patients who are likely to benefit have not been identified.

Design: PD-L1 (SP263) and CD8 expression in tumor cells and TILs were examined by immunohistochemistry (IHC) in 21 cases with stage III-IV lung cancer treated with Nivolumab, including 17 cases of adenocarcinoma and 3 cases of squamous cell carcinoma. Histologic subtypes, tumor size and other clinicopathologic conditions were compared with the density of their expression.

Results: PD-L1 expression in tumor cells was detected in 55.5% of the cases. PD-L1 positivity with CD8 TILs was significantly positively correlated with the objective response rate (figure). Cases featuring PD-L1 overexpression showed consistently dense CD8 positive TILs, even in subgroup analyses according to histological subtype, age and smoking status.

Conclusions: We found that PD-L1 overexpression with CD8 positive TILs was associated with a favorable response to treatment with Nivolumab. This may mean that assessment of PD-L1 and CD8+ TILs by IHC is valuable for predicting the response to treatment with Nivolumab. The PD-L1 status and presence or absence of CD8 positive TILs measured by IHC may be a candidate of biomarker that predicts the therapeutic response to immune checkpoint blockades.

1936 Tumor Budding and Single Cell Invasion Are Significant Prognostic Factors, Independent of Pathologic Stage, in Japanese Patients with Lung Squamous Cell Carcinoma (SQCC)

Kyuichi Kadota, Kosuke Inoue, Emi Ibuki, Ryou Ishikawa, Yumi Miyai, Naomi Katsuki, Yoshio Kushida, Toru Matsunaga, Masaya Okuda, Hiroyasu Yokomise, Nobuhiro Kanaji, Shuji Bandoh, Reiji Haba. Kagawa University, Kagawa, Japan.

Background: For lung SQCC, there are no pathological findings that have been universally accepted as prognostic factors, with the exception of pathological stage. We have previously demonstrated that tumor budding and single cell invasion were independently associated with an unfavorable prognosis among North American patients with resected lung SQCC (Kadota et al. J Thorac Oncol 2014). In this study, we validate whether tumor budding and single cell invasion can independently predict prognosis in Japanese patients with lung SQCC.

Design: All available tumor slides from patients with therapy-naive, surgically resected lung SQCC (1999-2012) were reviewed (n=216; stage I/II/III/IV, 134/56/22/4). Tumors were classified as keratinizing, non-keratinizing, and basaloid subtypes (2015 WHO Classification). Tumors were graded by means of tumor differentiation. Tumor budding (small tumor nests composed of less than 5 tumor cells) and single cell invasion were evaluated in a high-power field (HPF) of x200 magnification at the most invasive area. Tumor budding was assessed 2 ways: 1) the maximum number of buds per HPF (/1HPF) among the 10 HPFs and 2) the total number of tumor budding of 10 HPFs. Tumor budding was considered positive when the maximum number of buds was ≥5/1HPF or the total number of buds was ≥10/10HPF. Recurrence-free survival (RFS) and overall survival (OS) were estimated using the Kaplan-Meier method, and multivariate analyses were performed using the Cox proportional hazards model.

Results: Histological subtype and tumor differentiation did not correlate with RFS (p=0.86 and p=0.14, respectively) or OS (p=0.16 and p=0.57, respectively). On univariate analysis, maximum number of buds (/1HPF), total number of buds (/10HPFs), and presence of single cell invasion were associated with a worse RFS (p<0.001, p<0.001 and p<0.001, respectively) and OS (p<0.001, p<0.001 and p<0.001, respectively) . On multivariate analysis after adjustment for pathologic stage and lymphatic invasion, maximum buds, total buds and single cell invasion were independent prognostic factors for RFS (HR= 1.4; p<0.001, HR= 1.2; p<0.001 and HR= 4.9; p<0.001, respectively) and OS (HR=1.3; p<0.001, HR=1.2; p<0.001 and HR=3.2; p<0.001, respectively).

Conclusions: We found that tumor budding and single cell invasion, but not histologic subtype or tumor differentiation, were significant prognostic factors independent of pathologic stage among Japanese patients with resected lung SQCC.

1937 KRAS Mutation Is Highly Prevalent and Predicts Recurrence in Patients with Primary Invasive Mucinous Adenocarcinoma of the Lung

Mohamed K Kamel, Navneet Narula, Kyung Park, Brendon M Stiles, Jeffrey L Port, Helen Fernandes, Nasser K Altorki. New York Presbyterian Hospital - Weill Cornell Medicine, New York, NY.

Background: Invasive mucinous adenocarcinomas (IMA) of the lung have unique pathologic and genetic features. We sought to determine the effect of the presence and type of KRAS mutations on oncologic outcomes.

Design: Seventy-five tumors with IMA with known KRAS status were collected (2001-2016) at Weill Cornell Medicine. Pathologic diagnosis was based IASLC/ATS/ERS classification. Comparisons were made between clinical and pathologic characteristics and the presence and type of KRAS mutation status (transversion versus transition) on oncologic outcomes.

Results: The study included 75 patients (39% males, median age 71 years, and 60% smokers). Most patients (n=46,61%) had pT1 disease with median tumor size of 1.9 cm. Six patients (8%) had LN metastases and one had metastatic disease at the time of resection. Molecular analysis showed that 53% of patients had KRAS mutation of which 40% were transition type and 60% transversion type. The median follow up of the entire cohort was 32 months. At follow up, 18 patients (24%) developed recurrence (16 distant recurrence). The 5 year overall and disease free survival for stage I patients (n=46) were 89%, and 68%, respectively. There were no significant differences in clinical and pathologic characteristics in patients with and without KRAS mutation (Table).

Demographic and Clinical Data		KRAS Negative (n=35)	KRAS Positive (n=40)	P value
Age (years)		74 (67-78)	69 (65-75)	0.094
Gender (female)		21 (60%)	25 (62.5%)	0.824
Smoking (current/former)		19 (54.3%)	26 (66.7%)	0.276
Site of the tumor	Upper/Middle lobe	19 (54.3%)	15 (37.5%)	0.145
	Lower Lobe	16 (45.7%)	25 (62.5%)	
Tumor SUVmax		2.5 (1.3-6.1)	3 (1.4-6.1)	0.548
pStage	Stage I	21 (60%)	25 (62.5%)	0.824
	Stage II/III/IV	14 (40%)	15 (37.5%)	

However, KRAS –ve patients had higher probability of freedom from recurrence (85% vs 41%, P=0.02) compared to KRAS +ve patients (Figure).

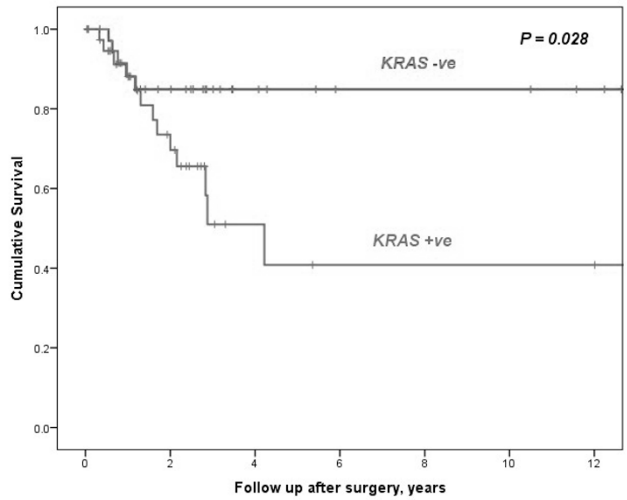

Furthermore, among KRAS +ve patients, there was a trend towards improved 5-year disease free survival in patients with transition mutation compared to those with transversion mutation (54% vs 30%, p=0.06).

Conclusions: KRAS mutation is highly prevalent in IMA patients. Patients with KRAS mutations have a higher probability of recurrence. Further studies should validate these results, and assess the role of adjuvant therapy in early stage disease with KRAS mutation.

1938 2015 WHO Thymoma Classification: Prognostic Value of Heterogeneity in Thymomas

Mohamed K Kamel, Navneet Narula, Brendon M Stiles, Jeffrey L Port, Nasser K Altorki. New York Presbyterian Hospital - Weill Cornell Medicine, New York, NY.

Background: The prognostic value of the impact of heterogeneity in thymomas is not known. The 2015WHO classification has refined the diagnostic criteria for thymoma subtypes and recommend that histologic subtypes in a thymoma be quantified in 10% increments. We sought to assess the prognostic value of the predominant histologic component on disease free survival (DFS) and to determine whether the presence of secondary components with higher grade subtypes than the predominant type affected patient outcomes.

Design: Pathology slides of patients who underwent thymectomy (2000-2014) were re-reviewed by a single pathologist to avoid inter-observer bias. Tumors were classified according to the 2015WHO criteria. DFS survival analysis was used to determine the impact of the presence of secondary components.

Results: 162 patients underwent thymectomy during the study period. Pathology slides were available for review in 130 patients (median age-55yr, 76-males), of them 113(87%) had thymoma and 17(13%) had a thymic carcinoma. Median tumor size was 7cm (70% Masaoka-stage I/II). Cox-regression analysis of thymoma patients (n=113) showed that the predominant subtype according to the 2015WHO criteria predicts DFS (Figure.1A, P=0.05). Survival curves showed ordered, wide uniform separation (A/AB carries best prognosis, B3 had the worst). Heterogeneity was found in only 22(19%) of thymomas (Table). In 14 patients the secondary component had a worse subtype compared to the predominant subtype. DFS curves of patients stratified by worst predominant/secondary subtypes showed narrower, non-uniform, separations with interchange of A/AB and B1 curves (Fig.1B), compared to those observed with the use of predominant subtype.
Conclusions: The 2015 WHO thymoma classification holds a prognostic value. Heterogeneity of subtypes within thymomas does not appear to be prognostic. The predominant subtype rather than the secondary subtypes should be used to assess patients' prognosis.

2015 WHO Primary Component	2015 WHO Secondary Component	No. of patients	Percentage from total
A/AB	B1/B2	1	5/55
	B2	3	
	B3	1	
B1	B2	2	2/13 (15%)
B2	AB	3	11/37 (30%)
	AB/B3	1	
	B1	1	
	B3	6	
B3	B2	4	4/8 (50%)
Total			22/113 (19%)

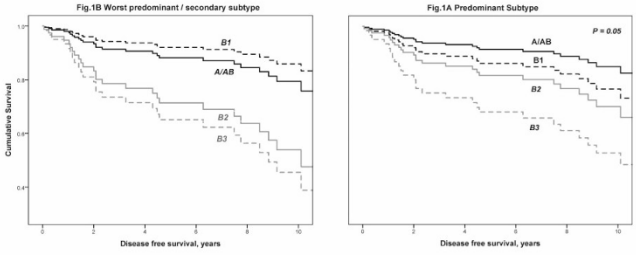

1939 A Clinicopathologic and Molecular Analysis of 34 Mediastinal Germ Cell Tumors (GCT) Supporting a Dual Histogenesis for Teratomas

Chia-Sui Kao, Dana Bangs, Thomas M Ulbright. Stanford University School of Medicine, Stanford, CA; Indiana University School of Medicine, Indianapolis, IN.

Background: Although mediastinal GCTs occur over a wide age range, they are most common in adult males. Teratoma is the most common subtype. Limited data exist on the chromosome 12p status of mediastinal GCTs. We studied the presence/absence of chromosome 12p amplification in mediastinal GCTs and correlated the results with histologic findings and clinical follow-up.
Design: 38 mediastinal GCTs were identified; all available clinical information was recorded. Fluorescence in situ hybridization (FISH) for chromosome 12p amplification was performed in all cases.
Results: 34 cases had successful hybridizations for FISH 12p amplification while 4 failed. Results are summarized in the table.

Tumor type	Age (years)	Gender	12p status	Treatment	Follow-up
Pure teratoma, no atypia/ disorganization (n=19)	0.2-52 (median 20)	9M, 10F	1 pos/18 neg	1 pre-resection chemo, followed by surgery and chemo; 17 surgery only; 1 NA	1 DOD, 17 NED, 1 NA (0.5-94 mos; avg 27.1)
Pure teratoma, with atypia/ disorganization (n=6)	19-30 (median 24.5)	6M	4 pos/2 neg		1 AWD, 5 NED (1.5-176 mos; avg 51.4)
Teratoma with secondary somatic malignancy (n=2)	29; 31	1M; 1F	1 pos/1 neg	Pre-resection chemo, followed by surgery and chemo; surgery only	DOD (16 mos); AWD (27 mos)
Non-teratomatous GCT (n=7)	18-46 (median 35)	7M	5 pos/2 neg		1 DOD, 1 alive, 2 AWD, 3 NED (1-43 mos; avg 13)

Conclusions: Mediastinal teratomas in children and females lack 12p amplification, and in the absence of secondary somatic malignancies, are benign. In postpubertal males, there is a higher frequency of benign pure teratomas in the mediastinum compared to the testis, and these are, in most instances, recognizable based on their lack of atypia and disorganized growth, although there are rare exceptions. Absence of 12p amplification in such cases correlates with a benign clinical course. The data support that mediastinal teratomas derive from two distinct pathways – benign teratomas predominate in children and women and form from non-transformed stem/germ cells; malignant teratomas occur almost exclusively in adult males and represent derivatives of malignant, non-teratomatous germ cell tumors that arise from transformed stem/germ cells. The former lacks 12p amplification and the latter demonstrates 12p amplification.

1940 PHH3 Immunostaining Reduces the Evaluation Time and Facilitates Histologic Assessment of Pulmonary Carcinoid Tumors

Babak Khoshkrood-Mansoori, Olga Sazanova, Michèle Orain, Sylvain Trahan, Serge Simard, Philippe Joubert. Université Laval, Quebec, QC, Canada; Quebec Heart and Lung Institute, Quebec, QC, Canada.

Background: Lung carcinoid tumors are divided into typical (TC) and atypical carcinoids (AC) based on the presence of necrosis and the mitotic count per 2mm^2. The mitotic count, which is done on hematoxylin and eosin (HE) stained slides, is time-consuming and subject to a high interobserver variability. The aim of this study was to test the usefulness of a sensitive and specific mitosis marker, the Phospho-Histone-H3 (PHH3) immunostaining, in the classification of lung carcinoid tumors and to compare it to the standard HE evaluation.
Design: Available carcinoid tissue blocks from lung resection specimens performed (1998 to 2013) were analyzed using HE and PHH3 stains. Mitotic count was carried out by two thoracic pathologists and two residents on HE and PHH3 stains according to the WHO guidelines and recorded as mitosis/2mm^2. The counting time was compared between the two methods. Interobserver agreement among the raters in terms of total mitosis count and mitotic count/2mm^2 was assessed for both methods with Cronbach's intraclass correlation analysis (ICC). Receiver Operating Characteristic (ROC) analysis was used to determine the optimal diagnostic cutoff for PHH3 staining.
Results: A total of 69 patients (82% TC, 18% AC) were included, for a total of 184 slides. Mitotic count with PHH3 was less time consuming than HE method for all raters (3.8 vs. 8.6 minutes per slide, $p < 0.001$), with a much greater gain for the residents. Compared to HE method, PHH3 stain detected more mitotic figures (10.8 vs. 3.9 mitoses per slide, $p< 0.001$) and per 2mm^2 (3.5 vs. 2.2, $p< 0.05$). The interobserver agreement was only slightly better for the PHH3 method than HE method in the examined areas (PHH3 ICC 0.876, Alfa 0.960; HE ICC 0.834, Alfa 0.939). For the PHH3 stain, a mitotic count of 4/2mm^2 was the optimal cutoff for separating TC from AC (Log-rank test, p=0.005).
Conclusions: Our data confirmed that histologic assessment of carcinoid tumors by PHH3 stain provides practical benefits in terms of significantly reduced scoring times, mitosis detection and reproducibility of mitotic counts. The gain of benefit is greater for less experienced pathologists. A mitotic count of 4/2mm^2 isproposed as the diagnostic cutoff for differentiating TC from AC. Validating this cutoff in a larger cohort of patients with a longer follow-up will help drawing more precise conclusions on the prognostic significance of PHH3 staining in terms of disease-free and overall survivals.

1941 *In Situ* Detection of MET Exon 14 Skipping in Lung Carcinoma via a Highly Sensitive BaseScope™ In-Situ Assay in FFPE Tissues

Jeff Kim, Xiao-Ming Mindy Wang, Nan Su, Rob Monroe, Xiao-Jun Ma, Hans-Ulrich Schildhaus, Emily Park. Advanced Cell Diagnostics, Newark, CA; University Hospital Goettingen, Göttingen, Germany.

Background: Non-small cell lung cancer (NSCLC) harboring particular genetic alterations, such as MET exon 14 (METex14) skipping, has been shown to be highly sensitive to targeted therapies. However, the identification of this specific splice variant can be challenging even to the extent of evading sensitive screens such as next generation sequencing. Here, we provide an invaluable tool to visualize and quantify METex14 skipping events across several lung cell carcinoma lines and patient biopsies.
Design: Five cell lines (EBC-1, H1993, H661, HCC827, and H596) and 16 lung carcinoma patient biopsies were examined for MET status via fluorescence *in situ* hybridization (FISH), DNA seq, RNA seq, immunohistochemistry, and BaseScope™, a highly sensitive RNA *in situ* hybridization assay capable of detecting precise exon junctions including spliced variants. METex14 skipping events were detected by specific probe designed on exon 13 and 15 junction (E13/15), compared to wt sequence detected by probe designed on exon 14 and 15 junction (E14/15). Signals detected by specific junction probes were quantified using image analysis software.
Results: The BaseScope™ assay positively identified METex14 skipping events in transcripts of the H596 cell line as distinct dots with the E13/14 probe, but not by the E14/15 probe. All other cell lines, which were wild-type for exon 14 status, were detected with the E14/15 probe only. Consistent with DNAseq information, five of the 16 patient samples were positively identified exhibiting METex14 skipping. Further, quantitative analysis was carried, revealing a distinct and heterogeneous expression of various MET exon junctions from cases with METex14 skipping.
Conclusions: Our findings indicate that the BaseScope™ assay is an innovative technology that is able to detect splice variants in FFPE clinical samples. This method provides therapeutically relevant genomic information in combination with RNA-expression levels in the context of tumor morphology making it suitable to serve as a predictive biomarker assay in lung cancer and other human neoplasms.

1942 A Combination of MTAP and BAP1 Immunohistochemistry Is Useful for Differentiating Malignant and Benign Mesothelial Proliferatons in Tissue and Cytological Specimens

Yoshiaki Kinoshita, Tomoyuki Hida, Makoto Hamasaki, Shinji Matsumoto, Tohru Tsujimura, Kunimitsu Kawahara, Kenzo Hiroshima, Yoshinao Oda, Kazuki Nabeshima. Fukuoka University School of Medicine and Hospital, Fukuoka, Japan; Graduate School of Medical Sciences, Kyushu University, Fukuoka, Japan; Hyogo College of Medicine, Nishinomiya, Hyogo, Japan; Osaka Prefectural Medical Center for Respiratory and Allergic Disease, Habikino, Osaka, Japan; Tokyo Women's Medical University Yachiyo Medical Cente, Yachio, Tokyo, Japan.

Background: Differentiating malignant pleural mesothelioma (MPM) from reactive mesothelial hyperplasia (RMH) is important for early diagnosis of MPM. Homozygous deletion of the 9p21 locus detected by fluorescence in situ hybridization (FISH) and loss of BRCA1-associated protein 1 (BAP1) expression detected by immunohistochemistry (IHC) are useful for differentiation between MPM and RMH. 9p21 FISH is a good

marker, but not all laboratories are equipped to perform FISH. We reported earlier that IHC expressions of protein product of the *methylthioadenosine phosphorylase* (*MTAP*) gene, which is localized in the chromosomal region 9p21, correlated with the deletion status of 9p21 FISH in MPM. In this study, we investigated whether a combination of MTAP and BAP1 IHC could distinguish MPM from RMH in tissue specimens and cell blocks obtained from pleural effusions.
Design: We examined tissues from 51 epithelioid MPM and 25 RMH cases and cell blocks from 25 epithelioid MPM and 21 RMH cases. The IHC expressions of MTAP and BAP1 in mesothelial cells in tissue sections and pleural effusion samples were evaluated.
Results: In histological analysis, both BAP1 and MTAP IHC had 100% specificity for differentiating MPM from RMH; their sensitivities were 60.8% and 45.1%, respectively. Upon their combination, the sensitivity was enhanced to 76.5%, which was higher than that of BAP1 IHC alone (60.8%) or 9p21 FISH alone (60.8%). In cytological analysis, BAP1 and MTAP had sensitivities of 44% and 36%, respectively, while their specificity was 100%. Their combination yielded 68% of sensitivity that was higher than that of BAP1 IHC alone (40%) or 9p21 FISH alone (30%).
Conclusions: A combination of BAP1 and MTAP IHC is useful for differentiating MPM from RMH. The combination shows good diagnostic sensitivity that is higher than that of BAP1 IHC alone or 9p21 FISH alone.

1943 Comparative Analysis of Lung Lesions of Systemic IgG4-Related Disease and Idiopathic Multicentric Castleman's Disease

Nariaki Kokuho, Yasuhiro Terasaki, Mika Terasaki, Shinobu Kunugi, Akira Hebisawa, Yoshinori Kawabata, Yuh Fukuda, Akira Shimizu. Nippon Medical School, Tokyo, Japan; NHO Tokyo National Hospital, Tokyo, Japan; Saitama Prefectural Cardiovascular, Respiratory Center, Saitama, Japan.
Background: Lung lesion of IgG4-related disease is a condition associated with IgG4-related disease and often mimics the lung lesion of idiopathic multicentric Castleman's disease. Because no clinical and pathological study compared the features of these diseases, we undertook this comparison with clinical data and surgical lung biopsies and an autopsy.
Design: Nine patients had lung lesion of IgG4-related disease (high serum IgG4 levels and $IgG4^+$ plasma cell infiltration in lung specimens; typical extrapulmonary manifestations). Fifteen patients had lung lesion of idiopathic multicentric Castleman's disease (polyclonal hyperimmunoglobulinemia, elevated serum interleukin-6 levels, and polylymphadenopathy with typical lymphadenopathic lesions).
Results: The mean data of age, the serum levels of hemoglobin, IgG4, and IgG4/IgG ratios were significantly higher in lung lesion of IgG4-related disease group, while the levels of IgG and CRP were higher in lung lesion of idiopathic multicentric Castleman's disease group. All lung lesions of IgG4-related disease showed myxomatous granulation like fibrosis (active fibrosis) with infiltration of lymphoplasmacytes and scattered eosinophils within lymphatic stroma itself such as peribronchial and perivascular areas, interlobular septa, and pleura. All samples had obstructive vasculitis. All 15 lung lesions of idiopathic multicentric Castleman's disease, however, had marked accumulation of polyclonal lymphoplasmacytes in lesions with lymphoid follicles and focal dense fibrosis in peribronchial and perivascular areas and mainly the alveolar area adjacent to interlobular septa and pleura. Five of 15 lung lesions of idiopathic multicentric Castleman's disease had cystic lesions, but no sample manifested obstructive vasculitis.
Conclusions: Although both lesions had lymphoplasmacyte infiltration, lung lesions of IgG4-related disease was characterized by active fibrosis with eosinophilic infiltration within lymphatic stroma itself with obstructive vasculitis, whereas lung lesion of idiopathic multicentric Castleman's disease was marked lymphoplasmacyte proliferating lesions mainly in the alveolar area adjacent to lymphatic stroma. These clinicopathological features may help differentiate them.

1944 Analysis of mTOR Signaling Pathways in Lymphangioleiomyomatosis

Ildiko Krencz, Anna Sebestyen, Judit Papay, Andras Jeney, Zoltan Hujber, Charles Burger, Cesar Keller, Andras Khoor. Semmelweis University, Budapest, Hungary; Hungarian Academy of Sciences, Budapest, Hungary; Mayo Clinic, Jacksonville, FL.
Background: Lymphangioleiomyomatosis (LAM) is a rare, progressive, cystic lung disease with features of a low-grade neoplasm. It is caused by TSC1 or TSC2 mutations, which are known to constitutively activate mTOR signaling. mTOR regulates cell functions through the activities of two multi-protein complexes: mTORC1 and mTORC2. Sirolimus, an mTORC1 inhibitor, has successfully been utilized to slow down disease progression in some, but not all patients. However, there is limited information available on the activity of mTORC2 in this disease. The aim of this study was to analyze the activities of both mTORC1 and mTORC2 in sporadic LAM.
Design: Lung tissue was available from 11 patients with sporadic LAM (8 explanted lungs and 3 wedge biopsies). We analyzed mTORC1 and mTORC2 activities using immunohistochemistry for phospho-S6 and Rictor, respectively. For semiquantitative immunohistochemical analysis, the H score was used. An expression was considered low if the H score was lower or equal to 100 and high if the H score was higher than 100.
Results: High phospho-S6 expression suggesting high mTORC1 activity was observed in 10 cases, whereas high Rictor expression suggesting high mTORC2 activity was observed in 6 cases.
Conclusions: These results suggest that, in addition to mTORC1 inhibitors, mTORC2 (or dual) inhibitors may also be potentially utilized in the treatment of sporadic LAM, particularly in cases with high mTORC2 activity. Furthermore, immunohistochemistry for phospho-S6 and Rictor may play a role in determining the appropriate individualized treatment.

1945 Similar Molecular Subtypes of Lung Injury Patterns in Interstital Lung Disease, Stem Cell and Lung Transplantation

Florian Laenger, Jens Gottlieb, Matthias Eder, Gregor Warnecke, Mark Kuehnel, Hans H Kreipe, Danny Jonigk. Medical School Hanover, Hanover, Germany.
Background: Loss of lung function is a severe and life threatening complication of interstitial lung disease (ILD), radiotherapy (RT) as well as stem cell (HSCT) and lung transplantation (LuTx). Here two important non-infectious lung injury patterns have been described: obliteration of bronchioles of the lung (BO) as well as collageneous obliteration of alveoli summarized as pleuropulmonary fibroelastosis (PPFE). Despite the shared morphology so far no comparative analysis of the similarities and differences on a molecular level has been reported. In this study we analyse the mediators of the fibrosis-associated pathways, especially TGF-β, BMPs and related effector molecules in BO and PPFE.
Design: We performed conventional histology, immunohistochemistry and stereological analysis on 63 lung explants from patients after LuTx, RT, HSCT and suffering from ILD. After compartment-specific laser microdissection of normal, BO and PPFE areas, gene expression analysis of 40 fibrosis associated genes was performed by low-density PCR panels. Statistical analysis of expression results was performed.
Results: Three key results emerged: I) "BO is BO", despite divergent clinical background molecular characteristics of BO were very similar II) "PPFE is PPFE", in all groups with PPFE pattern there were largely identical gene expression patterns III) BO concomittant to PPFE after LuTx showed a PPFE like molecular signature (as an exception to I).
Additionally we could show an evolutionary model of the PPFE pattern with a fibrin-rich acute injury pattern preceding a failed histiocyte-rich pattern and the final evolution of PPFE. Our expression data point toward a failure of the classical fibrinolytic pathway.
Conclusions: Our analysis of fibrosis-associated gene expression in BO and PPFE of the lung shows a shared and similar usage of these pathways regardless of the clinical background, identifying these patterns as rather unspecific acute injury patterns. Moreover our data point towards a sequential evolution of the PPFE pattern triggered by failed classical fibrinolysis following lung injury.

1946 Histopathologic Findings in Lung Biopsies from Patients with Primary Biliary Cirrhosis (PBC)

Hee Eun Lee, Jay H Ryu, Ana-Maria Bilawich, Andrew Churg, Henry D Tazelaar, Eunhee S Yi. Mayo Clinic, Rochester, MN; University of British Columbia, Vancouver, Canada; Mayo Clinic, Scottsdale, AZ.
Background: PBC, a progressive autoimmune disease of the liver,has been shown to be associated with various other diseases including interstitial lung disease (ILD). However, pulmonary histopathology in this setting has not been well characterized.
Design: 13 patients with a clinicopathologic diagnosis of PBC who underwent lung biopsies were identified from the surgical pathology files of 3 institutions. Medical records and imaging studies were reviewed. Histopathologic review was performed for the following: density and location of lymphocytic infiltrates; presence eosinophils or neutrophils; density, type, and location of granulomas; presence organizing pneumonia; pattern of interstitial fibrosis if present.
Results: All patients were women with a median age of 54 years (range, 41-79). Specimen types were lobectomy (n=1), VATS (n=9), CT-guided needle biopsy (n=1) and transbronchial biopsy (n=2). 12 of 13 biopsies showed lymphocytic inflammation, localized to peribronchiolar stroma (n=10), interstitium (n=12, either diffuse or centrilobular), and/or pleura (n=4). 11 of 13 biopsies revealed non-necrotizing granulomas, most of which were poorly-formed (n=10), reminiscent of those seen in the liver biopsies from PBC patients. The granulomas were found in the peribronchiolar stroma (n=8), interstitium (n=8), airspaces (n=5), and/or pleura (n=2). 4 cases also showed remarkable eosinophilic infiltrates. Organizing pneumonia was seen in 4 cases. 2 cases showed diffuse interstitial fibrosis with nonspecific interstitial pneumonia (NSIP) pattern and another 2 showed usual interstitial pneumonia (UIP) pattern. 1 patient underwent lobectomy for a mass lesion (2.3x2.2cm) diagnosed as light chain deposition disease with kappa-restricted MALT lymphoma based on ancillary studies.
Conclusions: The main histopathologic findings of the lung biopsies in our PBC patients included interstitial and peribronchiolar lymphocytic inflammation with poorly-formed non-necrotizing granulomas, which appeared to parallel the PBC histopathology in the liver biopsies. This set of findings should raise a question of underlying PBC when encountered in a lung biopsy from a patient with a radiologic impression of ILD. However, some patients have a fibrosing interstitial lung disease with features of NSIP or UIP.

1947 Inflammatory Pseudotumor Arising from Pulmonary Thrombi: Analysis of a Case Series

Xiaoyan Liao, Christine M Bojanowski, Eunhee S Yi, Huan-You Wang, Kim M Kerr, Justin Dumouchel, Grace Y Lin. UCSD, San Diego, CA; Mayo Clinic, Rochester, MN.
Background: Inflammatory pseudotumor (IPT), also known as plasma cell granuloma, is a rare lesion of unclear etiology reported in many organs, including the lung parenchyma. However, IPT arising in pulmonary arteries from chronic thromboembolic disease (IPT ex PT) has not been previously reported. This study sought to determine the incidence, clinical presentation, histopathological features, and diagnostic pitfalls of IPT ex PT at a single institution.
Design: A 17-year retrospective review of our surgical pathology database revealed more than 2,200 cases of pulmonary thrombus that underwent thromboendarterectomy. Histologic sections, final diagnosis reports, and available electronic medical records were reviewed and confirmed 5 cases of IPT ex PT. Another 5 cases, including 2 organizing/recanalizing thrombi, 2 pulmonary artery sarcomas, and 1 pulmonary arteritis, served as controls.

Results: All 5 patients with IPT ex PT were referred from outside hospitals, including 3 men and 2 women, with a median age of 41 (23~54) years old. One patient had a complex past medical history including pituitary prolactinoma and intraabdominal diffuse large B cell lymphoma status post ileocolectomy and chemotherapy. The other 4 had no significant past medical history. All patients presented with progressive dyspnea and imaging findings of saddle pulmonary embolism, and underwent anticoagulation therapy before surgery. The duration between symptom initiation to thromboendarterectomy ranged from 5 months to approximately 2 years.
Histological review of the 5 IPT ex PT cases demonstrates the following common features: prominent proliferation of spindle cells without cytologic atypia, increased mitoses, or necrosis; marked inflammatory infiltrate comprised mostly of plasma cells, lymphocytes, and histiocytes. Immunohistochemistry shows that the spindle cells are positive for SMA, but negative for ALK-1, EBV, HHV-8 (LANA), and S100. The background plasma cells are polytypic for kappa and lambda, and rarely positive for IgG4 (IgG4: IgG ratio <30%). No microorganisms are identified by Warthin-Starry, acid-fast, or GMS stains.
Conclusions: IPT ex PT is a very unusual condition, which has not been previously reported in literature. We present herein 5 cases of IPT ex PT and describe its clinical and histopathological features. It appears that organizing/recanalizing thrombus, IPT ex PT, and pulmonary artery sarcoma may represent the spectrum of a fibroblastic disorder in chronic pulmonary thromboembolism, yet the exact mechanism is not clear.

1948 SATB2 Expression in Adenocarcinoma of the Lung with and without Enteric Differentiation

Austin McCuiston, Daniel L Miller, Qing K Li, Ed Gabrielson, Peter Illei. Johns Hopkins Medical Institution, Baltimore, MD.
Background: A subset (10-12%) of lung adenocarcinomas (ACA) may express the gastrointestinal marker CDX2 making the distinction between metastatic colorectal ACA and primary lung ACA difficult. Special AT-rich sequence binding protein 2 (SATB2) was recently identified as a highly specific marker of the glandular epithelium lining the lower GI tract. SATB2 expression is retained in the large majority of colorectal ACA (85-97%) and is only uncommonly expressed in esophageal (6.7%), gastric (0%) and pancreas (4.2%) ACA. There is only very limited data available regarding SATB2 expression in lung ACA. Here we report our findings on SATB2 expression in 95 cases of lung ACA without intestinal differentiation and 10 enteric type ACA all with known CDX2 expression status.
Design: Four (4) micron sections of previously constructed tissue microarrays (TMA) containing 92 cases of lung ACA without enteric differentiation, as well as full sections of 3 mucinous ACA and 10 enteric type lung ACA were subjected to immunohistochemistry for TTF1, Napsin A, CDX2 and SATB2 using an autostainer and commercially available monoclonal antibodies. Tumors showing staining of any intensity (for SATB2 and CDX2) in greater than 5% of the tumor cells were accepted as positive.
Results: The TMA cohort consisted of 13 well, 52 moderately and 27 poorly differentiated ACA. Eighty-one tumor was positive for at least one lung adenocarcinoma marker with 68 tumors showing staining for both TTF1 and napsin A. Positive CDX2 staining was seen in 9 tumors (10%), while positive SATB2 staining was seen in only one tumor (1%). Focal (<5%) SATB2 staining was noted in 3 additional tumors. Six of 10 enteric type ACA were CDX2 positive, two of which were also SATB2 positive, while the remaining 4 enteric type ACA were negative for both CDX2 and SATB2. The 3 mucinous ACA were also double negative.
Conclusions: SATB2 is a novel marker that is highly specific for colorectal ACA and appears to be rarely expressed in primary lung adenocarcinoma. This is in contrast to CDX2, a widely used marker of gastrointestinal adenocarcinoma that is expressed in the majority of enteric typeACA and a subset of primary lung ACA without enteric features (10% in the current study) making the distinction between primary lung adenocarcinoma and metastatic colorectal adenocarcinoma problematic, especially in small biopsies where we rely more on immunohistochemistry to render a more specific diagnosis. SATB2 appears to be a promising marker that is superior to CDX2 for distinguishing between primary lung adenocarcinoma and tumors of the lower gastrointestinal tract.

1949 Whole Exome Sequencing Identifies Unique Gene Mutations and Copy Number Losses in Calcifying Fibrous Tumor of the Pleura

Mitra Mehrad, William A LaFramboise, Humberto Trejo Bittar, Samuel A Yousem. Vanderbilt University Medical Center, Nashville, TN; University of Pittsburgh Medical Center, Pittsburgh, PA.
Background: Calcifying fibrous tumor of the pleura (CFT) is a rare benign mesenchymal lesion with propensity to local recurrence, composed of paucicellular hyalinized collagenous tissue interspersed with bland spindle cells, and psammomatous/dystrophic calcifications. The pathogenesis is unknown and the diagnosis often requires exclusion of other common entities such as solitary fibrous tumor (SFT). Given the morphologic overlap with SFT we postulated that CFT may represent a sclerosing end-stage of SFT and attempted to study its genetic characteristics contributing to tumorogenesis.
Design: Surgical pathology files were searched and 3 paired cases of CFP and matched uninvolved lung tissue, the latter to serve as internal control, were identified. Immunohistochemistry (IHC) for STAT6, BCL-2, CD34, cytokeratin AE1/AE3, calretinin, desmin, and B-catenin was utilized on all tumor cases. Whole exome sequencing (WES) of DNA isolated from CFTs and matched uninvolved lungs was performed on all 3 pairs.
Results: Two patients were male and one female with age range of 21-32 years (mean: 28 years). Tumors were multifocal in 2 cases and solitary in 1, ranging in size from 1.0 - 5.0 cm. All IHC studies were negative in CFTs. While by WES there were no individual variants shared among the 3 cases, deleterious tumor-specific variants were identified in 3 genes including heterozygotic de-novo mutations in the Zinc Finger Protein 717 (*ZNF717*), fascioscapulohumeral muscular dystrophy-1 (*FRG1*) and cell division cycle 27 (*CDC27*) genes. In addition, WES revealed statistically significant tumor-specific copy number losses (CNL) shared in all CFTs, involving 114 genes (range: 1-32, mean 7.1) found on chromosomes 1, 3, 6, 12, 14, 15, 17 and 22, with substantial CNL at 6p22.2, resulting in loss of a cluster of 32 histone genes. Losses did not exhibit common copy number variations in healthy patients.
Conclusions: This is the first study to evaluate the molecular pathogenesis of CFT and to identify novel deleterious mutations most commonly found in *ZN717*, *FRG1* and *CDC27* genes as well as significant, non-random CNL on 8 chromosomes. These mutations are predicted to be damaging and perhaps contribute to the CFT tumorogenesis. The different IHC expression pattern in CFT compared to SFT and its unique genetic alterations suggest that CFT is a different clinicopathologic entity than SFT.

1950 Noninfectious Pulmonary Complications After Allogeneic Hematopoietic Stem Cell Transplantation: A Spectrum of Histopathological Patterns

Véronique Meignin, Françoise Thivolet-Bejui, Marianne Kambouchner, Claire Hussenet, Claire Danel, Anne Bergeron. Hôpital Saint Louis, Paris, France; Hospices Civils, Lyon, France; Hôpital Avicenne, Bobigny, France; Hôpital Bichat, Paris, France.
Background: Late onset noninfectious pulmonary complications (LONIPCs) frequently occur after an allogeneic hematopoietic stem cell transplantation (HSCT). As there is no consensus on the description of the pathological legends, pathologists reports and clinical conclusions are largely inconsistent in routine practice.
Design: Lung biopsies performed in 18 centers in patients diagnosed with an LONIPC were histopathologically reviewed. Infectious disease was excluded by clinical and radiological investigations and appropriate microbiological studies. For interstitial lesions, the observed patterns were classified according to the 2013 American Thoracic Society and European Respiratory Society classification of idiopathic interstitial pneumonia. For bronchiolar lesions, following features were studied: 1/ the size of the bronchioles (narrowed or ecatatic) , 2/ the presence or absence of fibrosis in the bronchiolar wall and 3/ the density and composition of the inflammatory infiltrate in the bronchiolar wall.
Results: We reviewed 60 lung biopsies, including 50 surgical lung biopsies, 4 post mortem biopsies and 6 lung explants. We found both bronchiolar (n=58) and interstitial lung diseases (ILDs, n=27). We described 2 types of bronchiolar lesions: ectatic (n=37) and narrowed fibrous and cellular lesions (n=43). We found a wide spectrum of ILDs including organizing pneumonia (n=8), nonspecific interstitial pneumonia (NSIP, n=9), diffuse alveolar damage ‘(n=6), lymphoid interstitial pneumonia (n=1), and pleuroparenchymal fibroelastosis (PPFE, n=2), as well as one case of associated PPFE and NSIP. Interstitial diseases were associated with bronchiolar lesions in 93% of thes cases. Lung inflammation was still present in lung explants from patients who underwent lung transplantation for post allogeneic HSCT endstage respiratory insufficiency due to LONIPC.
Conclusions: Herein, we described a wide spectrum of pathological post allogeneic HSCT LONIPCs which could help harmonizing pathological examination in routine practice.

1951 PD-L1 Expression Is Associated with *KRAS* and *BRAF* Mutations in Primary Lung Adenocarcinomas

Christine Minerowicz, Caitlyn Miller, Sanja Dacic. University of Pittsburgh Medical Center Presbyterian, Pittsburgh, PA.
Background: Programed cell death-ligand 1 (PD-L1) has emerged as an important immunotherapy target in lung carcinoma with improved tumor free survival and overall survival. The relationship between PD-L1 and driver mutations is not fully elucidated. The aim of this study was to characterize PD-L1 expression in primary lung adenocarcinoma (ADC) and squamous cell carcinoma (SQC) and correlate with gene mutations, amplifications and rearrangements.
Design: We selected 241 ADC and 120 SQC primary lung tumors as classified according to the 2015 WHO criteria for this study. Immunohistochemistry for PD-L1 was performed using a monoclonal anti-PD-L1 antibody (clone SP263 Ventana, Tuscon, AZ) on a Ventana BenchMark ULTRA staining system. Tumors exhibiting ≥25% cytoplasmic/membranous staining of any intensity were deemed positive. Ion AmpliSeq targeted next generation sequencing for *KRAS*, *BRAF, EGFR*, *MET* and *ALK* mutation, FISH for *MET* amplification, and FISH for *ALK, RET* and *ROS1* gene rearrangement was performed on all ADC tumors. FISH for *FGFR1* amplification was performed on a subset of 22 SQC tumors.
Results: PD-L1 expression was detected in 44% (105/241) of ADC and 17% (20/120) of SQC tumors (p=0.01). Wild type ADC (for panel tested) were PD-L1 positive in 38% (43/113) of tumors compared to 53% (31/58, p=0.01) of *KRAS* mutated tumors and 67% (8/12, p=0.04) of *BRAF* mutated tumors. There was no significant difference in PD-L1 expression in 21% (4/19) of *EGFR* mutated tumors and 0% (0/2) of *MET* mutated tumors as compared to wild type. PD-L1 expression was detected in 60% (6/10) of *MET* amplified tumors but did not reach statistical significance (p=0.09). PD-L1 expression was seen in 44% (4/9) of *ALK*, 50% (1/2) of *RET* and 0% (0/1) of *ROS1* gene rearrangement tumors. SQC positive for *FGFR1* amplification demonstrated positive PD-L1 staining in 40% (2/5) of tumors as compared to 18% (3/17, p=0.22) of SQC negative for *FGFR1* amplification.
Conclusions: In our cohort PD-L1 expression was more frequent in ADC than SQC. Positive PD-L1 expression was more likely in ADC tumors with *KRAS* and *BRAF* mutations than wild type tumors. Future studies should examine the clinical significance of co-existent PD-L1 expression and the presence of oncogenic mutations, amplifications and gene rearrangements.

1952 Tumor Metabolism in the Microenvironment of Squamous Cell Carcinoma of Lung

Mehri Mollaee, Marina Domingo-Vidal, Diana Menezes, Tingting Zhan, Ubaldo Martinez-Outschoorn, Madalina Tuluc. Thomas Jefferson University, Philadelphia, PA.

Background: Tumor microenvironment has a critical influence in tumor growth and spreading. Our group previously demonstrated tumor metabolism in head and neck squamous cell carcinoma, and anaplastic thyroid cancer, highlighting specifically the staining characteristic of monocarboxylate transporter 1 (MCT1), translocase of the outer mitochondrial membrane member 20 (TOMM20) a marker of mitochondrial oxidative phosphorylation (OXPHOS), and monocarboxylate transporter 4 (MCT4) as a marker of glycolysis. The current study aimed to investigate the mitochondrial metabolism alteration of squamous cell lung cancer (SCLC) by studying the same markers of mitochondrial metabolism.

Design: 22 subjects were enrolled in this retrospective cohort study. There were 11 SCLC samples (9 lobectomies, 3 wedge resections specimens) with the following pathological staging: 8/11 (stage IA), 1/11 (stage IB), 1/11 (stage IIA), 1/11 (stage IIB) and 11 cases of non-cancerous lung controls. All 22 cases were stained for MCT1, TOMM20 and MCT4. The expressions and pattern of Immunohistochemistry (IHC) in cancer cells and the stroma were visually scored as low <30%, intermediate 30%-70% and high >70% based irrespective of intensity. The percentages of positive cells were assessed and quantified by digital image analysis with Aperio scoring software using the co-localization and membrane algorithms.

Results: All 11 SCLC revealed notable membrane staining of cancer cells for MCT1, cytoplasmic staining for TOMM20 and stromal pattern of staining of MCT4. The cancer cells significantly expressed the MCT1 and TOMM20 (>70% both) as opposed to normal lung specimens that failed to show expression (<30%). The SCLC cases showed apparent expression of MCT4 stromal staining especially within the nests of proliferating cancer cells (>70%) compared to non-cancerous lung tissue. The percentage of MCT1, TOMM20 staining in SCLC tumor cells by Aperio software were highly significant as compared to non-cancerous tissue ($p < 0.001$, $p < 0.001$ respectively).There was also more significant percentage of MCT4 staining in stromal cells of SCLC as opposed to non-cancerous tissue (p=0.007 value).

Conclusions: The high expression of MCT1, TOMM20 and MCT4 in SCLC suggests a distinct mitochondrial metabolic feature in NSCLC from non-cancerous lung tissue. Hence we hypothesize targeting of these markers could be a potential therapeutic options.

1953 Histologic Patterns of Lung Cancers Associated with MET Exon 14 Splice Site Alterations (MESSA): A Study of 58 Cases

Joseph Montecalvo, Deepu Alex, Victoria Lai, Mark Kris, Alexander Drilon, Maria E Arcila, Marc Ladanyi, Natasha Rekhtman, William Travis. Memorial Sloan Kettering Cancer Center, New York, NY.

Background: MESSA have been reported in approximately 3% of non-small cell carcinoma (NSCC) cases and afford important treatment options. However, the histologic patterns associated with this molecular subset have not been described in detail. Here we describe the incidence and histologic features of lung carcinomas with MESSA.

Design: Using a hybrid capture based NGS assay analyzing mutations and copy number of 410 genes, we identified 58 cases with MESSA out of a total 1682 NSCC cases screened (3.4%). Histologic slides of the cases with MESSA were reviewed, including resection specimens [n=19], biopsy specimens [n=22], and cytology specimens [n=8], focusing on the histologic type and predominant histologic patterns. MET IHC (Ventana; clone SP44, prediluted) was performed on 10 MESAA-positive specimens, 5 of which showed *MET* amplification (by hybrid capture assay) and 5 of which did not.

Results: Of the 58 NSCCs with MESSA, the diagnostic categories included 1) adenocarcinoma (ADC) or NSCC, favor ADC [n=34], 2) squamous cell carcinoma or NSCC, favor squamous cell carcinoma [n=3], 3) NSCC, not otherwise specified [n=1], 4) pleomorphic carcinoma or NSCC with spindle or giant cell features (sarcomatoid carcinomas) [n=19], and 5) adenosquamous carcinoma [n=1]. One case consisted of a keratin negative resected spindle cell tumor. Predominant histologic patterns from resection, biopsy, and cytology specimens were as follows: spindle cell (31%), solid ADC (29%), acinar ADC (14%), lepidic ADC (12%), squamous cell carcinoma (6%), papillary ADC (4%), giant cells (2%), and micropapillary ADC (2%). MET IHC showed diffuse, strong, membranous staining regardless of MET amplification status.

Conclusions: The predominant histologic patterns of NSCC with MESSA are varied with the most common being spindle cells and solid patterns. Our findings support prior observations that MESSA are substantially over-represented in sarcomatoid carcinomas, which are rare but account for over 30% of cases with MESSA. We identified three cases of squamous cell carcinoma with MESSA, affording treatment options for a tumor which generally does not have a specific treatment. Although further study is needed, our MET IHC immunohistochemical results suggest that MET overexpression is not related to MET amplification in cases with MESSA. Given prior data on specificity of MESSA to lung carcinomas, the finding of MESSA in a keratin negative pleomorphic lung tumor appears to provide a new criterion for diagnosis of pleomorphic carcinoma.

1954 Neoplastic Architectural Remodeling as an Aggressive Histological Indicator of Early Stage Lung Adenocarcinoma

Noriko Motoi, Masaya Yotsukura, Aoi Sukeda, Hisao Asamura, Shun-ichi Watanabe, Nobuyoshi Hiraoka. National Cancer Center Hospital, Chuo-ku, Tokyo, Japan; Keio University School of Medicine, Shinjuku-ku, Tokyo, Japan.

Background: For an adequate therapeutic decision of lung cancer, an accurate assessment of invasion degree is important. In the 2015 WHO classification of lung tumor, invasion of pulmonary adenocarcinoma (AdCa) was defined as a presence of non-lepidic, so-called invasive subtypes and/or the cancer-associated active fibroblast (AF). The former has a matter of inter-observer discordancy. We hypothesize that the neoplastic architectural remodeling (NAR) is one of the morphological indicators of cancer aggressiveness and studied on its prognostic impact in early stage AdCa.

Design: Surgically resected 1,032 pulmonary AdCa of pStage 0 (n=166) and IA (n=866) with more than 5 years follow-up were recruited. We defined two subgroups of invasive AdCa: those with (INV-1) and without (INV-2) NAR. The NAR is defined as a neoplastic non-lepidic structure which destructs the original pulmonary framework that can be highlighted by an elastic stain. The clinicopathological characteristics and the postoperative recurrence of the tumor were analyzed in each group.

Results: Of the 866 stage IA, 696 (80.4%) and 170 (19.6%) were categorized as INV-1 and INV-2, respectively. AF was observed in all cases in the INV-2 but was not always present in the INV1. In the INV-2, the median diameter of the invasive component was 6 mm (range: 1-16), and none of the cases developed recurrence. In the INV-1, INV-2 and AIS group, the median follow-up period was 55, 61, 60 months (range: 2-104, 13-105, 17-100) and the estimated 5-year recurrence-free probability by the Kaplan-Meier method was 93.1, 100 and 100%, respectively. All cases with postoperative recurrence belonged to the INV-1. The INV-1 showed older age at operation (p=0.025), male dominant (p=0.039), association with cigarette smoking habits (p=0.046), lepidic subtype recessive ($p<0.001$), and a higher rate of lymphovascular invasion ($p<0.001$) compared to the INV-2. Tumor location and size of tumor did not show a significant difference between two subgroups.

Conclusions: Our study results indicate that a certain subset of pulmonary AdCa which defined as invasive by the presence of AF but does not have NAR assessed by an elastic stain had a very low risk of recurrence. Here, we propose the presence of NAR as an aggressive morphologic indicator of primary lung AdCa.

1955 Ultrasensitive ALK (D5F3) Immunohistochemistry in Inflammatory Myofibroblastic Tumor of the Lung and Trachea: A Multi-Institution Series of 34 Cases

Sanjay Mukhopadhyay, Deepali Jain, Andrea V Arrossi, Masakazu Soda, Charanjeet Singh, Junya Fukuoka, Lara Pijuan, John D Gentry, Ola El-Zammar, Sergej Griff, Jesse K McKenney, Carol Farver. Cleveland Clinic, Cleveland, OH; All India Inst of Medical Sciences, Delhi, India; Nagasaki University, Sakamoto, Nagasaki, Japan; Florida Hospital, Orlando, FL; Hospital del Mar, Barcelona, Spain; SUNY Upstate Med Univ, Syracuse, NY; HELIOS Kliniken Berlin, Berlin, Germany; Methodist Hospital, Omaha, NE.

Background: Most prior studies on inflammatory myofibroblastic tumor (IMT) are either from years prior to the availability of ALK FISH and ultrasensitive ALK immunohistochemistry (IHC) or have analyzed IMTs of the lung along with IMTs of other organs. The aim of this study was to compare the diagnostic utility of the ultrasensitive ALK antibody D5F3 to ALK-1, ALK FISH and conventional markers of myofibroblastic differentiation for IMTs of the lower respiratory tract (lung/trachea).

Design: IMTs of the lung and trachea were retrieved from the files of 8 institutions from 5 countries. FISH for ALK and IHC for ALK (D5F3, Cell Signaling), ALK-1, smooth muscle actin, desmin, actin and IgG4 was performed on whole-tissue sections in all cases where blocks were available.

Results: There were 34 IMTs (27 lung, 7 trachea) from 34 patients (19F/15M, mean age 26 years, range, 3-70y, 12 children/22 adults). IHC for ALK (D5F3) was positive in 28/31 (90%) cases and IHC for ALK-1 was positive in 23/33 (70%). ALK D5F3 staining was moderate or strong in 26 and weak in 2; distribution was diffuse in 27 and patchy in 1. In all tumors that were positive for both ALK antibodies, staining intensity with D5F3 was stronger than with ALK-1. Smooth muscle actin, muscle-specific actin (HHF35) and desmin stained 16/27 (59%), 8/20 (40%) and 6/25 (24%) cases, respectively. ALK FISH was positive in 19/33 (58%) cases tested (12 were negative and 2 were inconclusive). Five cases were negative for ALK-1 but positive for ALK D5F3. Ten cases were negative or inconclusive by ALK FISH but positive by ALK D5F3.

Conclusions: This study is the largest series of IMT of the lower respiratory tract to date. It shows that ALK D5F3 is a more sensitive marker for IMTs of the lung and trachea than ALK-1 IHC, myofibroblastic markers and ALK FISH. Additionally, ALK D5F3 staining intensity is consistently stronger than ALK-1, facilitating interpretation. In a subset of cases, ALK (D5F3) IHC is diagnostic when ALK FISH is negative or inconclusive. ALK D5F3 is the most effective ancillary marker for the diagnosis of IMTs of the lung/trachea.

1956 Enrichment of Immune Cells in Tumor Microenvironment Correlates with Long-Term Survival in Small Cell Lung Cancer

Prasuna Muppa, Simone BSP Terra, Aqsa Nasir, Nafiseh Janaki, Marie C Aubry, Eunhee S Yi, Aaron S Mansfield, Mariza de Andrade, Ping Yang, George Vasmatzis, Virginia P Van Keulen, Tobias Peikert, Farhad Kosari. Mayo Clinic, Rochester, MN.

Background: A small subset of small cell lung cancer (SCLC) patients survives for many years after their initial diagnosis. Tumor cytology and molecular factors that contribute to the long term survival (alive >4 years after surgery) remains unknown. We studied tumors from patients with long term survival (LS) and short survival (SS, died <2 years of surgery) to determine the histological, cytological, and molecular features of the differential outcomes.

Design: We identified 12 patients with LS and 14 patients with SS after surgery for this study. There were no statistical differences in age, gender, clinical TNM stage, curative versus non-curative intent surgery, and smoking status between the two cohorts. Tissue sections were stained for immune cell markers, including CD3, CD4, CD8, CD14, CD20, CD21, CD68, CD279 (PD-1), FoxP3, CD138, and Lysozyme. Concentrations of immune cells in intra-tumor areas, stroma, and tumor/non-tumor interface were assessed using an automated image analysis program (Aperio). Tumor areas were also macrodissected for gene expression profiling.

Results: We observed significantly higher concentrations of immune cells, including CD8 and PD-1 positive cells, in the tumor microenvironment, especially at the stromal and tumor/nontumor interface, in LS compared to SS ($p < 0.005$ for both markers). The total number of infiltrating immune cells (T-cells, B-cells, Plasma cells, monocytes and macrophages) was significantly higher in the tumor/non-tumor interface region ($p < 0.0005$) of the LS patients. Furthermore, over 200 genes were over-expressed in the tumors of LS compared with SS patients and the majority of these genes were either MHC or immunoglobulin related or had immune related functions (ex. cytokines).
Conclusions: Enrichment of immune cells, especially cytotoxic T-cells, in the tumor microenvironment, particularly at the tumor-stromal interface, may be a major contributor to the long term survival in SCLC.

1957 Lung Adenocarcinoma with GATA6 Expression Is Associated with Invasive Mucinous Adenocarcinoma Histology and HNF4alpha, but a Better Prognosis

Naoki Nakajima, Akihiko Yoshizawa, Hironori Haga. Kyoto University Hospital, Kyoto, Japan.
Background: GATA binding factor 6 (GATA6) plays a role in epithelial differentiation in development phase of the lungs. However, GATA6 expression status in lung cancer has not been well studied. The aim of this study was to analyze GATA6 expression in resected lung adenocarcinomas (LA) using immunohistochemistry (IHC) to define the clinicopathological characteristics.
Design: IHC analysis of GATA6 was performed using tissue microarray slides of 348 LAs. Scoring was based on the H score. The association between GATA6 expression and the following clinicopathological parameters was evaluated: sex; age; smoking status; tumor stage; tumor grade; lymphovascular invasion; pleural invasion; expression of TTF-1, HNF4alpha, MUC5B, MUC5AC, CDX2, and MUC2; mutation status of *EGFR*, *KRAS*, *BRAF*, and *HER2*; and fusion status of *ALK* and *ROS1*. Survival rates were calculated using the Kaplan–Meier method.
Results: Forty-seven (13.5%) cases were GATA6-positive. Most patients with GATA6-expressing tumors were younger (<65 years old, $p=0.005$). GATA6 expression was associated with well- to moderately differentiated tumors ($p<0.001$), absence of lymphatic invasion ($p=0.020$), and absence of vascular invasion ($p=0.011$), whereas it was not associated with sex, smoking status, tumor size, tumor stage, or pleural invasion. GATA6 expression was significantly associated with invasive mucinous adenocarcinoma (IMA) ($p<0.001$); *KRAS* mutations ($p=0.016$); positive expression of HNF4alpha ($p<0.001$), MUC2 ($p<0.001$), CDX2 ($p=0.006$), and MUC5AC ($p<0.001$); and negative expression of TTF-1 ($p=0.007$). Patients with GATA6-expressing tumors tended to have a better prognosis; however, this was not statistically significant ($p=0.346$). On the other hand, patients with HNF4alpha-expressing tumors had a significantly worse prognosis ($p=0.032$), although GATA6 expression was strongly associated with HNF4alpha expression.
Conclusions: The present study showed that LAs with GATA6 expression were associated with low-grade tumors with mucinous histology, IMA, and *KRAS* mutations. HNF4alpha, which is known to be an IMA marker, was strongly associated with GATA6 expression in this study. However, patients with GATA6-expressing tumors tended to have a better prognosis, while those with HNF4alpha-expressing tumors showed a significantly poorer prognosis. Taken together, clinicopathological characteristics of LAs with GATA6 expression seem similar to those with HNF4alpha expression; however, GATA6 might have a different role in LA development, compared to HNF4alpha.

1958 Intratumoral Heterogeneity of Programmed Cell Death Ligand-1 (PD-L1) Expression in Lung Cancers - Assessment by Spiral Array

Sayuri Nakamura, Kentaro Hayashi, Yuki Imaoka, Yuka Kitamura, Yuko Akazawa, Ruben Groen, Takeshi Nagayasu, Naoya Yamasaki, Tomoshi Tuchiya, Junya Fukuoka. Graduate School of Biomedical Sciences, Nagasaki University, Nagasaki, Japan.
Background: Assessment of PD-L1 expression in lung cancer tumors may predict the response to the programmed cell death-1 inhibitors. However, potential degree of intratumoral heterogeneity in PD-L1 expression which may cause false negative results is largely unexplored. Our aim was to examine the PD-L1 expression in surgically resected lung cancers by applying a novel method named Spiral Array.
Design: Total of 138 Lung cancer cases with surgical resection from 1998 to 2016 were selected, which included adenocarcinoma (n=60), squamous cell carcinoma (n=59), small cell carcinoma (n=12), and large cell carcinoma (n=7). Two orthogonally dissected sections from a paraffin embedded block were obtained. Sections were then reeled into cores and embedded into Spiral Array, which were subjected to immunohistochemistry using anti-PD-L1 (clone 28-8) antibody. Each core was separated into eight segments, which resembled the size of lung biopsy. The PD-L1 positivity of tumor cells was defined by four different thresholds (1%, 5%, 10%, and 50%).

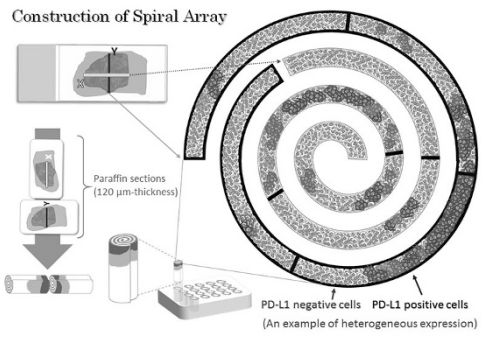

Results: Overall, Cases that had PD-L1 positive segments were 42 (30.4%), 39 (28.3%), 33 (23.9%) and 21 (15.2%) utilizing the threshold of 1%, 5%, 10%, and 50%, respectively. Majority of the tumors showed heterogeneous expression pattern regardless of thresholds [28/42 (66.7%), 29/39 (74.4%), 25/33 (75.8%) and 18/21 (85.7%), utilizing thresholds of 1%, 5%, 10%, and 50%, respectively]. Majority of the tumors with heterogeneous expression contained at least half of negative segments although the ratio of positive segments largely varied among the cases.

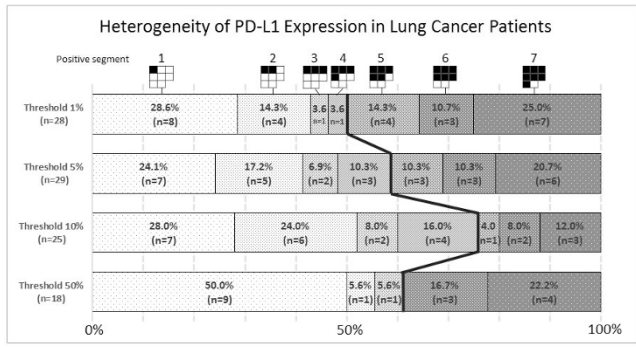

Conclusions: PD-L1 expression shows intratumoral heterogeneity in lung cancers. Our results by Spiral Array suggest that relatively high number of biopsy specimens may be required for PD-L1 companion diagnosis.

1959 Comprehensive Analysis of PD-L1 Expression in Primary Resected Squamous Cell Carcinoma of the Lung and Lymph Node Metastases

Christina Neppl, Manuel Keller, Yasin Irmak, Sean R Hall, Ralph A Schmid, Rupert Langer, Sabina Berezowska. University of Bern, Bern, Switzerland; Inselspital University Hospital Bern, Bern, Switzerland.
Background: Immunomodulation by inhibiting the PD1/PD-L1 pathway is a highly promising new therapeutic approach in non-small cell lung carcinoma treatment. The prognostic and predictive value of PD-L1 expression is still controversially discussed.
Design: We evaluated consecutive cases of primary resected squamous cell carcinoma of the lung, resected 2000-2013. Only p40 positive tumors were included. Two PD-L1 antibodies - E1L3N (E) and SP142 (SP) - were evaluated on 8 TMA cores per tumor and full slides, including lymph node (LN) metastases. Staining was scored as percentage of positive tumor cells, using the increments: <1, 1-<5, 5-<10, 10-<25, 25-<50, >50. CD3 and CD8 positive lymphocytes were scored. Results were correlated with clinico-pathological parameters.
Results: In total, 372 cases could be assessed on 8 TMA cores per tumor. Of 42 cases with N2-LN metastases, 41 full slides of LN metastases and paired primaries were included. PD-L1 expression was <1% in 163 (43%; E) and 231 (61%; SP) tumors, and >50% positive in 74 (20%; E) and 47 (12%; SP) tumors.
For both antibodies, there was a strong correlation between staining on full slides and TMA cores ($p<0.001$), and primary tumors versus LN metastases ($p<0.001$). Staining correlated between the antibodies used ($p<0.001$), but clone E was more sensitive.
Best prognostic cut off was 5% for E and 1% for SP for PD-L1 positivity associated with both shorter progression free survival (PFS; E: $p=0.009$, SP: $p=0.001$) and shorter tumor specific overall survival (OS; E: $p=0.004$, SP: $p=0.001$). PD-L1 expression was an independent prognostic factor in multivariate analysis for PFS (E: $p=0.008$, HR 1.7; SP: $p=0.001$; HR 1.98) and tumor specific OS (E: $p=0.003$; HR 2.09; SP: $p=0.001$, HR 2.25), together with age and T-stage. Both antibodies correlated positively with CD3 and CD8 numbers ($p<0.001$). Of note, CD3 and CD8 values had no prognostic value.
Conclusions: Staining with both PD-L1 clones E and SP strongly correlated, with higher sensitivity of clone E. PD-L1 expression is an adverse prognostic marker in squamous cell carcinoma of the lung. PD-L1 expression correlated between primary tumor and N2 LN metastases, rendering tissue from mediastinal LN metastases adequate for PD-L1 assessment.

1960 Characterization and Correlation of *ALK* Fusion Breakpoints in *ALK* FISH Rearranged Non-Small Cell Lung Cancer by Anchored Multiplex PCR and Next-Generation Sequencing

Catherine Nicka, Francine B de Abreu, Jason D Peterson, Gregory J Tsongalis, Laura Tafe. Dartmouth-Hitchcock Medical Center, Lebanon, NH.
Background: *ALK* rearrangement (AR) in 2-5% of lung non-small cell carcinoma (NSCLC) leads to constitutive activation of the ALK kinase domain which drives tumorogenesis. In our laboratory, break-apart FISH test is used to detect AR to determine eligibility for treatment with ALK targeted therapies. *ALK* FISH is a single-plex assay that cannot differentiate between partner genes or non-canonical breakpoints and can be challenging to interpret with various signal patterns (split signals and 5' deletion) considered positive for AR. We have recently introduced anchored multiplex PCR with next-generation sequencing (NGS) to detect somatic fusion events in FFPE tumor tissues. One of the main advantages of this assay is that it is able to detect fusions without prior knowledge of fusion partners or breakpoints by using universal adaptors. In the study, we sought to further characterize the *ALK* rearrangements and correlate with FISH signal patterns.
Design: DNA and RNA was extracted simultaneously from eight 4 micron unstained slides using the Qiagen AllPrep DNA/RNA FFPE Kit on the QIAcube. RNA underwent reverse transcription to cDNA and was tested for fusions associated with over 50 genes

using the Archer® FusionPlex® Solid Tumor Kit on the Illumina MiSeq instrument. Data analysis was performed using Archer Analysis software (v4.0.11); fusion partner genes or sequence variants are identified after aligning to the reference genome. *ALK* FISH was previously performed with *ALK* Break Apart FISH Probe Kit (Abbott Laboratories).
Results: In a series of 338 NSCLC cases, 12 (3.6%) showed AR by FISH (4 with 5' deletion, 2 with split signal). Six cases were available for the FusionPlex NGS assay; in all cases the translocation was confirmed and the -*ALK* partner gene was identified as *EML4* with breakpoints at exon 20 of *ALK* and at multiple exons of *EML4* (ex13-3; ex6-2; ex18-1). The *ALK* FISH pattern did not necessarily correlate with the fusion breakpoints detected by the FusionPlex assay. In three cases identified with *EML4* exon 13 breakpoint, two showed 5' deletion and one split signal patterns by FISH.
Conclusions: FusionPlex NGS correlated with *ALK* FISH results in a set of AR NSCLC. There is significant genomic heterogeneity in NSCLC gene rearrangements (e.g. *ALK*, *ROS1*, *RET*) and the anchored multiplex design of the assay allows for detection of multiple partner genes without prior knowledge and can be used complementary to FISH analysis in NSCLC to direct personalized care.

1961 Central versus Peripheral Carcinoid Tumors of the Lung

Daisuke Nonaka, George Papaxoinis, Wasat Mansoor. The Christie Hospital, Manchester, United Kingdom; The University of Manchester, Manchester, United Kingdom.
Background: Pulmonary carcinoid tumors occur in both central (endobronchial) and peripheral locations. Indeed, before the current WHO classification scheme became widely accepted, carcinoid tumor was often subdivided to three categories; central, peripheral and atypical, and subtle clinico-pathological differences have been observed between central and peripheral carcinoids, although the differences have been regarded as clinically not particularly relevant. Recently we reported OTP (orthopedia transcription factor) as a useful marker for the diagnosis of lung carcinoid, and, during the investigation, found differences between OTP-positive and negative tumors.
Design: 112 resected carcinoid tumors were subdivided to three subgroups based on OTP (polyclonal, Atlas Antibodies) and TTF1 (clone 8G7G3/1) expressions; type 1 (OTP-/TTF1-), type 2 (OTP+/TTF1-), type 3 (OTP+/TTF1+), and clinical and histopathological parameters were compared among those subgroups.
Results: There were 22 cases in type 1, 33 in type 2, and 57 in type 3. Significant differences were seen between type 1 and 3 in gender, presence of sustentacular cells (STCs), location, circumscription, cell morphology, presence of acinar growth, and presence of neuroendocrine hyperplasia (NH). Type 1 was characterized by male predominance, central location, absence of STC, well-circumscription, polygonal cell type, frequent acinar growth, and no association with NH. Type 3 was characterized by female predominance, peripheral location, presence of STC, and strong association with NH. Type 2 showed features in between. Interestingly, 7 out of 22 (32%) type 1 tumors arose in peripheral location while 9 out of 57 (16%) type 3 tumors occurred in central location.
Conclusions: Given the significantclinic-pathologic differences between type 1 and 3, lung carcinoid tumors may represent a group of tumors with heterogeneous pathogenesis. For instance, lung resection bearing type 3 carcinoid would require careful search for diffuse neuroendocrine hyperplasia. Further studies are required to confirm our findings.

1962 PD-L1 Expression in Thymomas and Thymic Carcinomas: Correlation with Clinicopathologic Features

Patricia P Odashiro, Michèle Orain, Daniela Furrer, Caroline Diorio, David Simonyan, André Moreira, Philippe Joubert. Quebec Heart and Lung Institute - L'IUCPQ, Québec, QC, Canada; Centre de recherche du CHU de Québec Université Laval, Québec, QC, Canada; New York University, New York, NY.
Background: Thymomas (TH) and thymic carcinomas (TC) represent the most common tumors of the mediastinum. The expression of Programmed Death-1 ligand (PD-L1) by tumor cells is an effective mechanism to escape anti-tumor immunity. PD-1/PD-L1 blockade by monoclonal antibodies (Ab) are emerging as an effective treatment option in multiple malignant tumors. Few studies have investigated PD-L1 expression in TH and TC. We aim to characterize PD-L1 expression in TH and TC using three differents PD-L1 Ab.
Design: 52 TH and 8 TC surgical resection cases were used. Tissue Microarrays (TMA) containing 5 representative cores of each tumor were constructed. PD-L1 expression was evaluated by immunohistochemistry (IHC) using three different PD-L1 Ab clones (E1L3N, 22C3 and 28-8). Image analysis software was used to assess PD-L1 staining. 4 cut-offs (1%, 5%, 10%, 50%) were used to classified the cases as positive or negative. Overall percent agreements (OPA) among the three antibodies were calculated for each cut-off. An optimal cut-off value for PD-L1 expression was calculated and used for statistical associations between PD-L1 expression and clinicopathologic features, and in the evaluation of disease-free survival (DFS) and overall survival (OS) curves.
Results: Thymoma B3 was associated with the highest mean PD-L1 expression (70-76%). The lowest mean PD-L1 expression was related with thymoma type AB (21-27%) and TC (20-25%). As expected, the highest and lowest percentage of PD-L1 positive cases was found with 1% cut-off (97-100%) and 50% cut-off (25-32%) respectively. Optimal OPA was found at 1% cut-off with all antibodies (22C3/E1L3N OPA; 96%, 22C3/28-8 OPA; 96%, 28-8/E1L3N OPA; 100%). Positive PD-L1 cases were associated with type B2/B3 TH, late Masaoka stages (III/IV), and age < 66 yo. Among thymomas, positive PD-L1 cases presented significant shorter OS (22C3 p = 0.0115; p = 0.0262).
Conclusions: Our data show that TH and TC express high levels of PD-L1, regardless of the clone used, and that there is a strong correlation in the level of staining between the three Ab studied. Given the high levels of expression of PD-L1 among the different thymic epithelial neoplasms, our study supports the relevance of clinical trials to test the efficacy of PD-1 inhibitors for the treatment of TH and TC.

1963 PDL-1 Expression in Synchronous Lung Nodules: Association with Driver Mutations and CD8+ Cytotoxic T Lymphocytes

Zehra Ordulu, Marina Kem, Tiffany Huynh, Dora Dias-Santagata, John Iafrate, Mari Mino-Kenudson. Massachusetts General Hospital, Boston, MA.
Background: Blockage of immune checkpoints, such as programmed cell death 1 (PD-1)/PD-1 ligand (PD-L1) axis has been shown to improve outcomes of lung cancer patients. PD-L1 expression on the tumor cells may be affected by the tumor-immune microenvironment, including CD8+ cytotoxic T lymphocytes, as well as the molecular alterations within the tumor genome, and could be heterogeneous within the tumor. Understanding the heterogeneity of PD-L1 expression and its mechanisms in patients with synchronous nodules may lead to better patient selection for immunotherapies.
Design: Patients with synchronous lung nodules resected at the same operation without neoadjuvant therapy were screened for mutations using SNaPshot. To assess clonality, cases with at least one tumor with a mutation are included. Membranous PD-L1 staining of any intensity on tumor cells (+: ≥1%) and CD8+ tumor infiltrating lymphocytes (TILs, abundant or not) were assessed by immunohistochemistry on a representative whole section each of the tumor. Several clinicopathologic parameters (age, gender, smoking status, tumor size, stage, predominant histologic pattern) were also collected.
Results: Analysis of 50 nodules from 25 patients (84% female; mean age of 70±8) revealed that there was concordant PD-L1 expression in paired lesions from all 8 (100%) patients with clonally related lung tumors (4 PD-L1(+) and 4 PD-L1(-) pairs) and 8 out of 17 patients (47%) with tumors harboring different clones (1 PD-L1(+) and 7 PD-L1 (-) pairs). Similarly, there was concordant CD8+ TIL scores in paired lesions from all 8 (100%) patients with clonally related lung tumors (four abundant). However, the majority of patients (14/17, 82%) with tumors harboring different clones also showed concordant CD8+ TIL scores between the tumors. Thus, the concordance of CD8+ TIL scores was higher than that of PD-L1 expression in tumors harboring different clones (82% CD8 concordant vs 47% PD-L1 concordant), suggesting that additional factors may influence the tumor-microenvironment. There was no association with the concordance of PD-L1 expression and that of CD8+ TIL scores nor other cliniopatholgic parameters.
Conclusions: The expression of PD-L1 may be heterogeneous in paired multifocal tumors from the same patient, and discrepant PD-L1 expressions indicate clonally different tumors in half of the cases. Our results indicate that a single biopsy in patients with multifocal lung cancer may not accurately capture PD-L1 expression status and emphasize the need for novel methods of patient selection for immunotherapy.

1964 PDL-1 Expression in Lung Adenocarcinoma Evaluated by Immunohistochemistry and RNA ISH Assay

Claudia Ormenisan Gherasim, Diane Lawson, Wanhong Jiang, Cynthia Cohen. Emory University, Atlanta, GA.
Background: Programmed death receptor (PD-1) and its ligand (PDL-1) are immunoregulatory proteins. The PD-1 pathway also has a key role in the tumoral microenvironment in the effector phase. Non-Small Cell Lung Cancer (NSCLC) bypasses the immune system through the induction of pro-tumorigenic immunosuppressive changes.The better understanding of immunology and antitumor immune responses has brought the promising development of novel immunotherapy agents like PD-1 checkpoint inhibitors (anti-PD-1 and anti-PDL-1 antibodies) that improve the capacity of the immune system to acknowledge and delete tumors. The aim of this study was to investigate the expression of PDL-1 in lung adenocarcinoma, comparing two different technologies:immunohistochemistry (IHC) by two methods versus RNA in situ hybridization (RISH).
Design: We selected 20 cases of adenocarcinoma (ADC) of the lung and 4 samples of metastatic colon adenocarcinoma. Evaluation of PDL-1 expression was performed by IHC (rabbit polyclonal Cell Signaling, Leica Bond III immunostainer, 1/200, >5% membranous cytoplasmic stain=positive), (Dako 22C3, Dako Autostainer Link 48, RTU, >50% membranous, cytoplasmic stain=positive) and RISH. RISH was performed using RNAscope (Leica, BioSystems, Buffalo Grove, IL), the Bond III immunostainer, and probe Hs-CD274 (Advanced Cell Diagnostics, Newark, CA). Specific staining signals were identified as brown, punctate dots present in the cytoplasm and/or nucleus. Both methods were scored in tumor cells and quantified using combined intensity and proportion scores.
Results: Eight of twenty (40%) lung ADC and two of four (50%) colon ADC were positive for PDL-1 with Cell Signaling IHC, and 65% lung ADC were positive by Dako IHC (13/20). All four cases of colon ADC were negative (low positive, <50% membranous and cytoplasmic staining). When evaluated by RISH, twelve lung ADC (60%) and one colon ADC (25%) were PDL-1 positive.

	PDL-1 Cell Signaling	PDL-1 Dako IHC	PDL-1 RISH
Sensitivity	40%	65%	60%
Specificity	50%	100%	75%
PPV	80%	100%	92%
NPV	14%	36%	27%

Conclusions: RNAscope probes provide sensitive and specific detection of PDL-1 in lung adenocarcinoma. Both IHC methods (Cell Signaling and Dako) show PDL-1 expression, with the Dako method more sensitive (40% vs 65%). Dako specificity is 100% compared to 75% by RISH and 50% by Cell Signaling IHC. This study illustrates the utility of RNA ISH and Cell Signaling IHC as complementary diagnostic tests, and FDA approved Dako IHC as a companion diagnostic test for treatment with pembrolizumab in lung ADC.

1965 Limited Molecular Testing (MT) of Multiple Pulmonary Tumors in a Single Resection Specimen: Correlation with Morphologic Staging

Carlos Pagan, Jonas Heymann, Mark Stoopler, Adrian Sacher, Catherine Shu, Naiyer Rizvi, John Crapanzano, Anjali Saqi. Columbia University Medical Center, New York, NY.

Background: Pathologic stage is a strong predictor of survival in patients with lung cancer. In the current (7th) edition of the AJCC manual, multiple synchronous lung tumors may be staged as multiple T1-2 or T3-4 (histologically similar tumors in the same or >1 ipsilateral lobe, respectively). Adenocarcinomas (ADCA) constitute a plurality of lung cancers. ADCA may have mixed histologic patterns and determination of morphologic similarity can be challenging. The aims of this study are to determine if morphology can accurately differentiate multiple T1-2 from T3-4 lesions using a targeted molecular panel as the gold standard.

Design: All lung carcinomas with pathologic stageT1, T2, T3 or T4 based on multiple nodules in single resection specimen were reviewed. Corresponding results from a limited MT panel for each tumor were reviewed as follows: *EGFR* mutation by Sanger (SS) or next-generation (NGS) sequencing, *KRAS* mutation by SS, Scorpion-ARMS or NGS, *BRAF* mutation by SS, real time-PCR or NGS, *PIK3CA* mutation by NGS, and *ALK* rearrangement by FISH.

Results: Lung carcinoma specimens [51 ADCA, 8 squamous cell carcinoma (SQCA), 11 other]were collected from 21 men and 49 women of median age 71.5 (range, 45-86) with pathologic stage T3 (29), T4 (4), or separate T1-2 (37) based on morphologic impression. MT was performed on >1 nodule in 35 cases (T1-2 =22; T3 =12; T4 =1). Of these, 11had identical mutations in *KRAS* (6), *EGFR* (4) and *PIK3CA* (1) , and 11 had disparate mutations, including 1 *BRAF* mutation. No rearrangements were identified in *ALK*. Based on MT, 31% (11/35) of patients would be restaged.

Conclusions: Morphologic impression does not always correlate with MT results. Current guidelines do not recommend routine use of MT to determine pathologic stage in the setting of multiple lung tumors. In this study, 31% of patients would be restaged after MT of a panel consisting of only 4 genes. Such restaging, along with identification of mutations in known oncogenes, will potentially have significant prognostic and therapeutic impact.

1966 Are Respiratory Bronchiolitis, Emphysema and Smoking-Related Interstitial Fibrosis (SRIF) Accurate Markers of Smoking Status? A Histologic Study of 119 Surgically Resected Lung Specimens

Andrea Pannunzio, Sanjay Mukhopadhyay. Cleveland Clinic, Cleveland, OH.

Background: Respiratory bronchiolitis (RB) and emphysema are widely accepted histologic manifestations of cigarette smoking. We undertook this study to determine (1) whether taking the severity of histologic findings into account or combining findings increases their predictive value as indicators of smoking status and (2) whether smoking-related interstitial fibrosis (SRIF) is a better marker of smoking status than RB or emphysema alone.

Design: An H&E-stained slide most representative of the non-neoplastic lung was selected from 119 consectuive surgically resected lung specimens (surgical lung biopsies, lobectomies, pneumonectomies, explants), and assessed for RB, emphysema and SRIF by a pulmonary pathologist blinded to smoking status. Histologic findings were assigned points as follows: possible/minimal RB: 1, possible/minimal emphysema: 1, definite RB: 2, definite emphysema: 2. Points were added to obtain a Smoking Likelihood Score (SLS) ranging from 0-4. SRIF (fibrosis + RB + emphysema) was scored directly as SLS 5. Smoking status was retrieved from medical records by a separate pathologist. Statistical analysis was performed using a 4x4 contingency table and Fisher's exact test.

Results: There were 68 men and 51 women (mean age 62, range 18-91); 89 were smokers and 30 were never-smokers. The association between histologic findings and smoking status is shown below:

Blinded histologic diagnosis	Number of cases	Smokers (current + ex)	Never-smokers	p value (two-tailed)
RB, definite	50	48	2	<0.0001
Emphysema, definite	37	36	1	<0.0001
SLS 2-4	67	57	10	0.0052
SLS 5 (SRIF)	9	9	0	0.1095
Total	119	89	30	

Patients with definite RB, definite emphysema or SLS scores of 2-4 were statistically signifcantly more likely to be smokers (Fisher exact test, 2-tailed). SLS scores of 0 and 1 were not associated with smoking status. All patients with an SLS score of 4 (definite RB + definite emphysema) were smokers. Similarly, all patients with an SLS score of 5 (SRIF) were smokers, although this finding did not reach statistical significance because of the small number of SRIF cases.

Conclusions: RB and emphysema are robust histologic markers of cigarette smoking, but only if the findings are definite/unequivocal. The combination of RB and emphysema increases the predictive value. SRIF occurs exclusively in cigarette smokers, and therefore may be a more reliable marker of smoking status than RB or emphysema alone.

1967 The Utility of E2F1 Protein Expression in Well-Differentiated Papillary Mesothelioma

Kyung Park, Yuis Jimenez, Robert Taub, Gleneara Bates, Alain C Borczuk. Weill Cornell Medicine, New York, NY; Columbia University Med Ctr, New York, NY.

Background: Well-differentiated papillary mesothelioma (WDPM) of the peritoneum is a rare disease often discovered as an incidental finding. It is associated with benign clinical course. It can be diagnostically challenging to differentiate WDPM from malignant mesotheliomas with large WDPM, WDPM with invasion, and papillary mesothelioma as particular problems. In this study, we investigated if E2F1 IHC could be a differential marker in mesothelioma subtypes.

Design: The cohort consisted of 189 abdominal mesotheliomas: 13 WDPM, 135 epithelioid mesotheliomas (EM), and 41 biphasic mesotheliomas (BM). IHC was performed on FFPE tissues using monoclonal mouse antibody against E2F1 (LifeSpan BioSciences, Inc., Seattle, WA). Nuclear E2F1 protein expression was evaluated by study pathologists and determined using a four-tier grading system: negative (positive in <1% of tumor cells), weakly positive (1+), moderately positive (2+), and strongly positive (3+). Statistical analyses were performed using SPSS software version 21.0

Results: Patients with WDPM were more likely to be younger and female.

		WDPM	EM	BM
Age [median (range)]		48 (20-84)	59 (30-88)	56 (15-79)
Sex	Male	6 (46%)	82 (61%)	29 (71%)
	Female	7 (54%)	53 (39%)	12 (29%)
E2F1 IHC Intensity	0	1 (8%)	7 (5%)	0
	1	12 (92%)	29 (21%)	10 (24%)
	2	0	76 (56%)	21 (51%)
	3	0	23 (17%)	10 (24%)
Median overall survival (days)		Not reached	1664	214

All WDPM showed 0 and 1+ nuclear expression of E2F1. In contrast, 73% and 76% of EM and BM, respectively, had strong (2+ and 3+) protein expression. The 2+ and 3+ cases were diffuse. The difference in intensity was statistically significant with p-value <0.01. Clinical follow-up was available for 187 patients; median overall survival was not reached in WDPM, 1664 days in EM, and 214 days in BM, respectively.

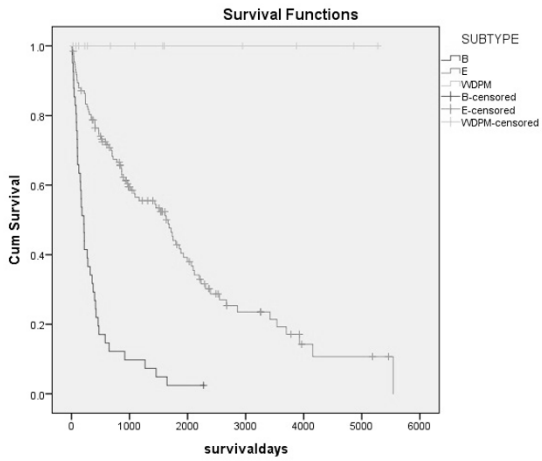

Conclusions: Our study underscores the importance of distinguishing WDPM from malignant mesotheliomas as it carries different prognosis and therefore may alter therapy. In conjunction with morphologic evaluation, strong E2F1 expression suggests that a mesothelial neoplasm is more likely to be malignant mesothelioma than WDPM.

1968 Morule-Like Changes in Lung Adenocarcinoma

Pallavi A Patil, Bassam Aswad, Maria L Garcia-Moliner. Brown University Rhode Island Hospital, Providence, RI.

Background: Morule-like changes in lung adenocarcinoma have been infrequently described in literature with conflicting reports on their significance. We conducted a retrospective analysis of lung adenocarcinoma cases to determine morule formation rate, associated clinocopathologic characteristics, and prognosis.

Design: Records from 2000-2008 were queried for lung adenocarcinomas. 96 cases with solitary adenocarcinoma were selected for slide review. Slides were reviewed and comprehensively subtyped according to 2011 IASLC/ATS/ERS classification. Percentage of morules was calculated. Parameters like age, sex, tumor size, predominant pattern (PrePat), pathological stage (pT stage), lymph node positivity (LN), lymphovascular invasion (LVI), spread through air spaces, pleural involvement (Pleura), and follow-up data were recorded.

Results: Clinicopathological characteristics with p values are summarized in Table 1.

Table 1: Comparison between cases with and without morules			
Parameters	Morule n=36	Non Morule n=60	P value
Age average (range)	69 (51-85)	67 (36-84)	N/A
Sex % Male Female	50 50	45 55	0.67 0.67
PrePat %Acinar Micropapillary Papillary Solid Lepidic	67 25 8 0 0	71 7 7 12 3	N/A
Tumor size cm	2.6 [0.9-7.0]	2.5 [0.7-8.5]	N/A
pT Stage %1a 1b 2a 2b 3	31 25 28 11 5	40 15 38 5 2	0.38 0.28 0.37 0.41 0.55
LN %	17	17	1.00
LVI %	14	23	0.30
Pleura %	36	23	0.24
Follow-up (months) Metastasis % Recurrence % Death of disease %	69 (1-171) 28 3 0	77 (1-179) 20 5 3	0.31 1.00 0.53

Morule formation was present in 37% cases, comprising from 5-30% of the tumor (average 10%). Micropapillary pattern was seen in 32/36 cases (89%) with morules and was PrePat in 9 (25%).

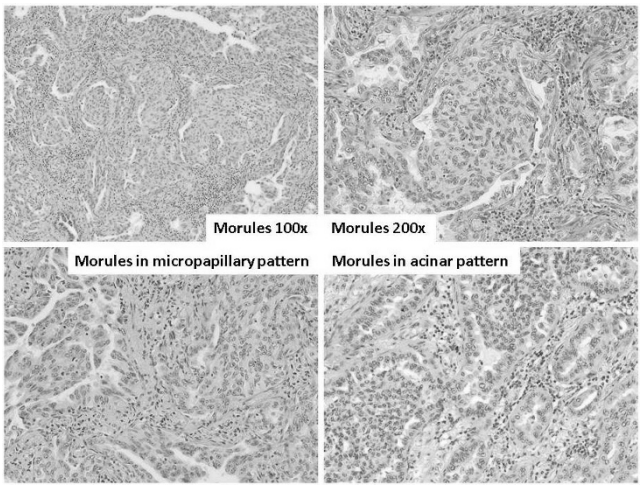

Conclusions: Morule formation was a minor (5-30%) component in 37% adenocarcinoma cases, seen in association with micropapillary pattern in 89 % cases and as suggested in literature, may represent an overgrowth of this pattern. The 4 cases without micropapillary pattern were acinar predominant and it is possible that micropapillary pattern was no longer recognized due to overgrowth of morules. Clinicpathologic characteristics or prognosis did not differ with presence or absence of morules.

1969 Effects of Delay to Formalin Fixation on Immunohistochemical Expression of Diagnostic Antibodies in Mesothelioma

John D Paulsen, Ryan Lau, Luis Chiriboga, Jonathan Melamed. New York University School of Medicine, New York, NY.

Background: Several immunohistochemical stains are used to aid in the diagnosis of mesothelioma, including WT1, calretinin, GLUT-1, D2-40 and BAP1. However, these antibodies have not been tested systematically to assess for loss of diagnostic utility with delay to formalin fixation. Our goal was to assess the variability of immunoreactivity for each antibody in formalin-fixed mesothelioma with timed fixation delays.

Design: Eight extrapleural pneumonectomy cases were sampled at time of resection and submitted to staged fixation. Using a tissue microarray, the immunoreactivities of diagnostic antibodies were studied to assess the effect of delay to formalin fixation. The tissue microarray was constructed from eight mesothelioma cases. Samples from each were fixed at different time points (0, 1, 2, 4, 6, 8, 12, 24 and 36 hrs). Immunohistochemical stains WT1, calretinin, GLUT-1, D2-40 and BAP1 were then performed on the tissue microarray. Staining was evaluated semiquantitatively using an H-score to evaluate both distribution and intensity of immunoreactivity.

Results: Mean reactivity for each antibody at 0 and 36 hours is listed.

Antibody	Reactivity (H-Score)	
	0 hrs, immediate fixation	36hrs (delay to fixation)
WT1	29.5	7.2
Calretinin	138.3	138.5
GLUT-1	92.1	131.7
D2-40	26.8	10.9
BAP1	Inconclusive	Inconclusive

In mesothelioma cases that stained strongly with WT-1 at 0 hrs, there was progressive loss of nuclear staining with delay to formalin fixation. Calretinin staining was overall maintained from 0 to 36 hrs, although nuclear staining was not evaluated separately. GLUT-1 remained intact with delay to fixation up to 36 hrs. D2-40 expression was patchy and appears to decline from 24 to 36 hrs, however results are not fully conclusive due to limited sample size and heterogeneous expression. BAP-1 staining was overall very weak and although staining appeared to be sustained in a few cases, lack of robust staining, heterogeneity and loss of internal controls yielded inconclusive results.

Conclusions: WT1 expression in mesothelioma is decreased with extended delay to fixation (prolonged cold ischemia time). This finding should be taken into account when interpreting diagnostic mesothelioma immunohistochemistry performed on specimens with long delays to fixation, such as autopsy material. Other diagnostic antibodies appear to have retained expression, however we plan further evaluation using whole sections to preclude analytic bias inherent in limited sampling in tissue microarray studies.

1970 Pathologic Grading of Malignant Pleural Mesothelioma: A REAL Evidence-Based Proposal

Giuseppe Pelosi, Anna Scattone, Andrea Marzullo, Angela De Palma, Alessandra Punzi, Federica Pezzuto, Elena Prisciandaro, Antonio Pennella, Anna Maria Catino, Gabriella Serio. University of Milan, Milan, Italy; Cancer Institute Giovanni Paolo II, Bari, Italy; University of Bari, Bari, Italy; University of Foggia, Foggia, Italy.

Background: A pathologic grading system (PGS) in malignant pleural mesothelioma (MPM) could be clinically warranted to better identify different risk categories of patients, plan therapy options and activate clinical trials.

Design: A cohort of 328 MPM patients was raised between October 1980 and June 2015. All original slides were jointly reviewed for consistency, blindly to asbestos exposure, overall survival, staging and (neo)-adjuvant chemotherapy. Histologic scoring was constructed by attributing to each parameter, independent upon multivariate analysis, different scores based on 50% increments of the corresponding hazard ratios (HR). Accordingly, final scores ranged from 0 to 12 points for each tumor patient.

Results: Histology (epithelioid, biphasic, sarcomatoid), necrosis (absent v. present), cell atypia (mild, moderate, severe), mitotic count per 1 mm^2 (cut-offs: 1-2, 3-5, 6-9, 10 or more) and Ki-67 labeling index on 2000 cells (cut-off 30%) were independent factors of survival after adjusting for confounding factors (stage, age and chemotherapy). Tumor patterns in epithelioid MGM or type of material (biopsy vs. resection) did not affect survival. PGS (AUC-ROC: 0.79) outperformed mitotic count (AUC-ROC: 0.68) and Ki-67 (AUC-ROC: 0.69). Patient survival progressively deteriorated from score 0 (median: 79.2 mo.) to score 12 (median: 1.3 mo.), with median survival values being 26.6 mo. (CI: 21.6-42.6), 15.1 mo. (CI: 13.3-16.8), 8.8 mo. (CI: 6.8-10.9) and 3.9 mo. (CI: 3.3-4.9) for 0-2, 3-5, 6-7, and 8-12 score, respectively. This PGS was effective not only in MPM considered as a whole, but also within epithelioid, biphasic and sarcomatoid subgroups, with HR values being 1.34 (CI: 1.27-1.41), 1.36 (CI: 1.27-1.46), 1.29 (1.12-1.49) and 1.44 (1.16-1.79) for each point of increase, respectively. Effectiveness of this PGS was then confirmed in an independent validation set dealing with further 60 MPM patients.

Conclusions: The combination of multiple parameters outperformed each single variable to construct a simple PGS, which predicted survival in diversely featuring MPM even at the level of an individual patient's cancer.

1971 Loss of BAP-1 Expression in Atypical Mesothelial Proliferations Helps to Predict Malignant Mesothelioma

Raghavendra Pillappa, Joseph J Maleszewski, William R Sukov, Patrick P Bedroske, Jennifer M Boland, Eunhee S Yi, Tobias Peikert, Marie C Aubry, Anja C Roden. Mayo Clinic, Rochester, MN.

Background: Distinguishing reactive mesothelial proliferation and malignant mesothelioma (MM) can be difficult, particularly on small biopsies that lack tissue to evaluate for invasion. In this scenario, a diagnosis of atypical mesothelial proliferation might be rendered. However, the distinction between a reactive process and MM is important for prognosis and treatment. Recently, loss of BAP1 expression and/or homozygous deletion of *CDKN2A* were identified in some MM, but not in reactive mesothelial proliferations. We studied BAP1 expression, deletion of *CDKN2A* and clinical outcome of cases diagnosed as atypical mesothelial proliferation.

Design: Institutional pathology archives were searched for atypical mesothelial proliferation (1995-2016). BAP1 (clone C-4, Santa Cruz Biotechnology, Santa Cruz, CA, USA) expression was reported as lost (no nuclear staining of mesothelial cells with positive internal control) or retained. FISH for *CDKN2A* was performed. Medical records were abstracted.

Results: The study included 37 cases (25 men; median age, 72 years, range (36-90+) of atypical mesothelial proliferation of the pleura (n=22), pericardium (n=4) or peritoneum (n=11) with a median follow-up of 34 months (range, <1-286). Sixteen of 37 patients (46%) were subsequently diagnosed with MM (13 on subsequent biopsies, 3 based on clinical evolution), 9 of 16 (56%) died of disease (median time to death 14 months; range <1-58), 7 (44%) were alive at a median of 54 months (range, 13-286). BAP1 results were available in 35 patients. BAP1 expression was lost in 5 of 15 (33%) patients subsequently diagnosed with MM. BAP1 was also lost in an additional patient who was diagnosed with lung adenocarcinoma (pT2N2M0) at time of biopsy; 8 months later a CT scan revealed visceral and parietal pleural thickening and effusion; the patient was subsequently lost to follow up. FISH (performed in 16 cases) found no homozygous deletion of *CDKN2A* in any of the cases tested.

Conclusions: Loss of BAP1 expression in atypical mesothelial proliferation helps to predict MM.

1972 HMGA2 Immunostaining Is a Straightforward Technique Which Helps to Distinguish Pulmonary Fat-Forming Lesions from Normal Adipose Tissue in Small Biopsies

Nicolas Piton, Émilie Angot, Florent Marguet, Jean-Christophe Sabourin. Rouen University Hospital, Rouen, France.

Background: Adipocytes may be observed in the lamina propria of tracheobronchial biopsies, which may complicate diagnosis of sampled lesions because these adipose cells may be part of the lesion (lipoma or pulmonary hamartoma), but may also be a normal component of the bronchial mucosa. Because endoscopic samples frequently miss their target, adipocytes observed in such biopsies usually lead to uncertainty regarding diagnosis. Both pulmonary hamartomas and lipomas have a high frequency of translocations involving *HMGA2*, resulting in over expression of the fusion protein. The literature suggests that only 31% of tracheobronchial lipomas are correctly diagnosed on biopsy, sometimes leading to unnecessary aggressive surgical resection.

Design: We performed retrospective study of tracheo-bronchial biopsies containing adipocytes using HMGA2 immunostaining in order to assess the diagnostic utility of this marker. Cases of tracheobronchial biopsies performed between 01/01/1990 and 01/03/2016 coded as lipoma or hamartoma were retrieved from the database of our center.

Results: In total, 13 adipose lesions biopsied in 12 patients were immunostained for HMGA2. Nuclear staining was detected in 7 out of the 13 lesions (54%), allowing us to diagnose a lipoma or hamartoma.

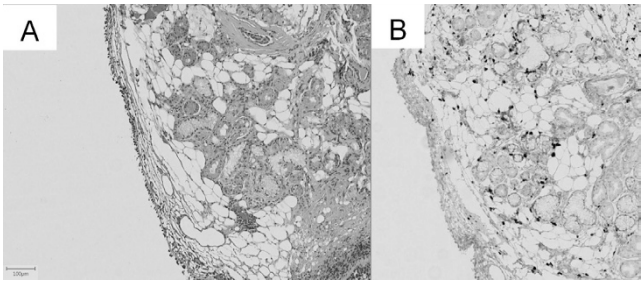

Conclusions: HMGA2 immunostaining is a straightforward technique for accurate description of biopsies containing adipose cells. When positive, a diagnosis of benign adipose lesion can be made with confidence since well-differentiated liposarcomas have never been described in the tracheobronchial tree. Our work enabled us to diagnose a benign adipose lesion in 54% of cases, well above the 31% reported in the literature, based solely on morphological analysis. We are convinced that HMGA2 immunostaining, if positive, is a straightforward method for accurate diagnosis of this rare cases.

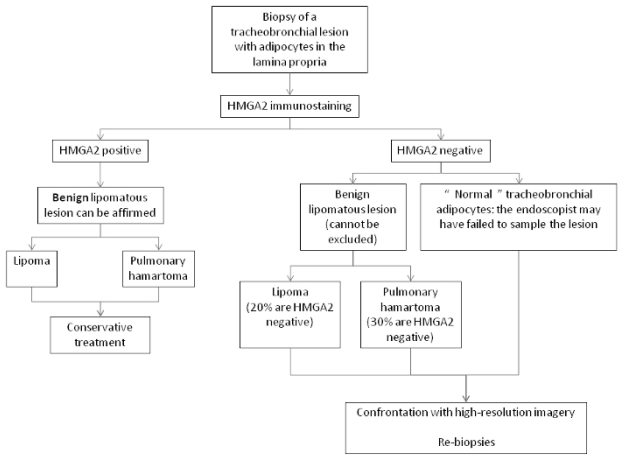

1973 Ligation Dependant-RTPCR : A New Specific and Low Cost Technique to Detect *ALK*, *ROS* and *RET* Rearrangements in Lung Adenocarcinoma

Nicolas Piton, Claire Gravet, Philippe Ruminy, Vinciane Marchand, Elodie Colasse, Luc Thiberville, Fabrice Jardin, Jean-Christophe Sabourin. Rouen University Hospital, Rouen, France; Centre Henri Becquerel, Rouen, France.

Background: Detection of *ALK*, *ROS1* and *RET* rearrangements in Lung ADenoCarcinoma (LADC) is usually performed by ImmunoHistoChemistry (IHC) screening followed by Fluorescence *In Situ* Hybridization (FISH), which is an expensive and difficult technique.

Ligation Dependant-RTPCR (Reverse Transcription Polymerase Chain Reaction) multiplex technique can detect gene rearrangements using probes specifically hybridized to either side of the breakpoint. PCR products are then sequenced by pyrosequencing or Next Generation Sequencing (NGS) in order to identify the 2 genes involved. The reagent cost is less than 15 dollars per patient and results are available in 2 days. We have developed a 47-probes LD-RTPCR kit especially for LADC.

Design: Fifty LADC were studied: 35 *ALK*+, 14 *ROS1*+ and 1 *RET*+. *ALK*+ and *ROS1*+ were IHC+ (D5F3 Ventana® for ALK and D4D6 Cell Signaling Technology® for ROS1) and all cases were FISH+ (Vysis ALK Breakapart Probe Abbott® for *ALK*, Zytolight SPEC ROS1 Dualcolor Breakapart Probe® for *ROS1* and Zytolight SPEC RET Dual Color Breakapart® for *RET*); 14 wild type samples were included as negative controls.

Results: Using LD-RTPCR, 15 rearrangements (48%) were detected in the *ALK* cases (gene partner: *EML4* in all cases), 9 rearrangements (64%) in the *ROS1* cases (gene partners: *CD74* in 8 cases and *SLC34A2* in 1 case) and 1 (100%) in the single *RET* case (gene partner: *KIF5B*). No rearrangement was found in the 14 negative control cases. Among the 20 *ALK* negative cases using LD-RTPCR, 8 (40%) contained very few tumor RNA molecule and therefore should be considered as non contributory. After excluding such cases, the positivity rate reached 56%.

Other *ALK*-negative cases using LD-RTPCR could be explained by some gene partners which were not included in our kit.

Conclusions: LD-RTPCR is more specific than IHC and less sensitive than FISH. We propose to use it in a daily routine according to the following flow chart:

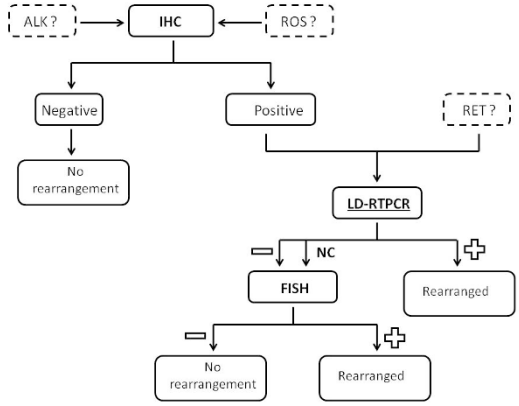

LD-RTPCR is a specific, simple and low-cost new promising technique to detect *ALK*, *ROS1* and *RET* rearrangements in lung adenocarcinoma. When positive, it could be a fruitful alternative to FISH.

1974 Increased PD-L1 and FOXP3 Expression Correlates to Worse Overall Survival and Nodal Disease in Patients with Lung Adenocarcinoma

Kate Poropatich, Rishi Raj, Kalliopi P Siziopikou, Kirtee Raparia. Northwestern University, Chicago, IL.

Background: Conflicting data raises questions of whether or not programmed death-ligand 1 (PD-L1) and FOXP3 are positive prognostic factors in patients with solid tumors. In this study, we examine the expression of these and other T cell markers in a cohort of lung adenocarcinoma patients and relate their expression levels to patient disease burden and overall survival (OS).

Design: Tissue micro-arrays containing 162 lung adenocarcinoma samples in triplicates were immunostained for CD3 (Dako), CD4 (Leica), CD8 (Leica), PD-L1 (E1L3N), and FOXP3 (Abcam). PD-L1 reactivity was recorded as the percent of membranous and cytoplasmic staining on both tumor and peritumoral lymphocytes as: Score 0 = <1%, 1= 1-4%, 2= 5-10%, 3= >10%. Foxp3 was scored as Score 1= <2%, 2= 2-5%, 3= >5%. OS analysis and other apporpiate parametric and nonparametric tests were calculated using Stata software (StataCorp).

Results: Patients included 57 men and 105 females. Mean time of follow-up was 61.67 months. Patients with elevated expression (Score 3) of PD-L1 (n= 29) and FOXP3 (n= 33) had a significantly worse OS (p= 0.007 and p= 0.03, respectively).

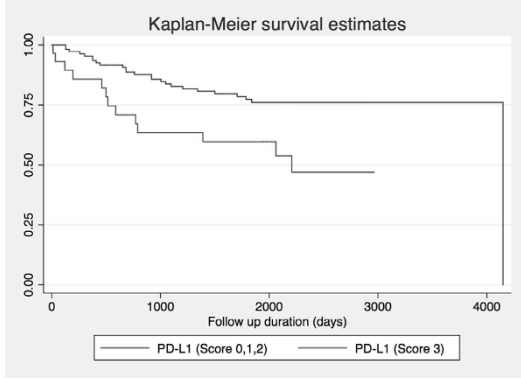

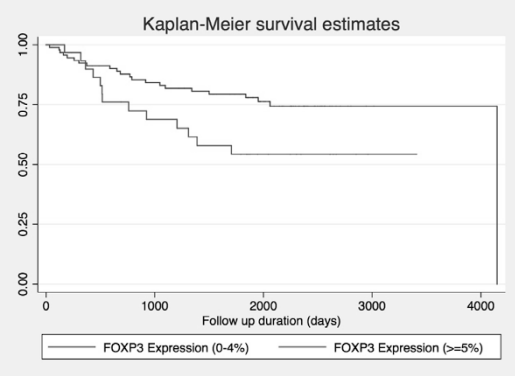

Almost half of all patients (42.86%) with an elevated Foxp3 expression also had elevated PD-L1 expression (p= 0.011). CD8 and PD-L1 levels positively correlated to one another (p= 0.0001). Patients with elevated PD-L1 expression levels were significantly more likely to have higher stage and nodal disease (p<0.0001 for botj). There was no correlation between PD-L1 expression and EGFR and KRAS molecular mutation status.
Conclusions: Elevated PD-L1 and FOXP3 expression levels are poor prognostic factors for lung adenocarcinoma and are more likely to be highly expressed in the same patients. Further work is needed to better understand how these immune parameters correlate to patient responsiveness to immunotherapeutic agents in lung adenocarcinoma.

1975 Identification of Criteria Predicting the Pertinence of Frozen Section Evaluation of Margins in Lung Cancer Resections

Étienne Racine, Michèle Orain, Sylvain Trahan, Yves Lacasse, Paula Ugalde, Serge Simard, Philippe Joubert. Laval University, Quebec City, QC, Canada; Quebec Heart and Lung Institute, Quebec City, QC, Canada.

Background: Frozen section (FS) evaluation of resection margins is routinely requested by thoracic surgeons during oncological lung surgeries. These procedures imply operating room delays and other additional costs. Positive margins remain relatively rare occurrences and do not necessarily change the course of the surgery. In this study, we propose to identify parameters associated with increased probability of positive margin, allowing to target specific patients for whom frozen sections are pertinent and will provide clinical benefits.
Design: Pathology reports of oncological lung resections performed at our institute between January 1st 2006 and July 20th 2015 were reviewed and included 1570 tumors. Collected data comprised histological diagnosis, tumor size, stage, margins, distance tumor-margin, invasions (pleural, lympho-vascular and nodal) and demographic parameters.
Results: 72 cases of positive margins (bronchial or vascular or parenchymal) were identified (4.6% of cases). Squamous cell carcinomas were overrepresented in patients with positive FS bronchial margins (65,2% vs 19,6%; p<0.0001). The average distance (*d*) between tumor and margin was found to be significantly shorter in positive FS bronchial margin cases (1.1 cm vs 3.5 cm; p<0.0001). Surprisingly, larger tumors were not significantly associated with positive FS bronchial margins (3.5 cm vs 3.0 cm; p=0.2723). Nodal (p=0.0006) and vascular (p=0.0295) invasions were both found to be significantly associated with higher probability of positive FS bronchial margin. Positive margins were shown to adversely affect survival (HR=2.18; 1.54-3.09). A cut-off distance *d* of 2.5 cm for performing frozen section on bronchial or vascular margins would have captured 90% of positive cases (missed cases at distance of 3.5 cm or greater). A cut-off on the ratio distance/tumor size equal to 1.0 yielded similar results.
Conclusions: We showed a significant association between the likelihood of finding positive FS bronchial margins and the following parameters: squamous cell carcinoma histology, distance between tumor and margin, lymph node invasion and vascular invasion. The size of the tumor and the presence of pleural invasion were not parameters correlated with a higher probability of positive FS bronchial margins. Our results will be useful to stratify patients and identify who should benefit from intra-operative frozen section evaluation of surgical margins.

1976 Correlation of Thyroid Transcription Factor (TTF-1) Immunostaining Status with Somatic Mutations in Lung Adenocarcinomas Detected by Targeted Next Generation Sequencing (NGS)

Rongqin Ren, Nabil Ashraf, Catherine I Dumur, Jorge A Almenara, Michael O Idowu, Adele O Kraft, Celeste N Powers. Virginia Commonwealth University Health System, Richmond, VA.

Background: TTF-1 immunohistochemical staining (IHC) has been routinely used for differentiating between pulmonary adenocarcinoma and squamous cell carcinoma. TTF-1 is positive in approximately 70-80% of lung adenocarcinomas. TTF-1 negativity in lung adenocarcinomas has been previously associated with the lack of *EGFR* mutation detected by allele-specific polymerase chain reaction assay. In this study we further investigate the correlation of TTF-1 IHC results with somatic variants detected by a 50-gene panel targeted NGS.
Design: A total of 92 surgical or cytological specimens diagnosed as lung adenocarcinoma from November 2015 to September 2016 were submitted for NGS analysis. TTF-1 IHC status was documented as either positive or negative. Formalin-fixed paraffin-embedded tissues or pre-stained smears were used to extract genomic DNA, which was subsequently analyzed by the Ion AmpliSeq™ Cancer Hotspot Panel v2 (CHP2) assay. Variant classifications were determined using our institutional knowledge base system. Only Pathogenic/Likely Pathogenic variants were reported. The presence of Pathogenic or Likely-Pathogenic variants in *EGFR* or other actionable genes were correlated with TTF-1 IHC status, using Chi-square statistics.
Results: Of 92 cases, 80 (87%) were positive for TTF-1 by IHC. *EGFR* and *BRAF* mutations were detected in 15/80 (19%) and 6/80 (8%) of TTF-1 positive cases, respectively (Table 1). No *EGFR* or *BRAF* mutations were detected in any of the TTF-1 negative cases (0/12). In addition, the presence of *KRAS* or *TP53* mutations was not significantly different (Yate's p-value = 0.7014) between TTF-1 positive and TTF-1 negative adenocarcinomas (Table 1).

TABLE 1: DISTRIBUTION OF SAMPLES BY TTF-1 STATUS AND SOMATIC VARIANTS

		EGFR	BRAF	KRAS	TP53	Other
TTF-1	Positive	15 (19%)	6 (8%)	27 (34%)	37 (46%)	18 (23%)
	Negative	0 (0%)	0 (0%)	3 (25%)	7 (58%)	5 (42%)

Conclusions: Based on these results, a negative TTF-1 IHC status may be used as potential screening test for the absence of *EGFR* and *BRAF* mutations. This may be especially beneficial for treatment decisions in a setting where molecular testing is not readily available or prohibitively expensive.

1977 *GNAS* Mutations in Mucinous and Non-Mucinous Lung Carcinomas

Lauren Ritterhouse, Marina Vivero, Mari Mino-Kenudson, Lynette M Sholl, John Iafrate, Valentina Nardi, Fei Dong. Brigham and Women's Hospital, Boston, MA; Massachusetts General Hospital, Boston, MA.

Background: *GNAS* mutations have been described in mucinous epithelial neoplasms, including appendiceal, pancreatic, and colon tumors, with hotspot *GNAS* codon 201 mutations being found in up to two-thirds of pancreatic intraductal papillary mucinous neoplasms (IPMN). Additionally, many *GNAS*-mutant tumors have concurrent mutations in the Ras/Raf pathway. However, the clinicopathologic features of *GNAS*-mutant lung carcinomas have not yet been characterized.
Design: All lung carcinomas that had been sequenced at either Brigham and Women's Hospital (BWH) (n=1413) or at Massachusetts General Hospital (MGH) (n=1108) on a targeted panel of known cancer genes by massively parallel sequencing were assessed for GNAS hotspot mutations in codons 201 and 227. Cases that were clinically considered metastases were excluded, and only those cases that were determined to be a primary lung carcinoma were included. TTF-1 immunohistochemistry was performed when material was available.
Results: Nineteen lung carcinomas with hotspot GNAS mutations were identified (19/2521, 0.7%) including 5 at codon 227 and 14 at codon 201 (Fig 1). GNAS-mutant lung carcinomas occurred predominantly in female patients (84%). 53% percent of GNAS mutated cases were invasive mucinous adenocarcinomas, all of which had GNAS R201 mutations and concurrent Ras/Raf pathway mutations (9 KRAS, 1 BRAF). GNAS R201 mutated tumors without concurrent Ras/Raf pathway mutations (n=4) did not have mucinous histology, and no tumors with GNAS Q227 mutations had mucinous histology. TTF-1 was positive in 86% of non-mucinous GNAS-mutated lung carcinomas (6/7) but only in 25% of mucinous GNAS-mutated lung carcinomas (1/4). Patients with non-mucinous GNAS-mutant tumors were more likely to have a history of smoking (100%) compared to patients with mucinous GNAS-mutant tumors (20%) (p=0.001).

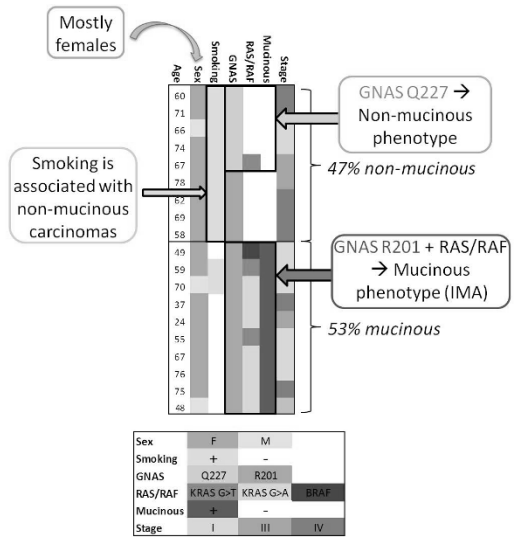

Conclusions: Hotspot GNAS mutations can occur in primary lung carcinomas, and the presence of concurrent mutations in the Raf/Ras pathway is associated with mucinous histology. Clinicopathologic correlation is necessary in these cases to determine the primary site of origin.

1978 Thymic Carcinoma Histology and Prognosis- A Single-Center Review

Rachel E Rominger, Michael A Balatico, Yesim Gokmen-Polar, Sunil Badve. Indiana University, Indianapolis, IN.

Background: Thymic carcinoma is a very rare malignancy accounting for less than 0.01% of all cancers. Most of the data is based on case reports and small series. Our objective was to examine a large series of thymic cancers in order to study patient characteristics and the relationship between tumor histology, degree of differentiation, and treatment with patient outcomes.

Design: Retrospective cases of histologically confirmed thymic carcinoma seen in the past 15 years were identified and available histological materials were reviewed. Histology was reviewed on the available cases using the current WHO classification of thymic tumors (2015). Tumor infiltrating lymphocytes (TILs) were also assessed in the stromal compartment. Tumor histology, differentiation and was correlated with outcome data.

Results: The review of the clinical database identified 184 cases of thymic carcinoma. In many cases the original histological slides had been returned to the referring institutions; this resulted in identification of histological materials for only 91 cases. There were 47 male and 38 female patients with an average age of 54.4 years. Histologically, most cases (n=81) were classified as of squamous histology with or without keratinizing features. There were 4 cases of clear cell carcinoma, 3 NUT-positive carcinomas, 2 cases each of basaloid carcinoma, adenocarcinoma, lymphoepithelial carcinoma, mucoepidermoid carcinoma and 1 case each of sarcomatoid carcinoma and micronodular carcinoma. The squamous cell carcinomas were further classified based on differentiation; the distribution was 30% well differentiated, 33% moderately differentiated, 28% poorly differentiated and 9% undifferentiated. TILs were rare in thymic cancers with the vast majority (~90%) of cases have less than 10% TILs in the stroma. Almost all patients (>90%) had received chemotherapy with or without radiotherapy. Outcome data was available in 59 of these 91 cases and consisted of time to progression, time to metastases and time to death. In general, progression of disease was noted in 34 patients in the series developed within 1 year of diagnosis, 43 patients developed metastases within 2 years and 8 patients died of disease within 4.5 years. There was no significant difference in the outcome based on histology, tumor differentiation or TILs.

Conclusions: Thymic carcinomas is predominantly a disease of late adulthood with a slight increase incidence in males. The tumors show squamous differentiation and lack significant tumor infiltrating lymphocytes. Prognosis is poor in spite of chemo-/radiotherapy.

1979 INSM1 Demonstrates Superior Performance to Synaptophysin, Chromogranin, and CD56 for Diagnosis of Thoracic Neuroendocrine Tumors

Lisa M Rooper, Rajni Sharma, Qing K Li, Peter Illei, William H Westra. Johns Hopkins Hospital, Baltimore, MD.

Background: Identification of neuroendocrine (NE) tumors is one of the most important distinctions in pulmonary pathology. However, diagnosis of small cell lung carcinoma (SCLC) and large cell neuroendocrine carcinoma (LCNEC) is often confounded by the suboptimal sensitivity and specificity of traditional NE markers. INSM1 is a transcription factor that is well-validated in laboratory studies to promote NE differentiation and has recently shown strong immunohistochemical expression in NE tumors from various anatomic sites. This study compares the performance of INSM1 to synaptophysin (SYN), chromogranin (CHR), and CD56 in hopes of improving the diagnosis of thoracic NE tumors.

Design: We built tissue microarrays (TMAs) to include a broad range of lung and mediastinal NE tumors, including 22 SCLC, 24 LCNEC, 18 atypical carcinoids, 16 typical carcinoids, and 8 paragangliomas. We also utilized existing TMAs containing 61 lung adenocarcinomas (ACA) and 95 lung squamous cell carcinomas (SCC). We performed immunohistochemistry for INSM1 (A-8), SYN (27G12), CHR (LK2H10), and CD56 (123C3.D5) on all tumors. Positivity was defined as any nuclear reactivity for INSM1 or any cytoplasmic staining for SYN, CHR, and CD56.

Results: Results of staining are summarized in Table 1. INSM1 demonstrated an overall sensitivity of 94% for thoracic NE tumors, compared to a collective 87% for SYN, CHR, and CD56. Notably, INSM1 showed 91% sensitivity for both SCLC and LCNEC, in contrast to just 68% and 82%, respectively, for the three traditional markers. INSM1 also had a specificity of 96%, versus 90% for the other markers combined.

	INSM1	SYN	CHR	CD56
SCLC	20/22 (91%)	13/22 (59%)	11/22 (50%)	14/22 (64%)
LCNEC	20/22 (91%)	14/22 (64%)	11/22 (50%)	13/22 (59%)
Atypical Carcinoid	17/18 (94%)	18/18 (100%)	18/18 (100%)	16/18 (89%)
Typical Carcinoid	16/16 (100%)	16/16 (100%)	16/16 (100%)	16/16 (100%)
Paraganglioma	8/8 (100%)	8/8 (100%)	8/8 (100%)	8/8 (100%)
ACA	2/61 (3%)	4/61 (7%)	1/61 (2%)	3/61 (5%)
SCC	4/95 (4%)	1/95 (1%)	0/95 (0%)	7/95 (7%)

Conclusions: Even in small tissue samples, INSM1 has better sensitivity and specificity for lung and mediastinal NE tumors compared to SYN, CHR, and CD56 combined. Moreover, INSM1 offers crisp nuclear staining that is easier to interpret than the cytoplasmic reactivity of traditional NE markers. These findings suggest that INSM1 could provide a standalone first-line marker for workup of thoracic NE tumors.

1980 Nuclear Grade, Necrosis and Solid Growth Pattern Predict Survival in Epithelioid Malignant Mesothelioma: An International, Multi-Institutional Study

Lauren E Rosen, Vijayalakshmi Ananthanarayanan, Alexander Gallan, Melissa Yuwono Tjota, Richard Attanoos, Fouad S Alchami, Luka Brcic, Kelly Butnor, Kenzo Hiroshima, Astero Klampatsa, Leslie Litzky, Alberto M Marchevsky, Filomena Medeiros, M Angeles Montero-Fernandez, David A Moore, Kazuki Nabeshima, Elizabeth N Pavlisko, Anupama Sharma, Michael Sheaff, Ann E Walts, Francoise Galateau, Nolwenn Le Stang, Thomas Krausz, Aliya N Husain. University of Chicago, Chicago, IL; Loyola, Maywood, IL; University of Wales, Cardiff, United Kingdom; Medical University of Graz, Graz, Austria; University of Vermont, Burlington, VT; Tokyo Women's Medical Center, Kawadacho, Japan; University of Pennsylvania, Philadelphia, PA; Cedars-Sinai Medical Center, Los Angeles, CA; Basildon & Thurrock University Hospital, Basildon, United Kingdom; Royal Brompton and Harefield Hospitals, London, United Kingdom; University of Leicester, Leicester, United Kingdom; Fukuoka University, Fukuoka, Japan; Duke University, Durham, NH; Veterans Affairs Pittsburgh Healthcare System, Pittsburgh, PA; Barts Health NHS Trust, London, United Kingdom; Centre Leon Berard, Lyon, France.

Background: A recently described nuclear grading system predicted survival in patients with epithelioid malignant pleural mesothelioma(EMM). The current study was undertaken to validate the grading system and to identify additional prognostic characteristics.

Design: We analyzed cases of EMM(biopsies&resections) from 16 institutions across the globe from 1998-2013. Nuclear grade was computed combining nuclear pleomorphism and mitoses into a grade(G) of 1-3 using the published system. Grade was scored by one pathologist for 3 institutions, the remaining were scored independently. The presence or absence of necrosis and patterns of growth were also evaluated. Overall survival(OS) was used as the primary endpoint. Data were examined using Student's t-test and Log-rank test.

Results: Of 532 cases, 183(34%) were G1, 259(49%) G2, and 90(17%) G3. The mean OS was 24 months. Higher nuclear grades were associated with worse OS(G1-35 months, G2-20 months, G3-13 months, G1 vs G2 $p<0.001$, G2 vs. G3 $p<0.005$, G1 vs. G3 $p<0.001$). G1&G2 tumors with necrosis behaved significantly worse than G1&G2 tumors without necrosis(G1:17 vs. 37 months, $p<0.001$, G2:17 vs 22 months, $p<0.05$), and more similarly to G3 tumors(G1:17 vs 13 months, $p=0.35$, GII:17 vs 13 months, $p=0.17$). Tumors with necrosis behaved worse than those without(29 vs 16 months, $p<0.001$). A solid growth pattern >50% (42%,193/457) was associated with worse OS(19 vs. 28 months, $p<0.001$).

Conclusions: This study confirms that nuclear grade predicts survival in EMM, and identifies the presence of necrosis as a predictor of G1&G2 tumors that behave like G3 tumors. Additionally, a predominat solid growth pattern, regardless of the nuclear grade, is associated with a worse OS.

1981 Appropriate Use of Immunohistochemistry in the Diagnosis of Lung Cancer on Biopsy: A Retrospective Comparison from Four Academic Centers

Lauren E Rosen, Hussein Alnajar, Vijayalakshmi Ananthanarayanan, Paolo Gattuso, Lifang Liu, Kirtee Raparia, Aliya N Husain. University of Chicago, Chicago, IL; Rush University Medical Center, Chicago, IL; Loyola University, Maywood, IL; Northwestern University, Chicago, IL.

Background: The discovery of EGFR and ALK alterations in lung adenocarcinomas has radically changed the approach to cancer therapy, and the current recommendation is to test for these alterations in all patients with advanced stage disease. The majority of patients are diagnosed by small biopsy, and it is essential to limit the number of stains used to subtype the tumor in order to conserve tissue for molecular studies.

Design: The purpose of this study is to evaluate the number and usefulness of immunohistochemical stains (IHC) performed on lung cancer biopsies. Records from 4 institutions were searched from 7/1/2015-6/30/2016. Metastases, neuroendocrine tumors and unusual tumors such as carcinosarcomas were excluded. Data collected included diagnosis and number and type of stains performed. If the diagnosis was clear morphologically (adenocarcinoma or squamous cell carcinoma) then IHC was considered unnecessary. For non-small cell lung carcinomas (NSCLC), TTF-1 and p40/p63 were considered as an initial panel, and if diagnostic, additional stains were deemed unjustified.

Results: Of 262 cases, 207 were inhouse and 54 were consults. An average of 1.9(range 1-5) H&E slides were cut for inhouse cases and 2.0(range 1-10) for consults. Morphologically differentiated tumors (adenocarcinoma, squamous cell carcinoma, adenosquamous) accounted for 136(66%) inhouse and 27(50%) consult cases. Unecessary stains were performed in 68(50%) of differentiated inhouse cases with an average of 2.5 stains/case and 19(70%) of differentiated consult cases with an average of 2.2 stains/case. NSCLC accounted for 71(34%) inhouse and 27(50%) consult cases. Unecessary stains were performed in 21(30%) of inhouse NSCLC cases with an average of 2.2 stains/case and 19(70%) consult NSCLC cases with an average of 3.0 stains/case. The combination of TTF-1 and p40/p63 immunostains alone was diagnostic in 63/87(72%) of NSCLC cases.

Conclusions: In the molecular era, unnecessary IHC are performed on far too many lung cancer biopsies. Only 1 H&E slide should be initially cut. Stains should not be performed on morphologically differentiated cancers, except when there is suspicion for metastasis. In NSCLC, TTF-1 and p40 should be the initial panel of stains. Further stains should only be performed if these initial stains are non-diagnostic. The number of slides cut per case can be reduced by up to an average of 4 by following these guidelines.

1982 MMP-1 as a Marker of Adverse Clinical Outcome of Pulmonary Adenocarcinoma Patients: The Correlation Between MMP-1 Overexpression and Clinicopathological Factors and EGFR-TKI Resistance

Ryoko Saito, Yasuhiro Miki, Naoya Ishida, Shuko Hata, Hironobu Sasano. Tohoku University School of Medicine, Sendai, Miyagi, Japan; Tohoku Medical and Pharmaceutical University, Sendai, Miyagi, Japan.

Background: MMP-1(matrix metalloproteinase-1) overexpression has been reported to be associated with metastasis and invasion in several human malignancies. However, the MMP-1 status in the patients with pulmonary adenocarcinoma (pADC), and its correlation with EGFR-TKI resistance postulated by in vitro analysis have remained virtually unknown.

Design: MMP-1 was immunolocalized in 59 cases with pADC obtained from surgery. The correlation between MMP-1 immunoreactivity evaluated by modified histological score and clinicopathological factors of the patients were analyzed. In addition, we also performed in vitro migration and invasion assays using PC-9, EGFR-TKI sensitive pADC cells, and EGFR-TKI resistant PC-9 (PC-9R) cells. We also treated PC-9 and A549 with EGF in order to clarify the possible mechanisms of MMP-1 induction and further analyzed the correlation between MMP-1 expression and EGFR pathway in pADC.

Results: High abundance of MMP-1 was significantly correlated with high stage ($p<0.05$) of the patients, tended to be associated with poor prognosis ($p<0.1$) and was also significantly associated with mucinous subtype ($p<0.0001$). MMP-1 status was significantly higher in PC-9R cells than PC9 cells. In PC-9R cells, MMP-1 knockdown using siRNA significantly inhibited migration and invasion ability of the cells. In addition, EGF significantly induced MMP-1 expression in a dose-dependent fashion in PC-9 and A549 cells.

Conclusions: Increased MMP-1 in carcinoma cells could represent the poor prognostic marker in pADC. MMP-1 also plays important roles in progression of cancer and could be a molecular target for the treatment in EGFR-TKI resistant pADC.

1983 Intratumoral Molecular and Proteomic Heterogeneity in Lung Adenocarcinoma. How Can We Address It?

Irene Sansano, Sherley Diaz, Javier Hernandez-Losa, Douglas Sanchez, Santiago Ramon y Cajal. HU Vall d'Hebron, Barcelona, Barcelona, Spain.

Background: For a long time, pathologists have been subtyping lung carcinoma based on the great diversity of intratumoral cell growth patterns. This morphological heterogeneity must be the translation of molecular variations. The aim of our study was to asses this heterogeneity by studying different mutations and protein expression throughout different parts of tumors.

Design: We analyzed 130 lung adenocarcinomas assessing histopathological features as well as immunohistochemical expression cell signaling factors (pMAPK, mTOR, 4E-BP1, p4E-BP1, eIF4E, peIF4E), and Epithelial-Mesenchymal Transition (EMT) factors (N-cadherin, YB1, pYB1). Levels of expression were evaluated semi-quantitatively as percentage and intensity of stained tumor cells (histo-score [H score]).Homogeneous expression was considered when >80% tumor cells displayed a strong positivity. We obtained 3 separate core-biopsies (acinar, papillary and micropapillary patterns) from 30 of these tumors and performed separate molecular studies. DNA was extracted for detecting mutations in EGFR and KRAS by PCR and RNA for screening transcription of 110 genes using NanoString technology. Correlations were analyzed using Kruskal-Wallis and Kaplan-Meier (log Rank) statistical tests.

Results: The predominant histological patterns were acinar, papillary and solid, with the latter associated with higher histological grade. Most cell signaling and EMT displayed heterogeneous and patchy distribution but p4E-BP1 and peIF4E that were homogenous. Moreover, the higher expression factors of eIF4E, 4EBP1 and YB1 was associated with higher recurrence rate, histological grade and metastases. Regarding RNA expression, 90% of cases showed significant heterogeneity. EGFR mutations were heterogeneous in about 20% of the cases while KRAS mutations were found in all the areas of the tumors.

Conclusions: We have found intratumoral heterogeneity in most cases of lung adenocarcinomas at proteomic, RNA and DNA levels, including EGFR mutations. These findings highlight the importance of studying different areas of the tumors. Moreover, we show a patchy expression of most signaling factors, such as pmTOR and pMAPK that could explain the partial clinical responses to specific inhibitors. Conversely, peIF4E (that displayed a homogeneous expression in most tumors) can have a potential role as a therapeutical target. Pathologists need to integrate the molecular, proteomic and histopathological data and apply biology systems and topologic approaches to enhance prognostic information and therapeutical options for each tumor and patient.

1984 Lung Transplant Outcomes in Emphysema Patients with Granulomas

Rex Michael Santiago, Tahani Al-Baqer, Zanobia Khan, Sassan Azad, Yizhuo Gao, Shaf Keshavjee, Ming-Sound Tsao, David Hwang. University Health Network, Toronto, ON, Canada.

Background: Fungal and non-tuberculous mycobacterial (NTM) infections are important complications in lung transplant recipients, and may be associated with significant morbidity and/or mortality. Infections in the transplanted lung may originate de novo from environmental sources, but patients may also be re-infected by microorganisms that are present in their native lungs and airways prior to transplantation. Patients with chronic obstructive pulmonary disease (COPD) are at increased risk of acquiring both fungal and NTM infections, and granulomas are commonly identified in the native lungs of patients with emphysema undergoing transplantation. However, it is uncertain whether the presence of granulomatous infections in the native lungs is associated with higher risk of adverse outcomes following transplantation, such as post-transplant infection, progression to chronic lung allograft dysfunction (CLAD), or death. We therefore initiated a study to assess whether the presence of granulomas in the pre-transplant native lungs of patients with COPD impacts on post-transplant outcomes.

Design: The pathology reports of patients receiving lung transplantation for emphysema from August 2001 to December 2010 were reviewed and assessed for the presence or absence of granulomas. Clinical follow-up and microbiologic data were acquired from the electronic patient records. Survival analysis was performed by Cox regression.

Results: A total of 175 cases of lung transplantation for emphysema were identified. Of these, survival and follow-up data were available for 144 patients, of which 39 patients showed granulomas in histologic sections (27%), while the remaining 105 patients (73%) showed no granulomas. Of the 39 patients with granulomas, acid-fast bacilli were identified in histologic sections in 17 (43.6%) and fungal organisms were detected in 8 (20.5%). Twenty six of 39 patients with granulomas and 60 of 105 of patients without granulomas died, with median survivals of 78 and 72 months, respectively (p=0.87).

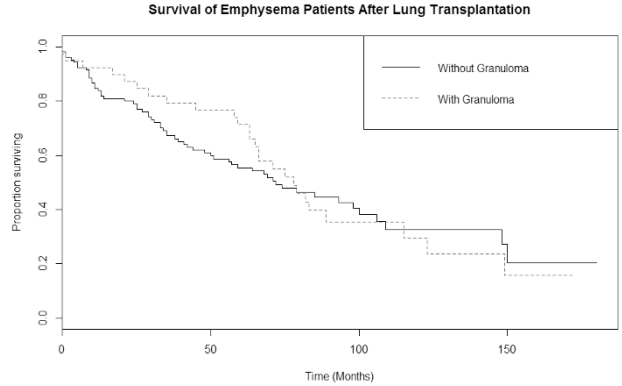

Conclusions: Granulomatous infections are common in the lungs of patients with end-stage emphysema. In our cohort, the presence of granulomas in the native lungs of emphysema patients was not associated with decreased post-transplant survival.

1985 Evidence of Welding Exposure Is Readily Seen but Under-Reported in Lung Neoplastic Pathology Specimens

Soma Sanyal, Judith A Crawford, Jerrold L Abraham. SUNY Upstate Medical University, Syracuse, NY.

Background: Welding and related occupations comprise a heterogeneous group that lead to generation of a variety of toxic fumes and gases. Respiratory effects of welding include bronchitis, increased infections, lung function changes, fibrosis and a possible increase in carcinoma. 'Welding bodies' (WB) are easily seen on H&E stained sections but are rarely recognized by pathologists. They have been described as mostly spherical structures having a golden, iron-rich coating and a central, opaque core particle, ranging in size from 1->10 μm.

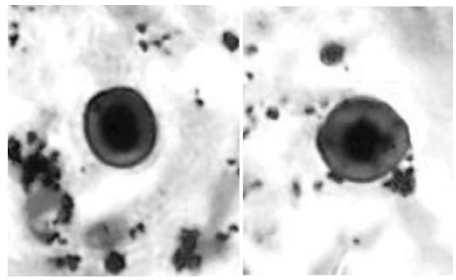

Design: Pathology reports and material (when available) of 100 consecutive lung resections for tumor (50 from our environmental/occupational pathology consultation cases (CC) and 50 from routine surgical cases (SC)) were reviewed for the presence and abundance of WB (abundant: >5 foci; rare: ≤5 foci). Statistics included means, frequencies, t-tests or χ^2 test.

Results: All cases had either a lung resection for a neoplasm or an autopsy. CC and SC differed significantly by age (73 vs 62 y) and gender (88% male vs 62% female, respectively). The median number of slides examined was 4 for CC and 7 for SC. The major primary diagnoses in CC were primary lung cancer and mesothelioma, and in SC primary lung cancer. None of the original reports for either group mentioned WB. Although we found WB in 52% of both groups, abundant WB was present in 65% of the CC vs only 34% of the SC. Presence of any WB and a greater abundance was more common in males, even among the SC, consistent with greater industrial/occupational exposure in men. Asbestos bodies were noted in 17 of the CC and 1 SC on H&E stained sections. Most CC had some history of asbestos exposure.

Conclusions: This study shows absence of reporting despite the frequent presence of WB in routine clinical lung pathology specimens. It is important to recognize exposure to welding because it: 1) provides additional documentation of inhalational exposure that a pathologist can identify, 2) is a marker of complex metal-working exposure that is easier to see than asbestos fibers and may trigger a further search for asbestos exposure (which is often a concomitant exposure in welding environments), 3) stimulates additional investigation into the complex effects of welding.

1986 *SMARCA4*/BRG1 Loss Occurs in Mediastinal and Pleural Tumors with Rhabdoid Morphology and Aggressive Behavior

Jennifer L Sauter, Rondell Graham, Anja C Roden, Jennifer M Boland. Mayo Clinic, Rochester, MN.

Background: BRG1 protein encoded by *SMARCA4* participates in a chromatin-remodeling complex that includes *SMARCB1*/INI-1 and suppresses tumor cell growth. *SMARCA4*/BRG1 inactivation is observed in high grade tumors with rhabdoid histology at several sites, including ovary, gastrointestinal tract, and thorax. Our aim is to evaluate the utility of immunohistochemistry (IHC) in identification of BRG1 deficient thoracic tumors, and describe their clinicopathological features.

Design: Slides were reviewed from mediastinum, pleura and lung tumors in our institutional surgical and consultation archives, with diagnosis keywords of rhabdoid, undifferentiated, or malignant neoplasm. Study cases (n=29) were selected with rhabdoid morphology. IHC was performed for BRG1 (EPNCIR111A, Abcam), pan-keratin, INI-1, desmin, NUT, S-100 and TTF1 (SPT24). Thymic carcinomas (n=11) were included as a comparison group. BRG1 loss was defined as negative tumor nuclei with positive internal control. Clinical data was obtained from medical records and referring physicians.

Results: Six of 29 undifferentiated thoracic tumors had BRG1 loss (21%): 5 of 14 in the mediastinum (36%), 1 of 5 in the pleura (20%), and 0 of 10 in the lung. INI-1 loss was present in 1 pleural tumor (retained BRG1), while all others had retained INI-1. All thymic carcinomas had retained BRG1 and INI-1. Morphologically, tumors with BRG1 loss showed sheets of monotonous discohesive ovoid cells with abundant eosinophilic cytoplasm, eccentric nuclei, and prominent nucleoli. Brisk mitotic activity and necrosis were universal, and occasional vague perinuclear hyaline inclusions were present. BRG1 deficient cases had focal keratin expression in 4 cases (67%), focal desmin in 2 (33%, negative myogenin), and weak TTF1 in 1 (keratin negative). All were negative for NUT and S-100. BRG1 deficient tumors occurred at mean age of 56 years (range, 44-69) with male predominance (5:1). Follow-up was available for 30 patients (mean, 39 months; range, 0.5-176), including 6 with BRG1 loss, 13 with retained BRG1, and 11 thymic carcinomas. All patients with BRG1 deficient tumors (100%) were dead of disease at a mean of 20.5 months (range, 1-108), compared to 46% in the BRG1 retained group and 73% in thymic carcinoma.

Conclusions: Thoracic tumors with BRG1 loss have a propensity for the mediastinum and pleura. They are histologically similar to tumors with INI-1 loss, with high grade rhabdoid appearance, and often show focal keratin expression. BRG1 deficient tumors are very aggressive, and may have a prognosis worse than other poorly differentiated thoracic tumors.

1987 Comparative Molecular Analysis of Typical and Atypical Pulmonary Carcinoid Tumors by Next Generation RNA Sequencing

Olga Sazonova, Babak Khoshkrood-Mansoori, Adréanne Gagné, Michèle Orain, Yohan Bossé, Philippe Joubert, Joël Tremblay Joël Tremblay Marchand. University Laval, Quebec, QC, Canada; Quebec Heart and Lung Institute, Quebec, QC, Canada.

Background: Pulmonary carcinoid tumors represent 3-5% of lung cancers and are divided into typical (TC) and atypical carcinoids (AC) based on the mitotic rate and the presence of necrosis. TC has a favorable prognosis and is usually cured by surgical resection while AC (intermediate grade tumor) more frequently recur and give metastases. To date, only few studies compared the molecular profile of typical and atypical carcinoids. Therefore, it is unclear which molecular alterations determine higher grade and more aggressive behavior of AC versus TC. The aim of this study was to compare the transcriptome of histologically well-characterized TC and AC.

Design: Patients that underwent lung resection for carcinoid tumors with available specimens in our biobank were reviewed. The case selection of TC and AC was done on the basis of mitotic counts. To minimize the impact of interobserver variability and issues related to the tumor heterogeneity, AC at the higher spectrum of the mitotic rate (5 to 10 mitoses per 2 mm²) were selected. A mitotic rate of less than 2/2mm² combined with the absence of necrosis were the criteria used for TC selection. Eight cases from both groups selected.

Gene expression levels of tumor samples were measured by paired-end RNA sequencing using the Illumina platform and compared between TC and AC. Differential expression analysis was carried out using three different algorithms. Pathway analysis linking differentially expressed genes were then performed to understand the molecular processes of these cancer subtypes.

Results: Ninety-five genes differentially expressed in TC versus AC were found. Most of these genes were primarily shown to participate in the processes of inflammation, cellular adhesion, migration and immune response. Genes known to be implicated in cancer and confirmed to be up- or down-regulated by at least 2 different algorithms were identified including *HIST1H1T, SPP-1, TREM-1, TYRO-3.* In addition, upstream analysis revealed the *MYD88* gene as a potential regulator. Surprisingly, no changes in gene expression associated with increased proliferation were found.

Conclusions: The current study highlights for the first time genes differentially expressed in TC compared to AC that are involved in inflammation, cellular adhesion, migration and immune response. These results are important to delineate the molecular basis and clinical behavior of AC and TC.

1988 Correlation of PD-L1 Expression with Molecular Driver Oncogene Mutations in Non-Small Cell Lung Cancer

Jason V Scapa, Haodong Xu. David Geffen School of Medicine at UCLA, Los Angeles, CA.

Background: Lung cancer has the highest mortality rates among malignancies worldwide, with non-small cell lung cancers (NSCLC) accounting for over 80% of lung cancer cases. Molecular driver oncogene mutations in NSCLC have been identified, particularly in the epithelial growth factor receptor (*EGFR*) and Kirsten rat sarcoma viral oncogene homolog (*KRAS*). Immune checkpoint pathways are implicated in T-cell unresponsiveness, allowing tumor cells to avoid the destruction by the host immune system. Blockade of interaction between the Programmed Death protein 1 (PD-1) and its ligand (PD-L1) provides tantalizing targets for immunotherapy. Previous studies suggest a correlation between molecular oncogene drivers EGFR/KRAS and PD-1/PD-L1 expression, although results remain inconsistent. Using pathologic and clinical data available at our large, academic medical center, we retrospectively examined the relationship between molecular driver oncogenes and PD-L1 expression in NSCLC.

Design: Using our pathology case database, we identified lung cancer cases in which PD-L1 immunohistochemistry (IHC) was performed using the 22C3 PD-L1 antibody clone. Many of these cases underwent molecular testing with our Molecular Lung Cancer Panel, which sequences for mutations in *EGFR*, *KRAS*, *NRAS*, *BRAF*, *ERBB2*, and *PIK3CA* in addition to cytogenetic studies for *ALK* and *ROS1* gene rearrangements. We characterized their demographic, pathologic, clinical, and molecular parameters in addition to PD-L1 IHC status in order to determine correlations between driver oncogenes' mutations and PD-L1 expression.

Results: We identified 76 NSCLC biopsies cases with both PD-L1 IHC and available molecular testing results. There were eight PD-L1 positive cases (over 50% of tumor cells staining) and ten cases with less than 50% of PD-L1 tumor cell staining. EGFR driver mutations in the PD-L1 positive group were not increased relative to the PD-L1 less than 50% of tumor cells staining and negative staining groups ($p = 0.3854$). However, KRAS driver mutations were present in higher proportion in the PD-L1 positive group ($p = 0.024$). Although not statistically significant, mutations were also found in other oncogenes including *BRAF*, *ERBB2*, *PIK3CA,* and *ALK*.

Conclusions: The relationship between PD-L1 and EGFR remains controversial. We did not find an increase in EGFR mutations in our PD-L1 positive cases using the 22C3 antibody clone. However, KRAS driver mutations did appear in a higher proportion in our PD-L1 positive group and may represent a driver mutation associated with PD-L1 expression.

1989 A Comparative Analysis of PD-L1 Distribution in Primary NSCLC and Metastatic Tumors to the Lung

Wijendra Senarathne, Peggy Gates, Semir Vranic, Zoran Gatalica. Caris Life Sciences, Phoenix, AZ; University of Sarajevo, Sarajevo, Bosnia and Herzegowina.

Background: Expression of programmed death-1 ligand (PD-L1, CD274) in non-small cell lung cancer (NSCLC) is associated with a benefit to PD-1/PD-L1 blockade targeted therapy. Expression of PD-L1 is believed to be an immune surveillance evasion mechanism. In the present study, we investigated expression of PD-L1 in the tumor microenvironment (TMA) in carcinomas metastatic to the lungs and compared them to primary lung carcinomas.

Design: 205 formalin-fixed paraffin-embedded tissue samples [81 primary NSCLC and 124 metastatic tumors to the lung (colon, breast, gynecologic, head and neck, unknown primary site carcinomas, and soft tissue tumors)] were evaluated for PD-L1 expression (anti-PD-L1 SP142 antibody) using the automated immunohistochemical method. PD-L1 positivity was defined as membranous expression (2+) in ≥5% in tumor cells (TC) or tumor infiltrating immune cells (IC). All cases were stratified into four categories based on the presence or absence of PD-L1 expression on TC's or IC's.

Results: PD-L1 TC's postivity in primary NSCLC was significantly higher than in metastatic tumors (28% vs. 9%, $p<1.001$). In contrast, PD-L1 expression in IC's was significantly higher in metastatic tumors than in the primary NSCLC (23% vs. 0%, $p<0.001$). No significant difference in PD-L1 expression was observed within the NSCLC histologic subgroups and within the metastatic tumor types. When stratified on the basis of combined PD-L1 distribution (TME: TC + IC) primary and metastatic tumor exhibited significantly different patterns ($p<0.001$).

TME category (PD-L1 expression)		TC+/IC+	TC-/IC-	TC+/IC-	TC-/IC+	Total
Histotype	Primary Lung	0 (0%)	58 (72%)	23 (28%)	0 (0%)	81
	Metastatic tumors	4 (3%)	87 (71%)	7 (6%)	24 (24%)	122
Total		4	145	30	24	203

Conclusions: PD-L1 distribution differs significantly between the primary (NSCLC) and metastatic tumors to the lung with predominance of PD-L1 expression on tumor cells in NSCLC and on tumor infiltrating immune cells in metastatic tumors to the lung. Further clinical studies recommended elucidating the therapeutic relevance (response rates) of these observations.

1990 The Clincopathological and Mutation Analysis of Pulmonary Mucin-Producing Adenocarcinoma

Guoguo Shang, Yan Jin, Yuan Li. Fudan University Shanghai Cancer Center, Shanghai, China.

Background: Pulmonary mucin-producing adenocarcinoma is an adenocarcinoma that includes invasive mucinous adenocarcinoma and adenocarcinoma with abundant extracellular mucin or signet ring cells. The correlation between morphological characteristics and mutational status of pulmonary mucin-producing adenocarcinoma is still unclear. We performed a retrospective study to investigate the association between mutation status and specific morphologic characteristics of pulmonary mucin-producing adenocarcinoma.

Design: In this study, 106 pulmonary mucin-producing adenocarcinomas were collected, which were reclassified according to predominant, secondary histological patterns, the presence of abundant extracellular mucin, goblet or columnar tumor cell, signet ring cells, psammoma body and spread through the air space (STAS). We investigated differences in morphologic characteristics and a spectrum of well-identified driver-gene mutations, including EGFR, KRAS, HER2, BRAF, ALK, ROS1, MET and RET.

Results: Of the 106 mucin-producing adenocarcinomas, 91 (86.8%) harbored known mutations, including 23 (21.7%) ALK rearrangements, 21 (19.8 %) KRAS mutations, 30 (28.3%) EGFR mutations, 2 (1.9%) HER2 mutations, 2(1.9%) BRAF mutations, 4 (3.8%) ROS1 rearrangements, 8 (7.5%) RET rearrangements and 1 (0.9%) MET mutation. Divided 106 mucin-producing adenocarcinomas into mucin more than 90% group (42 cases) and mucin less than 90% group (64 cases), we found that mucin more than 90% group had more frequency of ALK rearrangements (33.3% vs. 14.1%, p=0.019) and KRAS mutations (35.7% vs. 9.4%, p=0.001) than mucin less than 90% group, but lower frequency of EGFR mutations (9.5% vs.40.6%, p=0.001). ALK rearrangements were significantly more frequently detected in mucin-producing adenocarcinomas with special morphological characteristics, including the presence of STAS (p<0.001), cribriform (p<0.001) and psammoma body (p<0.001). KRAS mutations were significantly more frequently detected in invasive mucinous adenocarcinoma with goblet cell feature (p=0.004).
Conclusions: The frequency of major oncogenic driver mutations in mucin-producing adenocarcinomas varies with morphological characteristics and the presence of the extent of mucin. The findings suggest that it will be clinically valuable to investigate the morphological characteristics of mucin-producing adenocarcinomas.

1991 ALK Gene Rearranged Pulmonary Adenocarcinomas: Demographics, Clinicopathologic, and Treatment Profile in a Cohort of South East Asian Patients

Shivani Sharma, Lata Kini, Samriti Arora, Aurobinda Samal, Shipra Garg, Arbind Singh, Mohit Kumar, Beklaswar Salona, Sankar Mohan, Ajay Pandita, Rahul Katara, Sambit K Mohanty. CORE Diagnostics, Gurgaon, Haryana, India.
Background: ALK gene rearrangement in the lung adenocarcinomas is the second most common (1.6-11.7%) targetable genomic alteration, following EGFR mutation(s). However, the data on the frequency, clinicopathologic features, and treatment profile of ALK-rearranged lung adenocarcinomas from South East Asia has been very rarely explored. Therefore, we sought to study the incidence and phenotypic (clinicopathologic and treatment) profile of ALK-rearrangement in a cohort of pulmonary adenocarcinoma from South East Asia.
Design: All pulmonary adenocarcinomas were screened for ALK gene rearrangement utilizing ALK break-apart dual color FISH assay. Demographics, smoking status, EGFR mutational status, TNM stage, and treatment response were recorded.
Results: Of 512 cases screened, 42 cases exhibited ALK-gene rearrangement (8.2%) by break-apart FISH assay.

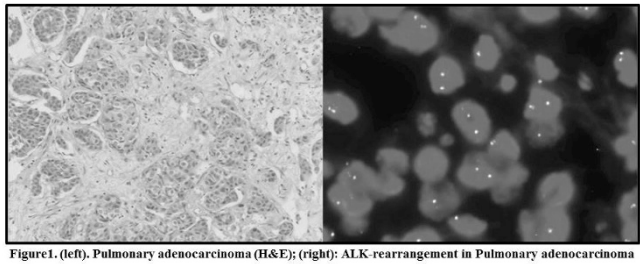

Figure1. (left). Pulmonary adenocarcinoma (H&E); (right): ALK-rearrangement in Pulmonary adenocarcinoma

The male to female ratio was 1.33:1 and the patients' age ranged from 24 years to 81 years (mean = 57 years). Smoking history was available in 5/42 (11.9%) cases of which two were smokers and the rest were non smokers.The morphologic patterns noted were solid (19/42,45.2%), acinar (9/42,21.4%), signet ring (4/42,9.5%), papillary (4/42,9.52%), mucinous (3/42,7.1%), micropapillary (2/42,4.76%), and clear cell (1/42,2.3%).The EGFR mutational analysis was performed on 35.7% cases, all of which showed a wild type status. The TNM stage was known in (12/42,28.5%) cases, all of which were stage IV. Out of eight patients who received crizotinib, two had partial response, three had stable disease after two years, and the rest three had no response. Further analysis on various determinants is currently under progress.
Conclusions: ALK-rearranged lung adenocarcinomas account for a minor proportion of non small cell lung cancer with prevalence similar to that reported in the literature. However, in contrast to the published data, in our series, patients were in older age group and had solid pattern on morphology. The survival and treatment response analyses in the rest of the patients is underway.

1992 Alveolar Framework Alterations in Fibrosing Interstitial Lung Disease: A Three-Dimensional Reconstruction Study

Angela Shih, Xiujun Fu, Lida Hariri, Tiffany Huynh, Eugene Mark, Yukako Yagi, Mari Mino-Kenudson. Massachusetts General Hospital, Boston, MA.
Background: Fibrosing interstitial lung disease (ILD) consists of several histologic patterns, the full spectrum of which encompasses a vast number of etiologies. As distinct etiologies have varying prognoses that may be modified by pharmacologic agents, it is problematic that the patterns cannot always be distinguished by conventional radiographic and histologic methods. This study analyzes alveolar framework alterations in fibrosing ILD to determine if specific architectural changes can be suggestive of certain histologic patterns.
Design: Four cases of fibrosing ILD were selected for 3D reconstruction of an approximately 0.5 mm thick section of FFPE. After multidiscplinary discussion, the wedge biopsies were given the following histological diagnoses: airway-centered interstitial fibrosis with organizing pneumonia (OP) [Case 1]; usual interstitial pneumonitis (UIP) with cystic dilatation [Case 2]; non-specific interstitial pneumonia (NSIP) [Case 3]; and end-stage UIP [Case 4]. Reconstruction for each case was performed on an average of 75 H&E and 24 EVG stains using *Voloom* software.
Results: Case 1 shows homogeneous interstitial fibrosis with evidence of OP and preservation of the underlying alveolar framework. In contrast, Case 2 demonstrates markedly convoluted alveolar architectural distortion as well as check valve-type morphology. Case 3 shows a preserved alveolar framework with striking smooth muscle accentuation extending from the bronchiolar walls. Case 4 illustrates end-stage architectural remodeling with check valve-type morphology; its extensive fibrosis is remarkable for a disproportionate loss of elastic fibers.

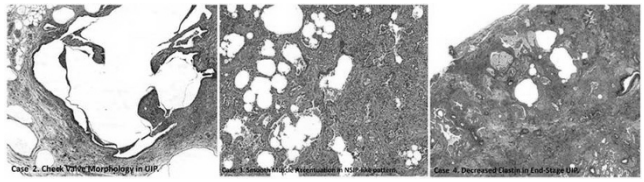

Conclusions: UIP is characterized by honeycomb morphology, which may in part be a consequence of check valve-type mechanisms contributing to cyst formation; additionally, the markedly decreased amount of elastic fibers in fibrotic areas is suggestive of significant destruction of the alveolar framework. Both OP and NSIP show alveolar architectural preservation. Using elastic stains as a means of highlighting the underlying alveolar framework may provide some indication of specific histological patterns in the spectrum of fibrosing interstitial lung disease. Additional clinicopathologic studies with evaluation of elastic stains is ongoing.

1993 Reproducibility in Classification of Small Lung Adenocarcinomas: An International Interobserver Study

Angela Shih, Hironori Uruga, Alona Muzikansky, Emine Bozkurtlar, Jin-Haeng Chung, Lida Hariri, Yuko Minami, Andre L Moreira, He Wang, Akihiko Yoshizawa, Mari Mino-Kenudson. Massachusetts General Hospital, Boston, MA; Marmara University, Istanbul, Turkey; Seoul National University, Bundang Hospital, Seongnam, Republic of Korea; National Hospital Organization, Ibarakihigashi National Hospital, Naka, Japan; NYU Langone Medical Center, New York City, NY; Temple University School of Medicine, Philadelphia, PA; Kyoto University Hospital, Kyoto, Japan.
Background: The 2015 WHO classification for lung adenocarcinoma (ACA) provides criteria for diagnosis of ACA in-situ (AIS), minimally invasive ACA (MIA), and invasive ACA (INV). Differentiating these entities can be difficult, and as understanding of prognostic significance increases, inconsistent classification is problematic. This study assesses agreement within an international panel of lung pathologists and identifies factors contributing to inconsistent implementation of WHO criteria.
Design: 60 cases of lung ACAs (≤2cm) were reviewed digitally by 6 lung pathologists in 3 rounds with intervening washout periods. The panel independently reviewed each case to assess predominant pattern, invasive component size, and final diagnosis (AIS, MIA, or INV). Round 1 provided baseline assessment; round 2 occurred after a consensus conference; and round 3 involved concomitant examination of elastic stains highlighting alveolar architecture to help differentiate lepidic from other patterns. Statistical analysis was performed.
Results: The overall kappa value for AIS versus MIA and INV decreased from 0.340 (round 1) to 0.286 (round 2) and 0.287 (round 3). The kappa value for AIS and MIA versus INV decreased from 0.438 (round 1) to 0.296 (round 2), with an increase to 0.338 (round 3). Misinterpretation of WHO criteria resulted in 18 instances of misclassification in round 1, which decreased to 4 instances in round 3. A mucinous ACA had a wide range of diagnosis across raters. In round 1, the raters had 100% agreement on final diagnosis in 12 cases, which decreased in round 3 to 6 cases. The intraobserver kappa coefficient between round 1 and 3 ranged from 0.53 to 0.73.
Conclusions: Interobserver agreement on small lung ACA diagnosis between 6 raters was fair, and improved minimally with concomitant elastic stain evaluation. Poor agreement is primarily attributable to subjectivity in pattern recognition, although there is moderate to substantial intraobserver agreement. Misinterpretation of the WHO criteria contributing to inconsistent classification may be resolved by education. More reliable markers to differentiate histologic patterns may be necessary to improve interobserver agreement in small lung ACA classification.

1994 Pulmonary Squamous Cell Carcinoma with Lepidic Pattern- A Study of 9 Cases

Hemlata Shirsat, Ashley E Stueck, Mathieu C Castonguay, Zhaolin Xu. Dalhousie University, Halifax, NS, Canada.
Background: Pulmonary squamous cell carcinomas are thought to arise from metaplastic bronchial epithelium through a metaplasia-dysplasia-carcinoma sequence and are often centrally located. In contrast, bronchogenic adenocarcinomas are thought to arise from bronchial epithelium and peripheral pulmonary units; occurring as peripheral tumours. A lepidic growth pattern is frequently seen in adenocarciomas, but has rarely been reported in association with squamous cell carcinomas. Squamous cell carcinoma sometimes may entrap benign reactive pneumocytes; in such cases, classification as adenosquamous carcinoma is often entertained.
We embarked on this study to evaluate cases of squamous cell carcinoma showing lepidic-like areas and explore the mechanism(s) of development of peripheral squamous cell carcinoma.
Design: Nine cases of resected pulmonary squamous cell carcinomas with lepidic-like areas were identified over a 6-year period. These cases were analyzed using H&E-stained tumour sections and p40 and TTF1 (SPT24 clone) immunohistochemical (IHC) studies.
Results: All cases were peripheral invasive squamous cell carcinomas with focal lepidic-like areas. Two patterns of immunohistochemical reactivity were noted: 1, five cases showed superficial reactive pneumocytes undermined by squamoid/squamous

cells, both reactive to TTF1 (with more intense reactivity in pneumocytes), and only squamous cells reactive to p40; 2, three cases showed only superficial pneumocytes reactive to TTF1 and basal squamoid cells reactive to p40. One case demonstrated the conventional metaplasia- dysplasia –carcinoma sequence of ciliated bronchial epithelium with both bronchial epithelial and squamous cells staining for TTF1. Among those, three cases showed significant entrapped hyperplastic reactive pneumocytes giving a pseudoglandular appearance.

Conclusions: In many cases, the proliferating basal squamoid cells were not morphologically identical to the cells in invasive component. This makes true lepidic growth, extending from the invasive component into the alveolar walls, unlikely, and raises the possibility that peripheral squamous carcinoma may arise from squamous metaplasia of type 2 pneumocytes with further dysplasia-carcinoma sequelae. Lepidic-like growth does exist in squamous cell carcinoma of the lung. Entrapped pneumocyte hyperplasia can mimic adenosquamous carcinomas. Careful evaluation of architecture and morphology of type 2 pneumocytes with appropriate IHC can help distinguish them.

1995 Frequency of Neuroendocrine Cell Proliferations in Lungs Explanted for Fibrotic Interstitial Lung Disease and Emphysema

Susan Shyu, Jonathon E Heath, Allen P Burke. University of Maryland School of Medicine, Baltimore, MD.

Background: Definitions for neuroendocrine cell hyperplasia (NECH) and diffuse idiopathic neuroendocrine cell hyperplasia (DIPNECH) have recently been proposed. Using these criteria, we sought to determine the incidence of NE cell proliferations in a series of lung explants. Although an association between NECH and chronic lung disease has been suggested, the frequency of secondary NECH has not been reported. Series of neoplasia associated with parenchymal lung disease include non-small cell carcinomas, but not neuroendocrine tumors.

Design: Synaptophysin staining was performed on 2 representative sections each from a series of lungs explanted for fibrotic lung disease and emphysema between December 2013 and June 2016. Cases were defined as NECH (≥3 bronchioles with ≥5 endocrine cells), borderline diffuse neuroendocrine cell hyperplasia (DPNECH) (1-3 tumorlets with or without NECH), and DPNECH (≥3 tumorlets with NECH).

Results: There were 60 explants with ILD (57 usual interstitial pneumonia, 2 nonspecific interstitial pneumonia, 1 sarcoidosis), and 11 with centrilobular emphysema. There were 4 cases of DPNECH in the ILD group (7%), 1 case of borderline DPNECH (2%) and 21 cases of NECH (35%). There were no cases of DPNECH in the emphysema group, with 1 borderline DPNECH case (9%) and 5 NECH (45%). One DPNECH in UIP had 26 tumorlets and 50 bronchioles with NECH. An unexpected finding was the presence of synaptophysin positivity in reactive pneumocytes adjacent to fibroblastic foci in 36 cases of UIP (63%).

Conclusions: NECH is common in ILD and emphysema, and includes DPNECH in 7% of ILD in this series. These results suggest that fibrotic lung disease is a predisposing factor for neuroendocrine cell proliferation, in addition to the known risk of epithelial carcinomas.

1996 Circulating Tumor Cell Detection via a Novel FISH Assay Prior to Lung Biopsy Enables Accurate Prediction of Pulmonary Malignancy

Amber L Smith, Tanweer M Zaidi, Namita Shanbhag, Duy Truong, Sara Shkedy, Brenda L Namer, Joshua D Kuban, Ruth L Katz. MD Anderson Cancer Center, Houston, TX.

Background: Patients at risk for lung cancer (LC) may present with indeterminate pulmonary nodules. However due to cost, morbidity, and high rate of negative biopsies (bx), many patients are followed by CT scans alone. An accurate adjunctive biomarker that could predict for LC would be advantageous to make an early diagnosis of LC so that serial CT scans or unnecessary biopsies could be avoided. We performed a prospective study using a four-color FISH probe, which was developed based on data derived from CGH arrays from Non-Small Cell Lung Cancers (NSCLC) and was designed to detect circulating tumor cells (CTCs) in the peripheral blood of LC patients. Our aim was to test the utility of our CTC test to predict LC in indeterminate lung nodules.

Design: Patients who had no prior history of LC were eligible. Prior to needle bx, blood was collected. I-FISH was performed on blinded samples enriched for peripheral blood mononuclear cells using a custom probe set comprising 3 tel,3p22.1, cep 10, and 10q22.3. Intact cells (500) were analyzed by an automated instrument (Bioview Il) optimized to select for larger cells, and classified into subclasses based on gains and / or losses of fluorescent signals. CTCs were defined as cells with increased copy number of 2 ≥ genes. A positive assay was defined as 4 ≥ CTCs; negative assay was CTCs<4.

Results:

Total cases	33
Classification	Malignant (25) Suspicious (2) Negative (6)
Tumor types	Primary LC (23) Adenocarcinoma (17) Squamous cell carcinoma (4) Neuroendocrine carcinoma (1) NSCLC (1) Melanoma (2)
Average age	69.6 years (50-85 years)
Male: Female	18:15
Average tumor size	Malignant 2.5 cm (0.7 – 7.5 cm) Negative 1.8 cm (1 – 5 cm)
Lung cancer stage	Early (7) Late (13) Unknown (2)

By CTC assay using bx as gold standard there were 24 true positives, 6 true negatives, and 2 false negatives called "suspicious" for LC. There were no false positives. Sensitivity for the detection of malignancy was 92.6%; positive predictive value was 100%, specificity was 100%.

Conclusions: Our FISH-based CTC test was highly sensitive to detect malignant cells of NSCLC; however, unsuspected metastatic melanoma was also detected. This pilot study is being validated, however, it appears to hold great promise as an adjunctive biomarker for triaging patients with positive blood tests for needle bx of indeterminate lung masses, whereas patients with negative CTC tests, may be followed by CT scan.

1997 Poorly-Differentiated Non-Keratinizing Squamous Cell Thymic Carcinoma: A Clinicopathologic, Immunohistochemical and Molecular Genetic Study of 25 Cases

David Suster, Alexander C Mackinnon, German Pihan, Saul Suster. Beth Israel Deaconess Medical Center, Boston, MA; Medical College of Wisconsin, Milwaukee, WI.

Background: Poorly-differentiated non-keratinizing squamous cell carcinoma of the thymus is a rare, aggressive variant of thymic carcinoma whose clinicopathologic, immunohistochemical and molecular features have not been well-characterized.

Design: The clinicopathologic features of these tumors were abstracted and a broad panel of immunohistochemical stains were assayed. Tumor enriched DNA was extracted from FFPE blocks for all 25 cases and sequenced with the Ion AmpliSeq™ Cancer Hotspot Panel v2. Variants were analyzed using Torrent Suite 5.2.0 and annotated with the GenomOncology Workbench.

Results: The patients were 5 women and 20 men aged 20-85 years (mean: 59.8). Symptoms included shortness of breath, chest pain and weight loss. The lesions presented as well-defined anterior mediastinal masses without a history or evidence of similar tumor elsewhere. The tumors were grossly lobulated, tan to white, with areas of hemorrhage and necrosis and measured from 2.0 to 13.5 cm (mean: 6.0 cm). Histologically the tumors were characterized by irregular cords and islands of tumor cells comprised of atypical cells with large vesicular nuclei and prominent nucleoli. Tumor cells displayed brisk mitotic activity (>10 mitoses per 10 HPF). The stroma showed dense lymphoplasmacytic infiltrates in 17 cases (lymphoepithelioma-like pattern) and a dense sclerotic stroma in 9 cases (desmoplastic pattern). Immunohistochemical stains showed strong positivity of the tumor cells for cytokeratin AE1/AE3, CK5/6, CK18, MOC31, p40 and p63. MIB-1 showed on average 35% nuclear positivity. CD117 was positive in 21/25 cases and CD5 was positive in 20/25 cases. PDL-1 showed strong membranous positivity in 17/23 cases. EBER in-situ hybridization was positive in only 2/24 cases. High quality sequence data was obtained for 22 of 25 cases. Variants with allele frequency between 5% and 45% and quality scores >50 were classified as somatic. 19/22 cases had one or more somatic variants of unknown significance. One case showed an IDH1 p. R132C mutation.

Conclusions: Poorly-differentiated non-keratinizing thymic squamous cell carcinoma is an aggressive type of primary thymic epithelial neoplasm with a distinctive phenotype. The lack of common, clinically actionable somatic variants (i.e., BRAF, EGFR, or KRAS) suggests that alternative genetic aberrations may contribute to the development and growth of these tumors.

1998 Temporal and Spatial Heterogeneity of Programmed Cell Death-Ligand 1 Expression in Malignant Mesothelioma

Simone BSP Terra, Aaron S Mansfield, Tobias Peikert, Anja C Roden. Mayo Clinic, Rochester, MN.

Background: Programmed Cell Death-Ligand 1 (PD-L1) and Programmed Death Protein 1 (PD-1) blocking antibodies are promising immunotherapies for malignancies. We have shown PD-L1 expression in 40% of malignant mesothelioma (MM); however, the temporal and spatial heterogeneity of its expression has not been thoroughly studied. We compared PD-L1 expression between primary and metastatic MM and primary and recurrent/persistent MM.

Design: Pathology files (1995-2016) were searched for cases of MM that had tissue from multiple sites and/or time points. Cases were reviewed by a thoracic pathologist. PD-L1 (SP263, Ventana Medical Systems, Inc., Tucson, AZ, US) expression was reviewed by 2 authors; membranous staining of tumor cells was scored as <1% (considered negative), 1-10%, >10-50%, >50%. Disagreement was solved by consensus.

Results: 64 patients (53 men, median age at diagnosis, 64 years, range, 37-76) with epithelioid (N=50), biphasic (N=11) or sarcomatoid (N=2) MM or well differentiated papillary mesothelioma (N=1) (pleural, N=56; peritoneal, N=8) were included. Subsequent biopsies revealed an additional histologic MM component in 11 cases. Patients had a subsequent specimen from the primary site (N=48, 0.1-132 months [median, 4] after initial specimen), from a metastasis (N=6, 7-120 months [median, 17]), or both (N=10, 0.3-57 months [median 4.5]). Reviewers agreed on PD-L1 expression in 135 of 151 (89%) specimens. In the initial specimen, PD-L1 expression was <1% (N=33), 1-10% (N=19), >10-50% (N=7) or >50% (N=5). PD-L1 expression is summarized in the table.

PD-L1 expression in initial specimen	PD-L1 expression in follow-up specimen/metastasis	MM at different time points (N=58), N (%)	Primary MM and metastasis (N=16), N (%)
Concordant			
Neg	Neg	23 (40)	7 (44)
Pos	Pos, % expression = initial specimen	18 (31)	1 (6)
Discordant			
Neg	Pos	6 (10)	3(19)
Pos	Neg	5 (9)	2 (12)
Pos	Pos, % expression > initial specimen	1 (2)	3 (19)
Pos	Pos, % expression < initial specimen	5 (9)	0

There was agreement of PD-L1 expression between paired primary lesions obtained at separate time points in 41 of 58 (71%) and between paired primary and metastatic lesions in 8 of 16 (50%) cases.

Conclusions: In MM PD-L1 expression can differ between specimens from multiple time points and between primary sites and metastases. This heterogeneity could affect treatment selection with the use of PD-L1 as a predictive biomarker; however, the degree of sampling error we observed emphasizes the need for better biomarkers for PD-1/PD-L1 axis inhibitors.

1999 Mediastinal Synovial Sarcoma: Clinicopathological Analysis of 20 Cases with Molecular Confirmation

Simone BSP Terra, Scott W Aesif, Joseph J Maleszewski, Andrew L Folpe, Jennifer M Boland. Mayo Clinic, Rochester, MN; University of Wisconsin, Madison, WI.

Background: Synovial sarcoma (SS) is a translocation-associated sarcoma characterized by *SS18-SSX* fusion, which is most common in the extremities of young adults. SS can be monophasic, consisting of monomorphic spindle cells, or biphasic, which also have an epithelial component. Some cases of SS are poorly differentiated, with increased cellularity and high grade nuclear features. The mediastinum is an exceedingly rare primary site, and the literature consists mainly of case reports and small series without molecular confirmation. The aim of this study is to report the clinicopathological characteristics of 20 molecularly confirmed mediastinal SS, the largest series to date.

Design: Cases were identified by searching our institutional surgical and consultation archives. Existing slides were reviewed, including surgical excisions (8), incisional biopsies (3), and small biopsies (9). Diagnoses were confirmed by either *SS18* FISH (n=5) or RT-PCR for *SS18-SSX* fusion (n=15). Clinical information was acquired from medical records and referring physicians.

Results: The 20 mediastinal SS occurred in patients aged 21-75 years (mean, 38). Only 1 patient (5%) was older than 50 years. A male predominance was observed (14 men, 70%). Only 1 confirmed biphasic example was identified based on available samples (5%), while 11 cases were poorly differentiated (55%). Average tumor size was 17 cm (range, 6.4-23), and they occurred in the anterior, posterior and superior mediastinal compartments. Presenting symptoms included pain, dyspnea, cough, dysphagia, hemoptysis, and Horner syndrome. Specific fusion transcripts were known in 10 cases, with 6 *SYT-SSX2*, and 4 *SYT-SSX1* including the biphasic SS. Follow-up was available for 13 patients (mean, 20 months; range, 5- 45). Local recurrence occurred in 9 cases, and metastasis in 6 cases (lung, pericardium, brain). Nine patients died from disease (5-32 months from diagnosis), and 4 were alive with disease at last follow-up (range, 6-45 months).

Conclusions: Mediastinal SS is a rare and aggressive malignancy most common in patients younger than 50 years. Most are monophasic and reach large size before detection. Poorly differentiated morphology is common. SS should be included in the differential diagnosis of spindle cell, biphasic and poorly differentiated mediastinal tumors. Due to the rarity at this site, molecular confirmation is prudent to confirm the diagnosis.

2000 A Comparison of *ALK* Gene Rearrangement and ALK Protein Expression in Primary Lung Carcinoma and Matched Metastasis

Humberto Trejo Bittar, Sanja Dacic. UPMC, Pittsburgh, PA.

Background: The CAP/IASLC/AMP guideline for *EGFR* and *ALK* testing in lung carcinoma indicates that either the primary tumor or the metastasis are suitable for testing. While the heterogeneity of gene mutations has been extensively studied, similar reports on gene rearrangements are limited. The aim of this study was to determine if the *ALK* status between primary tumor and matched metastasis differs.

Design: 2116 non-small cell lung carcinomas were tested by ALK-FISH using the Vysis ALK Break Apart FISH kit. A total of 34 cases (68 tissue samples) had sufficient tissue samples from primary tumor and matched metastases available. ALK immunohistochemistry was performed in the selected cases usign the ALK D5F3 clone (Ventana ALK D5F3 CDx Assay).

Results: Of the 34 cases, there were 15 cases positive for *ALK* rearrangement and 19 cases negative for *ALK* rearrangement. Overall, there were 30 cases (30/34; 88%) with concordant *ALK*-FISH results, and 32 cases (32/34; 94%) with concordant ALK-IHC results. FISH discordant cases included three cases with *ALK*-FISH positive primary tumors and *ALK*-negative matched metastases. One case showed *ALK*-FISH positive metastasis, while primary tumor was negative. All samples from four FISH discordant cases were ALK-IHC negative. Discordant cases included small biopsy and cytology samples with a tendency towards lower percentage of *ALK*-FISH positive tumor cells (average 23%; range 18-31%). The two ALK-IHC discordant cases showed ALK expression in the primary tumor only.

Conclusions: Our study suggests that the *ALK*-FISH results show more frequent discordances between primary tumor and matched metastases than ALK-IHC most likely due to technical challenges of the FISH assay and sample quality. This observation indicates that the quality of sample and technical expertise of the laboratory should guide decision about *ALK* testing in clinical practice.

2001 Immune Profile of Ciliated Muconodular Papillary Tumors

Emiko Udo, Sayuri Nakamura, Mikiko Hashisako, Junya Fukuoka. Graduate School of Biomedical Sciences, Nagasaki University, Nagasaki, Japan.

Background: Ciliated muconodular papillary tumors (CMPTs) are newly recognized rare peripheral lung nodule, consisting ciliated columnar, goblet, and basal cells, and the diagnosis is always challenging between inflammatory nodules and mucinous adenocarcinoma. Due to the rarity, immune profile of CMPTs related to oncogenesis including programmed cell death ligand 1 (PD-L1) is not well examined. We reviewed cases of CMPTs and immunohistochemically evaluated for mucinous adenocarcinoma related markers and PD-L1.

Design: Four cases of surgically resected CMPT were identified between 2012 and 2016. We performed immunohistochemistory using antibodies to HNF4-alfa (clone H1415), MUC5B (polyclonal), p53 (clone DO-7), TTF-1 (clone SPT24) and PD-L1 (clone SP142). HNF-4alfa and MUC5B were scored as follows: -; negative, 1+; focal, 2+; diffuse. p53 expression was assessed by intensity as follows: 1+; weak and sporadic pattern, 2+; frequent positive but unclear for over expression, 3+; diffusely positive with clear over expression. PD-L1 expression was scored by percentage of PD-L1 positive cells among tumor cells.

Results: In the four cases, all cases were positive for HNF4 alfa and TTF-1 in nuclear. Two cases showed diffuse and strong intensity for HNF4 alfa as seen in mucinous adenocarcinoma or colorectal carcinoma. Different from mucinous adenocarcinoma, all cases showed diffuse TTF-1 positive and one case indicated possible overexpression. Cytoplasmic staining of MUC5B is also detected in all cases which is very rare in normal lung parenchyma but common in mucinous adenocarcinoma. Nuclear expression of p53 was found with more frequent positive cells for two cases and with clear over expression in one case.

Additionally, we performed immunostaining for PD-L1, three cases showed <1% PD-L1 in tumor cell membrane and one case showed 1-5% positive. The case with higher frequency of PD-L1 did not show abnormal staining of p53. These findings suggest that CMPTs are neoplastic condition, tumors originated from terminal respiratory units, and show similarity to mucinous adenocarcinoma.

Immune Profile of Ciliated Muconodular Papillary Tumors (CMPTs) of Lung

	PD-L1 (SP142)	HNF4-α	MUC5B	p53	TTF-1
case 1	<1%	++	+	++	+
case 2	<1%	+	++	+++	++
case 3	<1%	++	++	++	+
case 4	1-5%	+	++	+	+

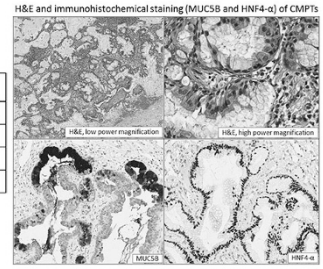

Conclusions: Our study showed that CMPTs are likely to be neoplasia of terminal respiratory unit origin and possess similar profile as mucinous adenocarcinoma of the lung.

2002 The Role of IL-24 in Lung Adenocarcinoma

Shigeaki Umeda, Koji Okudela, Yoko Tateishi, Mai Matsumura, Kenichi Ohashi. Yokohama City University, Yokohama, Kanagawa, Japan.

Background: Lung cancer research has been changed drastically by combining genetic information and morphology in recent years. Histological subtypes of lung adenocarcinoma were well correlated with driver oncogene abnormality such as *EGFR* and *KRAS* mutation. Molecular targeting agents have been developed for each cancer types. Even though EGFR and KRAS share MAP kinase cascades, *EGFR* mutated adenocarcinoma and *KRAS* mutated adenocarcinoma were contrasted and often separately discussed owing to the mutually exclusive relationship. Roles of the genes involved in the common signal pathway to promote lung adenocarcinoma development are still largely unknown.

Design: During the search for common downstream targets modulated by both oncogenic KRAS and EGFR transduction in immortalized human airway cells, we focused on IL-24 in the present study. We performed expression analysis of IL-24 in lung cancer cell lines with quantitative real time PCR. To evaluate the expression regulation of IL-24 in human lung cancer cells, treatment with an inhibitor for a DNA methyl-transferase (5-AZA-dc) in combination with an inhibitor for histone deacetylase (trichostatin A, TSA) was performed. Moreover, we investigated the potential effects of IL-24 transduction on cell growth and migration activities in both a *KRAS* mutant cell line and an *EGFR* mutant lung cancer cell line. To elucidate its role in lung adenocarcinoma progression, we investigated associations between the levels of IL-24 expression and histopathological parameters in surgically resected primary lung cancers.

Results: IL-24 mRNA expression levels were markedly decreased in adenocarcinoma cell lines. In addition, the expression in some of the cancer cells was restored by 5-azacytidine and trichostatin A treatment. A forced expression of IL-24 inhibited migration in A549 and in PC-9 human lung cancer cells, which had lost the IL-24 expression. Immunohistochemical study with semi-quantitative measurement of 143 lung adenocarcinoma cases revealed invasive predominant subtypes had significantly lower scores of IL-24 expression than a lepidic predominant subtype (p=0.0240).

Stage I adenocarcinoma cases showed significantly higher scores than Stage II or more advanced cases (p=0.0252). Although the statistical significance was not confirmed between the groups harboring *EGFR* or *KRAS* mutation, *EGFR* mutation positive or *KRAS* mutation positive adenocarcinoma cases tended to have the higher IL-24 scores than those without the mutations.

Conclusions: Our results suggested IL-24 could play a role in the common oncogenic pathway, intrinsically suppress invasion early and disappear late in lung adenocarcinoma progression.

2003 Pathologic Patterns of Inflammatory Lung Injury Following Anti-PD-1 Immunotherapy in Asymptomatic Patients

Moises J Velez, Charles Leduc, Matthew Hellmann, Jamie Chaft, Jarushka Naidoo, Janis M Taube, Patrick M Forde, Valerie Rusch, William Travis, Natasha Rekhtman. Memorial Sloan Kettering Cancer Center, New York, NY; The Johns Hopkins University, Baltimore, MD.

Background: PD-1/PD-L1 immune checkpoint blockade is an emerging treatment option for many cancers and works by potentiating the host immune response against tumor. Pneumonitis is an uncommon but recognized immune-related adverse event (irAE) associated with anti-PD-1/PD-L1 agents, with clinical manifestations ranging from asymptomatic to fatal. We examined the histopathologic findings in the non-tumor lung tissue of a series of patients following pre-operative anti-PD-1 treatment, and compared the findings to those in patients with lung samples obtained for clinically evident PD-1-related pneumonitis.

Design: We evaluated the nonneoplastic lung in 9 patients who underwent surgical resection following pre-operative anti-PD-1 treatment for non-small cell lung cancer. The histologic findings were compared with biopsy or surgical specimens from 11 patients with clinically evident pneumonitis associated with anti-PD-1/PD-L1 therapy recently reported from our institution (Naidoo et al. J Clin Oncol. 2016 PMID: 27646942).

Results: All 9 patients who received pre-operative anti-PD-1 had pathologic evidence of inflammatory injury in the non-neoplastic lung, including organizing pneumonia (n=1), cellular interstitial pneumonia (CIP) (n=3, one also with non-necrotizing granulomas), necrotizing granulomatous inflammation (n=1), non-necrotizing granulomatous inflammation (n=2) and non-specific chronic inflammation (n=2). There was no evidence of infection in any samples based on special stains, cultures and viral PCR, when available. Of these 9 patients, only one (with CIP) had clinical evidence of pneumonitis prior to surgical resection. These findings were similar in the phenotypic spectrum and severity to those in 11 recently reported patients with known, clinically recognized pneumonitis with the exception that diffuse alveolar damage was identified only in those with known pneumonitis.

Conclusions: The patterns of lung injury in asymptomatic patients treated with anti-PD-1 are highly varied, and the findings are etiologically non-specific. Nevertheless, the lack of other apparent etiology and the overall similarity of the findings to those in symptomatic patients makes it likely that the observed inflammatory lesions represent subclinical irAE. The clinical significance of this potentially common feature of PD-1 blockade will require further study.

2004 Loss of BAP1 Expression Is Useful in the Distinction of Thymic Carcinoma from Thymoma

Julie A Vrana, Marie Christine Aubry, Eunhee S Yi, Anja C Roden. Mayo Clinic, Rochester, MN.

Background: Both somatic and germline mutations of *BRCA1-Associated Protein 1 (BAP1)*, a tumor suppressor gene, are known to occur in uveal melanoma and malignant mesothelioma. Most *BAP1* mutations are associated with loss of BAP1 protein expression. Loss of BAP1 expression has recently been shown in a subset of malignant mesotheliomas but not in reactive mesothelial proliferations. However, BAP1 expression has not been thoroughly investigated in other neoplasms. We studied BAP1 expression in thymic epithelial tumors (TET) and explored the value of loss of BAP1 expression in the distinction of thymic carcinomas from thymoma.

Design: Institutional TET database (1996-2014) was searched for WHO type A and B3 thymomas and thymic carcinomas. All cases were reviewed blindly by 3 thoracic pathologists who independently agreed upon the WHO classification. Thymic carcinomas were staged according to TNM staging. All cases were stained with BAP1 (clone C-4, Santa Cruz Biotechnology). BAP1 expression was reported as lost (no nuclear stain of epithelial tumor cells but presence of nuclear stain in other cells) or retained.

Results: 13 thymic carcinomas [moderately (MD) (n=1) and poorly (n=6) differentiated squamous cell, undifferentiated (n=2), sarcomatoid (n=1) and MD adenosquamous carcinomas (n=1), atypical carcinoid tumors (n=2)], 9 type A and 3 type B3 thymomas were included. Loss of BAP1 expression was found in 2 (of 13, 15%) thymic carcinomas (MD squamous cell carcinoma, undifferentiated carcinoma) but none of the type A and B3 thymoma. 1 (of 2) patients with BAP1 loss underwent complete resection of a 7.5 cm tumor (pT3N0M1), developed metastasis and recurrence and died of disease 1.6 years following surgery. The other patient underwent complete resection of a 5.5 cm tumor (pT4N0M0) and died 2.7 years after surgery of unknown cause. The median follow up time of the 11 patients with BAP1 retained thymic carcinoma was 2.7 years (range, 0.2-13.1). 4 (of 11, 36.4%) patients had recurrence/metastasis; 6 (54.5%) patients died at a median time from surgery of 2.3 years (range, 0.2-7.5), 3 of disease.

Conclusions: Loss of BAP1expression can be useful in the distinction of thymic carcinoma from type A and B3 thymoma. However, if BAP1 expression is retained, thymic carcinoma cannot be excluded. Although thymic carcinomas with BAP1 loss appear to behave as rather aggressive tumors, larger studies are necessary to evaluate for the prognostic significance of this finding.

2005 Detecting ALK, ROS1 and RET Gene Translocations in Non-Small Cell Lung Cancer (NSCLC) with the NanoString Platform

Hangjun Wang, Anke F Rijk, Zari Dastani, Jason Agulnik, Victor Cohen, David Small, Carmela Pepe, Lama Sakr, Goulnar Kasymjanova, Anna Y Wang, Alan Spatz, Leon C van Kempen. Jewish General Hospital, McGill University, Montreal, QC, Canada.

Background: Lung cancer is the most common cause of cancer-related death worldwide. ALK and ROS1 gene rearrangements in NSCLC often occur in younger patients or non-smokers. It is important to identify those gene fusions efficiently and treat patients with Crizotinib quickly. ALK translocations are commonly identified through a multi-step process using ALK-1 immunohistochemistry (IHC) followed by ALK break-apart probe fluorescence in situ hybridization (FISH) for confirmation. In this study, we evaluated the nanoString nCounter technology as a single tube RNA-based assay for the simultaneous detection of ALK, ROS1 and RET transcripts in formalin-fixed and paraffin embedded tissues (FFPE).

Design: The series of 39 selected cases of NSCLC (EGFR wild type, ALK-1 IHC positive or negative in cases of non-smoker or <50 year old patient) were assessed for ALK, ROS1 and RET fusion transcripts by nanoString nCounter profiling.

Results: The series included 10 ALK-1 IHC positive cases (9 IHC+/FISH+, 1 IHC+/FISH-). Twenty-eight ALK-1 IHC negative cases of nonsmokers and/ or < 50 years old were selected (8 IHC-/FISH-, 3 IHC-/FISH+, 17 IHC-/FISH not tested). One case was IHC equivocal/FISH-.

An ALK fusion transcript was detected in all 10 ALK-1 IHC positive cases: five EML4-ALK A6;A2, one EML4-ALK E18;A20, and four ALK transcripts with an unknown fusion partner. The single case with an ALK-1 IHC equivocal/FISH- did not reveal any ALK fusion transcript. NanoString analysis could not be performed for two of the 28 ALK-1 IHC-negative cases because of high RNA degradation. The 26 remaining samples contained a RET fusion transcript (KIF5B-RET K15;R11), two ROS fusion transcripts (SLC34A2-ROS1 S4:R33 and EZR-ROS1 E10;R34), two unknown ALK fusion transcripts (FISH not tested) and one unknown ROS1 fusion transcript. The three ALK-1 discrepancy cases (ALK-1 IHC-/FISH+) did not contain an ALK, ROS1 or RET fusion transcript.

Conclusions: NanoString nCounter is a valuable method for the analysis of fusion transcript in lung cancer FFPE tissue. The results are highly concordant with the current standard methods of ALK-1 immunohistochemistry and can provide a definitive answer in case of a discrepancy between immunohistochemistry and FISH. In addition, ROS1 and RET fusions as well as two unknown ALK fusion were detected in ALK-1 negative immunostaining cases. NanoString profiling can be an alternative for a one tube test for ALK, ROS1 and RET translocations in a selected NSCLC patient group.

2006 Metastatic Basal Cell Carcinomas to Thorax and Bone: A Clinicopathological and Immunohistochemical Study of 14 Cases

Annikka Weissferdt, Neda Kalhor, Cesar Moran. MD Anderson Cancer Center, Houston, TX.

Background: Cutaneous basal cell carcinoma (BCC) is the most common neoplasm worldwide. While the majority of these tumors are cured following complete excision, metastatic BCC (mBCC) is an exceedingly rare phenomenon with an estimated incidence of <0.003 to 0.5%. Metastasis most commonly occurs to lymph nodes, lungs, and bone and is associated with an aggressive clinical course and median survival from metastasis to death of only 8-10 months. We report the clinicopathological and immunohistochemical features of 14 mBCC to organs of the thorax and bone.

Design: Fourteen cases of mBCC to the lung (n=10), bone (n=3) and heart (n=1) were identified among 5311 cases of BCC (0.0026%) diagnosed at our institution between 2002-2015. All cases were analyzed for clinicopathological parameters. In 11 cases, immunohistochemical studies with antibodies directed against bcl-2, BerEP4 and EMA were performed on the metastatic deposits.

Results: The patients were white males with a mean age at diagnosis of BCC of 53 years and mean age at metastasis of 65 years. Primary BCC were primarily located on the torso and head and neck. Microscopically, the primary tumors included 6 BCC, not otherwise specified, 4 nodular, 2 mixed and 1 each of morpheaform and microcystic types. Three cases showed focal squamous differentiation. Nine patients had tumor recurrence or multifocal disease. Ten cases metastasized to the lung, 3 to the bone and 1 to the heart. Immunohistochemically, 7/10 metastatic cases (70%) were positive for bcl-2, 9/11 for BerEP4 (81%) and 0/10 for EMA. Treatment consisted of surgery +/- chemo or radiotherapy. The median time from primary diagnosis to metastasis was 89 months and from metastasis to last follow-up was 27 months. Eight patients died at a median interval from metastasis to death of 20 months and 6 patients were alive at a median interval from metastasis to last follow-up of 34 months.

Conclusions: mBCC to the thoracic organs and bones is a rare occurrence mainly affecting older white males. Often mBCC is not suspected in a patient presenting with metastatic disease who has a history of BCC leading to inadequate patient management. Our cases confirm that lung and bone are common sites for mBCC and for the first time describe such occurrence in the heart. Compared to previous published data, our results seem to suggest slightly better prognosis for these patients possibly due to improved multimodal treatment strategies. Metastasis from a BCC should be included in the differential diagnosis in a patient with metastatic disease of unknown primary and history of BCC.

2007 Are All PD-L1 Antibodies Created Equal? A Multiinstitutional Survey of FDA- and Non FDA-Cleared Immunohiostchemistry Assays on 157 NSCLC Cancers

Hadi Yaziji, Judy Pang, Dafydd G Thomas, Clive R Taylor, Jeffrey L Myers. Vitro Molecular Laboratories, Miami, FL; University of Michigan, Ann Arbor, MI; University of Southern California, Los Angeles, CA.

Background: Programmed cell death axis is in the spot light of targeted therapy of a myriad of cancer types including non-small cell lung cancer (NSCLC), with promising clinical outcome. Available PD-L1 antibodies were FDA approved as either companion or complementary immunohistochemistry assays. However, each targeted therapy agent requires a different PD-L1 antibody testing, making it unrealistic to incorporate all available PD-L1 antibodies in order to cover all targeted therapy applications. FDA-approved assays are also more expensive than analyte specific reagents. Finally, large-scale technical validation and comparison of performance characteristics has not been established independently of biopharmaceutical industry. This study aims at comparing the performance characteristics of the most common PD-L1 antibodies in a large cohort of NSCLCs.

Design: Tissue microarrays of 157 patients with NSCLC (adenocarcinomas, n = 97; squamous carcinomas, n = 60) were evaluated. Patient age ranges from 43 to 84 years, with roughly equal F/M ratio and wide TNM stage range. Two FDA approved antibodies (rabbit monoclonal clone 28-8/Abcam; mouse monoclonal antibody clone 22c3/Dako) were compared to a third antibody (rabbit monoclonal clone E1L3N/Cell Signaling Technology). Antibodies were optimized using calibrated control cell lines with four established levels of expression. For comparison purposes, cutoff of >1% positive tumor cells was selected.

Results: E1L3N showed the most sensitivity on adenocarcinomas and squamous carcinomas (positive on 15% and 16% respectively) followed by 28-8 (5% and 4%) and 22c3 (4% and 2%), in addition to a stronger signal intensity noted with E1L3N.

Conclusions: This study provides the technical validation of three widely used PD-L1 monoclonal antibodies showing signficantly higher sensitivity of E1L3N compared to 28-8 and 22c3. These results suggest expanding the utility of E1L3N to cover broad clinical applications. The results also have economic repurcussions: Non-FDA cleared antibodies are inherently less expensive than FDA-approved ones. The combination of higher sensitivity and lower cost makes E1L3N clone more desirable for PD-L1 targeted therapy testing in lung cancer. Once it undergoes stringent clinical validation, E1L3N can potentially be suited as a better alternative to FDA-approved assays for the determination of treatment eligibility with PD-L1 targeted therapy.

2008 BAP1 Loss in Well-Differentiated Papillary Mesothelioma May Be Associated with Malignant Transformation

Eunhee S Yi, Hee Eun Lee, Julian R Molina, Debra A Bell, Anja C Roden, William R Sukov. Mayo Clinic, Rochester, MN.

Background: BRCA1-associated protein 1 (BAP1) is a tumor suppressor that has been implicated in the development of several tumors including malignant mesothelioma (MM). BAP1 immunohistochemistry (IHC) can be helpful in distinguishing benign from malignant mesothelial proliferations. Well-differentiated papillary mesothelioma (WDPM) is a distinct tumor of mesothelial origin with papillary architecture, bland cytological features and a tendency towards superficial spread without invasion. WDPM is generally regarded as a clinically, morphologically and prognostically separate entity from conventional MM. In the present study, we examined the BAP1 expression in WDPM cases that has not been well known.

Design: Six patients diagnosed as WDPM were identified from the surgical pathology file at Mayo Clinic Rochester. Adenomatoid tumor (n=8) and conventional MM (n=39) were included as controls. BAP1 IHC (C-4, Santa Cruz Biotechnology, Santa Cruz, CA) and p16 fluorescence in situ hybridization (FISH) were performed on a representative block from each case after reviewing all HE slides. Clinical information was obtained from the medical records.

Results: Six patients with WDPM were composed of 3 women and 3 men with the age ranging 30-77 (median, 62 years). Two patients had multiple biopsies. One patient developed MM in 2016 after the initial diagnosis of WDPM in 2006 that showed BAP1 loss, as did in the subsequent biopsies with WDPM in 2006 and with MM in 2016. Another patient had synchronous pleural and peritoneal involvement verified by multiple biopsies over one year, which revealed synchronous and metachronous MM. BAP1 loss was found in both WDPM and MM in this patient as well. The remaining 4 patients showed WDPM with intact BAP1 and had no evidence of disease on follow up at 1-122 months (median 36.5 months). All adenomatoid tumors had intact BAP1 expression, while 19 of 39 MM revealed BAP1 loss. FISH did not show p16 deletion in all 5 WDPMs and 8 adenomatoid tumors tested. One MM tested for p16 FISH showed heterozygous deletion.

Conclusions: Two of 6 WDPM patients showing BAP1 loss developed MM, suggesting that BAP1 loss in WDPM might predict a malignant transformation. All adenomatoid tumors had intact BAP1 expression and 48.7 % of MM showed BAP1 loss, in keeping with the results reported in previous studies.

2009 Histopathologic Features of IgG4-Related Lung Disease Associated with Carcinomas in the Lung: Report of 4 Cases

Eunhee S Yi, Hee Eun Lee, Thomas V Colby, Mathieu C Castonguay, Charles H Aust, Jr., Henry D Tazelaar. Mayo Clinic, Rochester, MN; Mayo Clinic, Scottsdale, AZ; Dalhousie University, Halifax, NS, Canada; Lutheran Hospital of Indiana, Fort Wayne, IN.

Background: Previous studies have suggested that IgG4-related disease (IgG4-RD) may predispose patients to cancers or that some cancers may be associated with the subsequent development of IgG4-RD. However, the direct association of IgG4-RD with a cancer has not been documented. We report 4 cases showing histopathologic features of IgG4-related lung disease (IgG4-RLD) associated with carcinomas in the lung.

Design: 3 cases with histologic features of IgG4-RLD associated with adjacent primary or metastatic lung carcinomas were identified in the consult files of the Mayo Clinic. An additional case was identified by a systematic review of 159 resected lung adenocarcinomas over a one year period at Mayo Clinic Rochester (0.6%). Clinical history, pathology, and radiologywere reviewed. IgG and IgG4 immunostains were performed on all cases and additional stains for CD3, CD20, IgD, kappa, and lambda were performed as needed.

Results: 3 of 4 patients were women with a median age of 68 years (range, 63-79). Patients underwent lobectomy (n=2), wedge resection (n=1), or lobectomy and wedge resections of other lobes (n=1). 3 patients had primary lung adenocarcinoma (ADC) and 1 had a metastatic squamous cell carcinoma. All cases showed histologic features consistent with IgG4-RLD, including prominent fibroinflammatory mass-like inflammation nearly obliterating the adjacent carcinomas, with exuberant lymphoplasmacytic infiltrates (4 of 4 cases), eosinophils (4/4), storiform fibrosis (4/4), obliterative phlebitis (3/4) or arteritis (1/4), and increased IgG4-positive plasma cell counts (median, 103/HPF; range 47-132/HPF) and IgG4/IgG ratio (median, 63.3%; range 45– 65%). In 1 patient, there were 2 separate nodules of ADC in one lobe, both of which had the features of IgG4-RLD around the tumors. In addition, there was a separate fibroinflammatory nodulewith the features of IgG4-RLD in a different lobe that did not have carcinoma. None of our cases had a clinical suspicion for IgG4-RD. The radiologic features were mostly nonspecific. Serum IgG4 level was within normal range in 1 patient; the remaining patients were not tested.

Conclusions: Histopathologic features of IgG4-RLD can be seen in association with lung cancers, suggesting the IgG4-RLD features as a peculiar immune reaction to tumors. Additional follow-up will be necessary to determine the clinical significance of this finding.

2010 Aberrant mTOR Pathway Signaling Associated with Sclerosing Pneumocytoma

Eunhee S Yi, Hee Eun Lee, Emily G Barr Fritcher, Jesse S Voss, Benjamin Kipp. Mayo Clinic, Rochester, MN.

Background: Sclerosing pneumocytoma (SP) is a tumor of pneumocytic origin histologically characterized by presence of two cell types, cuboidal surface cell and round cell. SP is generally considered a benign neoplasm and usually present as a single mass treated by simple resection. However, SP can rarely present with distant metastasis or as multiple nodules which may not be amenable for surgical treatment. Targeted therapy might be useful in such cases but the molecular profile of these tumors is not well known.

Design: Nine SP cases were identified from the Mayo Clinic surgical pathology files. NGS mutational analysis was performed on 8 cases using a lab developed NGS assay that assesses the entire coding regions of 50 cancer-associated genes. Foundation One (Cambridge, MA) mutation testing was performed on the remaining case.

Results: All patients were women with median age of 48 years (range, 17-63). Procedures included wedge resection (n=6), segmentectomy (n=1), lobectomy (n=1) and one fine needle aspiration biopsy (FNAB) (n=1). Seven patients presented with a single pulmonary nodule, one patient had two, and the remaining one patient had numerous nodules. NGS sequencing results identified *AKT1* alterations in 4 of 8 (50%) specimens including the common E17K (x2) mutation and an in-frame indel (Q79_W80delinsKR x2), all within the Pleckstrin homology domain. One patient had a co-existing *AKT1* E17K and *CTTNB1* S33A mutation. The patient that presented with numerous pulmonary nodules is a 22-year-old woman who was first diagnosed with SP at age 14 with multiple wedge resections and recently had FNAB for a further work-up. Genomic sequencing of the FNAB by Foundation One revealed *PTEN* and *PIK3R1* (both involved in the mTOR pathway) mutations. She has been treated with the mTOR inhibitor everolimus.

Conclusions: Our findings suggested that aberrant PI3K/AKT/mTOR signaling pathways play a major role in pathogenesis of SP and mTOR pathway inhibitor may be an effective therapeutic target for a subset of SP patients.

2011 BAP1 Immunohistochemistry Differentiates Pleural Mesothelioma Not Only from Reactive Mesothelial Hyperplasia but Also from Metastatic Pleural Tumors

Masayo Yoshimura, Yoshiaki Kinoshita, Makoto Hamasaki, Shinji Matsumoto, Tomoyuki Hida, Yoshinao Oda, Kazuki Nabeshima. Fukuoka University School of Medicine and Hospital, Fukuoka, Japan; Graduate School of Medical Sciences, Kyushu University, Fukuoka, Japan.

Background: For the diagnosis of malignant pleural mesothelioma (MPM), differentiating MPM from pleural metastatic tumors and reactive mesothelial hyperplasia (RMH) is important. Recently, it has been reported that immunohistochemical detection of loss of BRCA-associated protein 1 (BAP1) protein expression permits differentiation of MPM from RMH. Moreover, BAP1 protein loss has rarely been detected in lung carcinoma. In this study, we examined BAP1 protein expression in 9 different types of tumors (total 175 tumors) that sometimes metastasize to the pleura.

Design: Between the years 2001 and 2015, pleural metastases were observed in 9 different types of tumors. Thus, we examined BAP1 protein expression in 51 cases of MPM as well as in the 175 cases of 9 different types of tumors [87 lung carcinoma (68 adenocarcinoma, 10 squamous cell carcinoma (SqCC), 9 pleomorphic carcinoma), 20 breast carcinomas (15 invasive carcinoma of no special type, 5 invasive lobular carcinoma), 10 bladder carcinomas, 5 thymic carcinomas, 2 type B3 thymomas, 5 esophageal SqCC, 6 hypopharyngeal SqCC, 16 gastric carcinomas (11 tubular adenocarcinoma, 5 signet ring cell carcinoma), and 24 renal cell carcinomas (RCC) (20 clear cell RCC, 4 non-clear cell RCC)]. Tumor nuclei that stained with intensity equal to or stronger than that of the surrounding stromal cells or lymphocytes were designated BAP1 positive. The cutoff was set at 25% with a safe margin based on ROC analysis in MPM and RMH cases.
Results: Loss of BAP1 protein expression was detected in 60.8% (31/51) of MPM cases, while none of the lung (0/87), breast (0/20), bladder (0/10), thymic (0/5), esophageal (0/5), hypopharyngeal (0/6), or gastric (0/15) carcinomas and type B3 thymomas (0/2) showed BAP1 loss. Only 15% (3 of 20) of clear cell RCC revealed BAP1 loss.
Conclusions: In addition to the utility of detecting BAP1 loss in discriminating MPM from RMH, anti-BAP1 antibody can also be added to the antibody panel to differentiate pleural metastatic carcinomas from MPM. Loss of BAP1 indicative of presence of MPM rather than metastatic tumors. However, possibility of metastatic clear cell RCC should be carefully considered morphologically and immunohistochemically, since clear cell RCC shows BAP1 loss in about 15% of cases.

2012 Differential Expression of Immune Inhibitory Markers in Association with the Immune Microenvironment in Resected Lung Adenocarcinomas

Mingjuan L Zhang, Marina Kem, Meghan J Campo, Tiffany Huynh, Justin F Gainor, Mari Mino-Kenudson. Massachusetts General Hospital, Boston, MA.
Background: Programmed cell death ligand 1 (PD-L1), indoleamine 2,3-Dioxygenase 1 (IDO1) and B7-H4 have been shown to exert potent immunosuppressive effects and be variably expressed in human lung cancer. We have reported the association of PD-L1 expression with CD8+ cytotoxic T lymphocytes (CTL)/Th1 microenvironments in resected lung adenocarcinomas (ADC), but the association between PD-L1, IDO1, and B7-H4 expression with subtypes of tumor-infiltrating lymphocytes (TILs) and molecular alterations has not been well-characterized in ADC.
Design: PD-L1, IDO1, and B7-H4 expression were evaluated in 261 resected ADC using tissue microarrays and H-scores. Associations between expression and clinicopathologic variables, TILs, molecular mutations, and patient outcomes were examined.
Results: There was expression of PD-L1 in 89 (34.1%), IDO1 in 74 (28.5%), and B7-H4 in 3 (1.2%) cases using a cutoff H-score ≥5. Of those, co-expression of PD-L1 and IDO1 was present in 49 (18.8%) cases, with no overlap of either with B7-H4. Both PD-L1 and IDO1 expression were significantly associated with smoking history, aggressive pathologic features, and abundant CD8+ and T-bet+ (a marker for Th1 pathway activation) TILs. In cases with isolated IDO1 expression, abundant CD8+ and T-bet+ TILs were present in 0% and 8.0%, respectively, vs. 71.4% and 26.5% of PD-L1+/IDO1+ and 60.0% and 27.5% of PD-L1 only cases ($p<0.001$, respectively). PD-L1 expression was significantly associated with EGFR wild-type ($p<0.001$) and KRAS mutants ($p=0.021$). However, there was no difference in IDO1 expression, in particular isolated IDO1 expression, between different molecular alterations. In regard to patient outcomes, PD-L1 expression was significantly associated with decreased progression-free (PFS) and overall survival (OS) by univariate and multivariate analyses, while IDO1 expression was associated only with decreased OS by multivariate analysis. Interestingly, there was a significant difference in the 5-year PFS and OS ($p=0.004$ and 0.038, respectively), where cases without PD-L1 or IDO1 expression had the longest survival, and those with PD-L1 alone had the shortest survival.
Conclusions: While PD-L1 +/- IDO1 expression is observed in association with CTL/Th1 microenvironments, EGFR wild-type, and KRAS mutations, isolated IDO1 expression does not demonstrate these associations, suggesting that IDO1 may serve a distinct immunosuppressive role in ADC. Thus, blockade of IDO1 may represent an alternative and/or complementary therapeutic strategy to reactivate anti-tumor immunity.

2013 Morphologic Findings in Native Lungs from Single Lung Transplant Recipients: An Autopsy Study of 11 Cases

Xiaotun Zhang, Eunhee S Yi, John P Scott, Anja C Roden. Mayo Clinic, Rochester, MN.
Background: Single lung transplantations have become more frequent in patients with end-stage lung diseases. Complications of the native lung might impact post-transplant morbidity and mortality. We have studied histomorphologic findings in native lungs of single lung allograft recipients at time of autopsy.
Design: Autopsy files (1995-2014) were searched for patients with single lung allografts. Archived autopsy sections from the native lungs were reviewed by a pulmonary pathologist. Medical records and autopsy reports were studied.
Results: Eleven patients (5 men) who had received a single lung allograft at a median age of 57 years (range, 38-64) were included. Indications for transplantation and morphologic findings are summarized in the table.

Indication for Transplantation (N)	Morphologic Findings of Native Lungs at Autopsy*(N)
Idiopathic pulmonary fibrosis/ UIP** (4)	Fibrosis most consistent with UIP (4)ALI*** (1)Alveolar hemosiderosis (1)
Alpha1-Antitrypsin Deficiency (3)	Severe panacinar emphysema (3) ALI (3) Alveolar hemosiderosis (2) Mycetoma (1)Bronchiectasis (1)Acute hemorrhage (1)Marked capillary proliferation (1)
Emphysema (2)	Extensive centrilobular emphysema (2)ALI (1)Alveolar hemosiderosis (1)Non-necrotizing granulomas (1)
Scleroderma-associated interstitial lung disease (1)	Lymphangitic carcinomatosisNon-specific interstitial pneumoniaALI Emphysema
Restrictive lung disease, constrictivebronchiolitis (1)	Constrictive bronchiolitisALIAlveolar hemosiderosisSevere pleural fibrosis with previous talc pleurodesis

*Some patients had multiple findings; **UIP, usual interstitial pneumonia; ***ALI, acute lung injury (diffuse alveolar damage, acute bronchopneumonia, acute or organizing fibrinous pneumonia)
Patients died at a median of 17 months (range, 0.5-113) after transplantation from acute lung injury (n=5), pulmonary aspergillosis, sepsis due to biliary lithiasis, complications of systemic scleroderma or acute on chronic lung allograft failure (n=1, each). Two patients died perioperative from surgical complications.
Conclusions: Our study suggests that acute lung injury can complicate native lungs in patients with single lung transplantation and directly cause or at least contribute to the death of these patients. In addition, native lungs commonly show alveolar hemosiderosis and can occasionally develop carcinoma. Findings in the native lung are important for clinical management and outcome of this patient population.

2014 Programmed Cell Death Ligand 1 Is Expressed in a Subset of Pulmonary and Systemic Langerhans Cell Histiocytosis

Xiaotun Zhang, Eunhee S Yi, Robert Vassallo, Anja C Roden. Mayo Clinic, Rochester, MN.
Background: Pulmonary Langerhans cell histiocytosis (PLCH) is a rare histiocytic disorder that is distinct from systemic Langerhans cell histiocytosis (SLCH) by its association with adult smokers. Although both diseases can be effectively managed by current treatment approaches, a subgroup of patients still progress despite ongoing therapy. Since immune dysregulation is a key feature of both diseases, we sought to determine the expression of the immune regulatory molecule Programmed Cell Death Ligand 1 (PD-L1) in the current study.
Design: All cases identified in pathology files (1995-2014) were reviewed by a thoracic pathologist. Clinical features were abstracted from the medical record. Immunohistochemical stains of CD1a (MTB1, Leica Biosystems Newcastle Ltd, UK) and PD-L1 (SP263, Ventana Medical Systems Inc, Tuscon, AZ, US) were done on serial sections. Membranous PD-L1 expression in Langerhans cells was scored as <1% (considered negative), 1-9%, 10-49%, or ≥50% by 3 reviewers separately. Disagreement cases were solved by consensus.
Results: Twenty-three PLCH cases and 14 SLCH cases were included in the current study. Clinical features were summarized as table 1.

	Age (year) Median (range)	Smoking history (N)				Pack Year Median (range)	Gender (M:F)
		Never	Quit	Current	Unknown		
PLCH (N=23)	43 (21-74)	0	4	18	1	25 (6-80)	10:13
PD-L1 +	39 (21-62)	0	0	8	1	22.5 (6-68)	6:3
PD-L1 -	46 (25-74)	0	4	10	0	30 (9-80)	4:10
SLCH (N=14)	22 (1-66)	7	2	5	0	n/a	9:5
PD-L1 +	25 (1-66)	4	1	4	0	n/a	6:3
PD-L1 -	21 (8-27)	3	1	1	0	n/a	3:2

Langerhans cells expressed CD1a in all cases (100%). Nine (39.1%) PLCH cases and 9 (64.3%) SLCH cases showed PD-L1 expression. The immunohistochemical stain results were summarized as Table 2.

PD-L1 in Langerhans cells (%)	PLCH (N=23), N (%)	SLCH (N=14), N (%)
<1 (negative)	14 (60.9)	5 (35.7)
1-9	8 (34.8)	5 (35.7)
10-49	1 (4.3)	3 (21.4)
50-100	0	1 (7.2)

Due to the small sample size, PD-L1 positivity did not correlate with age, smoking history or gender, but does appear to be more frequent in SLCH ($p=0.04$).
Conclusions: PD-L1 expression appears to be more common and more extensive in SLCH than PLCH. This suggests that modulation PD-L1 signaling by relevant blocking antibodies might provide a novel therapeutic target for management of SLCH.

2015 Increased IgG4 Density and IgG4:IgG Ratios in Interstitial Lung Disease Are Associated with Rheumatologic Diseases and Usual Interstitial Pneumonia

Yang Zhang, Allen P Burke, Nevins W Todd. University of Maryland Medical Center, Baltimore, MD.

Background: IgG4-related lung disease has expanded to include an interstitial inflammatory pattern similar to non-specific interstitial pneumonia (NSIP) and even usual interstitial pneumonia (UIP). It is unknown how often NSIP or UIP have IgG4 plasma cell infiltrates, or what defines an abnormal number of IgG4+ cells in interstitial lung disease (ILD).

Design: We selected 14 cases of cellular NSIP, and 6 cases of UIP based on the presence of numerous plasma cells on routine staining. No patient had a history of IgG4 disease. Immunohistochemical staining identified IgG positive and IgG4 positive plasma cells. In areas of maximal numbers, IgG4 density and IgG4:IgG ratios were quantitated per high-power field (hpf) and averaged over 4 hot spots. There were 9 explants and 11 wedge biopsies.

Results: There were 9 women and 11 men; five patients had a history of autoimmune disease. No case had fibroinflammatory lesions suggestive of IgG4-related masses. Mean IgG4 density was 3.9 ± 4.8 in cases of NSIP (highest 14) vs. 8.2 ± 7.6 in cases of UIP (highest 22) (p=0.15). Mean IgG4 ratio was 6.8% (range 0-31) in cases of NSIP vs. 19.3% (range 5-32) in cases of UIP (p= 0.016). The highest IgG4 ratio in the NSIP group (31%) was in a woman with an elevated serum IgG4 level. There was a significant increase in mean IgG4+ plasma cells between patients with rheumatologic disease and those without (p=0.04). By multivariate analysis, a history of autoimmune disease (p=.006) and UIP histologic pattern (p=0.01) were associated with increased IgG4 ratio, as well as between autoimmune disease and IgG4 density (p=0.01).

Conclusions: IgG4+ cells are associated with autoimmune ILD, and are more numerous in UIP vs. NSIP. Although there is a wide range, an upper normal limit of interstitial plasma cells would be approximately 20/hpf, with an IgG4:IgG ratio of over 25%.

Quality Assurance

2016 Detecting Incidental Gallbladder Adenocarcinoma: When to Submit the Entire Gallbladder

Ashwin Akki, Qiang Liu, Sun M Chung, Kathryn E Tanaka, Nicole C Panarelli. Montefiore Medical Center, Bronx, NY.

Background: Gallbladder adenocarcinomas are rare and a substantial proportion is detected incidentally in routine cholecystectomy specimens. It is currently unclear which findings in initial sections are associated with incidental adenocarcinoma, and sampling practices are highly variable when intestinal metaplasia (IM), low-grade dysplasia (LGD), or high–grade dysplasia (HGD) are found upon routine review. The purpose of this study was to correlate findings in initial sections of cholecystectomy specimens with final diagnoses, in order to determine whether detection of any of these features warrants more extensive sampling.

Design: We retrospectively reviewed all cholecystectomy specimens over a 26-month period in order to identify those that had additional sections submitted following review of the original slides. Four pathologists with an interest in gastrointestinal pathology, who were blinded to the original diagnoses and findings on the additional sections, reviewed the initial slides (mean: 2, range 1-7) to assess for the presence or absence of IM, LGD (including BilIN 1 and 2), HGD (BilIN 3), or adenocarcinoma. Diagnostic discrepancies were resolved by consensus.

Results: Additional sections were submitted in 51 of 4059 (1%) cases. These contained IM (n=44, 86%), LGD (n=18, 35%), and HGD (n=5, 10%). A mean of 10 additional cassettes were submitted (range: 2-26). All cases with dysplasia were submitted entirely. Interobserver agreement was fair (κ=0.4) for LGD and high (κ=0.8) for HGD. The diagnosis of IM was agreed upon by all pathologists in all cases. Five incidental adenocarcinomas were detected, including 2 (40%) that were not present in initial sections. These two cases displayed HGD in the original slides, which was independently diagnosed by all four pathologists. The remaining 3 adenocarcinomas were associated with HGD in the background mucosa. Incidental cancers were not detected in cases with only IM or LGD on initial sections; LGD was detected in 8 cases with IM on initial sections, and 2 cases with LGD displayed HGD upon further sampling.

Conclusions: The presence of HGD should prompt complete submission of cholecystectomy specimens, as they may harbor adenocarcinoma and require further treatment. Pathologists should consider seeking a second opinion when LGD is present and submitting additional sections that target abnormal areas; examination of the entire specimen is needed if these yield HGD. Cases that show IM are adequately examined with routine sampling in the absence of gross abnormalities.

2017 Should the Prenatal Cell-Free DNA Screening Test Replace the Quad Screen for Detection of Fetal Trisomies?

Lubna A Alattia, Abhilasha Ghildyal, Menchu Ong, James G Traylor, Diana M Veillon. LSU Health Shreveport, Shreveport, LA.

Background: Cell-free DNA (cfDNA) Screening Test is a non-invasive genetic test that is used to identify chromosomes 13, 18, and 21 and the sex chromosomes. The assay can detect the most common autosomal trisomies and some sex chromosome abnormalities. The test utilizes a maternal blood sample, can be used from 10 weeks through the duration of the pregnancy, and is the only 3rd trimester screening test. The assay is significantly more expensive than the Quad Screen and is currently not covered by most third party payers or Louisiana Medicaid.

Design: We routinely receive requests for either a Quad screen or a cfDNA Screening Test. Our department recently noticed an increase in cfDNA test requests. Retrospectively, we reviewed requests for the Quad Screen or Cell-Free DNA Screening Test over the last 9 months.

Results: There were 57 requests identified. Forty-three were for cfDNA testing with alpha-fetoprotein (AFP), and 14 were for Quad screen with cfDNA testing. Thirteen of 14 Quad screen test results were negative and correlated with cfDNA findings. One patient had a positive Quad Screen suspicious for trisomy 18 but a negative cfDNA result. Fifty-five patients had negative cfDNA results. Two patients had positive cfDNA test for Trisomy 21. Results of cfDNA tests accurately predicted clinical outcome.

Conclusions: Our study suggests that the cfDNA test has higher sensitivity and lower false positive rate than a Quad Screen. The utilization of cfDNA test may decrease the use of more invasive testing such as amniocentesis. Ordering cfDNA test combined with AFP appears to have a greater accuracy, is a more cost effective approach for the evaluation of fetal trisomies, and is available in the first trimester.

2018 Discordances in Evaluation of Melanocytic Lesions and Its Impact on Management: A Study of 1518 Cases

Rami Al-Rohil, George Jour, Priyadharsini Nagarajan, Phyu P Aung, Michael T Tetzlaff, Jonathan L Curry, Carlos A Torres-Cabala, Doina Ivan, Victor G Prieto. Vanderbilt University, Nashville, TN; MD Anderson Cancer Center at Cooper, Camden, NJ; MD Anderson Cancer Center, Houston, TX.

Background: Accurate diagnosis of melanocytic lesions carries a significant clinical implication as appropriate management does not only depend on the correct diagnosis but varies according to the pathologic stage. The objective of this study is to evaluate the degree of discordance between primary histopathologic diagnosis and secondary review of melanocytic lesions, parameters of melanoma, and the subsequent impact on clinical management and follow-up.

Design: In a retrospective review of 1518 referral cases to MD Anderson Cancer Center (MDACC) of melanocytic lesions from 1/2010 to 1/2011, initial diagnoses from the referring institution were compared to the MDACC second opinion reports. If any discordance was noted at time of review, a consensus diagnosis by at least 4 different dermatopathologists was rendered prior to approving the discordance. The discordances were classified as (i) major discordance if they resulted in change in diagnosis and stage of melanoma and thus, the clinical management and (ii) minor discordance if there was no impact on clinical management.

Results: The concordance rate was 100% among metastatic melanoma, (n=214 cases, 14%). Discordance in primary melanocytic lesions occurred in 10.7% of cases (140/1304). Minor and major discordances were found in 38% (n= 53) and 62% (n=87) of the primary melanocytic lesions, respectively. Major discordance categories included inaccurate mitotic count 40/87 (46%), followed by change in diagnosis 39/87 (44.9%), change in Breslow thickness 6/87 (6.9%), change in Breslow thickness and mitotic count 1/87 (1.1%), and change in Breslow thickness, mitotic count and ulceration 1/87 (1.1%). Follow-up ranged between 6 to 131 months (mean 52 months). Among cases with major discordance, 80% (n=69) showed no evidence of residual/recurrent disease, 7% (n=6) died of disease, 2% (n=2) died of other causes, 2% (n=2) are alive with disease, and 9% (n=8) were lost to follow-up.

Conclusions: Our results show that critical review of melanocytic lesions may lead to significant changes in the diagnosis of melanoma, tumor classification as well as staging, thus resulting in critical changes in clinical management and impacting patient survival.

2019 Checklist Implementation for Intraoperative Consultations: Improved Quality and Safety

Kevin Anderson, Jia Xu, Yigu Chen, Jeffrey D Goldsmith, Yael K Heher. Beth Israel Deaconess Medical Center, Boston, MA; Boston Children's Hospital, Boston, MA.

Background: Intraoperative consultation (IOC) is a fundamental part of surgical pathology, providing surgeons with real-time information central to patient care. Correct IOC slide labeling, typically manually performed in a time pressured setting, is critical to avoid patient harm. A recent serious adverse event due to IOC labeling mixup prompted workflow redesign. A checklist was implemented aimed at standardizing slide labeling and monitoring other data points central to quality management. Checklist effects on slide labeling defect rates and frozen section TAT were studied.

Design: Data were collected for all IOC cases over a 9 month period. Slide labeling defect rates and IOC TAT were recorded and compared for the pre and post implementation periods. A slide labeling defect was defined as a lack of any 3 elements on a slide label per hospital policy: patient name, medical record number (MRN), and specimen designation by surgeon.

Results: 839 IOC cases were analyzed. Pre-intervention slide labeling showed that the patient's name, MRN and specimen designation were absent in 23%, 39% and 84% of cases, respectively, with 85% of cases containing at least one defect (n=565). Post intervention, labeling data revealed that the patient's name, MRN and specimen designation were absent in in 18%, 15% and 24% of cases, respectively, with 27% of cases containing at least one defect (n=274). There was statistically significant improvement in all aspects of slide labeling (P<0.001 on all 3 elements). Mean TAT was 21.55 minutes pre-intervention versus 23.21 minutes post-intervention and the change was insignificant (P=0.071). Post-implementation, there was a significant decrease in the number of cases with TATs of exactly 15 or 20 minutes (55% pre and 35% post, p=0.024). This suggests more honest TAT reporting with a shift towards normally distributed values.